

UNIVERSITY OF OKLAHOMA

GRADUATE COLLEGE

THE NATURE OF WATER IN BACTERIAL SPORES, SPORICIDAL ACTIVITY
OF CHLORINE DIOXIDE AGAINST SPORES, AND CRYOPROTECTANT
PROPERTIES OF POLY(ADENYLIC) ACID

A DISSERTATION

SUBMITTED TO THE GRADUATE FACULTY

in partial fulfillment of the requirements for the

Degree of

DOCTOR OF PHILOSOPHY

By

ANTHONY WILLIAM FRIEDLINE

Norman, Oklahoma

2013

THE NATURE OF WATER IN BACTERIAL SPORES, SPORICIDAL ACTIVITY
OF CHLORINE DIOXIDE AGAINST SPORES, AND CRYOPROTECTANT
PROPERTIES OF POLY(ADENYLIC) ACID

A DISSERTATION APPROVED FOR THE
DEPARTMENT OF CHEMISTRY AND BIOCHEMISTRY

BY

Dr. Charles V. Rice, Chair

Dr. Robert L. White

Dr. Zhibo Yang

Dr. Ronald L. Halterman

Dr. Andrew S. Madden

© Copyright by ANTHONY WILLIAM FRIEDLINE 2013
All Rights Reserved.

ACKNOWLEDGEMENTS

First and foremost, I must acknowledge the support of my family, especially my mother, Tammy, my sister Shawna, and most importantly, my late father, Craig, who passed away before this work could be completed. His own dedication—obtaining a bachelor’s degree online through Utica College, and being able to obtain the degree before his death from cancer—and his words of encouragement have always driven me to do my best throughout my life, and has ensured that I could not, and would not, simply settle for less in my education.

I have to also acknowledge the continued support from my extended family, from both sides—Friedlines and Dyes alike.

I am indebted to the Camp Hill School District and Susquehanna University, for having provided me with the education necessary to get into graduate school, and for promoting my natural curiosity about science and technology. While I won’t say that if I had gone to larger institutions I would have had a worse education, the small size and more hands-on interactions between me and my teachers and professors was, I feel, instrumental in keeping my education from being rote or formulaic.

Also to be acknowledged is the University of Oklahoma, and the Department of Chemistry and Biochemistry, for being willing to accept me as one of their own for these five years, and for their continued support and aid.

I have to mention fondly the members of the Rice Group that I have been fortunate to have worked with through the course of my time here. Each of

them provided something to me, either active assistance with my research or encouragement and support, and for that they have my thanks. I have to mention the post-doctoral members, Drs. Ravi Garimella and Karen Johnson; some of the former members of the group, Jeff Halye, Kevin Pastoor, William Harrison, and Malcolm Zachariah; Kieth Thomas, the closest in year to me in the lab; and two undergraduate and post-graduate researchers who, hopefully, will continue the research I have started in the future, Amy Middaugh and Erin Scull.

My thanks have to go out to the members of my graduate Advisory Committee, for taking time from their schedules to assist in ensuring I have kept myself on track to complete this work: Drs. Robert White, Zhibo Yang, Ronald Halterman, and Andrew Madden. In addition, thanks are also necessary for Dr. Richard Taylor, who was on the Committee for most of my time here and only left owing to his own decision to retire after a long career at OU.

Of course, I cannot conclude my acknowledgements without the grateful, heartfelt, appreciation of my advisor and mentor, Dr. Charles V. Rice, and his wife Toni. Their enthusiasm and full-throated support of my research—coupled with a generous helping of gentle poking and prodding—have ensured that I didn't take this work lightly and strove to do my best. Their generosity of heart in that period of time when I was dealing with the illness and death of my father, the way they opened their home and treated me and my father with a warm smile and stories and best wishes...all of this makes it hard to put into words my gratitude and thanks for their support and efforts. Even setting aside the

financial assistance that he and the University have provided me through these years, these simple and yet generous acts of support have, in my opinion, made my time here at OU more productive and fruitful, and I can do nothing but express my deepest appreciation and thanks to Dr. Rice and Mrs. Rice for all they have done for me these years.

TABLE OF CONTENTS

	Page
Acknowledgements	iv
Table of Contents	vii
List of Tables	xii
List of Figures	xiii
Abstract	xxiii
CHAPTER 1: THE RNA WORLD HYPOTHESIS AND THE COLD ORIGIN OF LIFE	1
Introduction	1
The RNA World	2
RNA World and a cold origin of life	5
RNA World and compartmentalization	8
Evolving beyond the RNA World	11
Cold origin of life: when?	12
Conclusion	14
CHAPTER 2: EXTREMOPHILIC ORGANISMS	16
Introduction	16
Extremophiles: definitions and significance	16
Psychrophiles	18
Thermophiles	19
Halophiles	21
Radiation resistance	23

Piezophiles/Barophiles	24
Acidophiles and alkaliphiles	25
Conclusion	27
CHAPTER 3: RHODAMINE B FLUORESCENCE STUDIES OF	
POLY(ADENYLIC) ACID, A POTENTIAL CRYOPROTECTANT, IN RELATION	
TO LIPOTEICHOIC ACID	28
Introduction	28
Structure and function of teichoic acids	29
Principles of fluorescence; structure and function of rhodamine B	32
Experimental Procedure	36
Results	38
Conclusions	40
CHAPTER 4: GENERAL PRINCIPLES OF DEUTERIUM NUCLEAR	
MAGNETIC RESONANCE SPECTROSCOPY	
Nuclear spin and degeneracy; RF pulses and free induction decay	43
Dipolar coupling and chemical shift anisotropy effects	47
Deuterium NMR spectroscopy	51
CHAPTER 5: VARIABLE-TEMPERATURE DEUTERIUM NMR OF	
POLY(ADENYLIC) ACID AND OTHER POTENTIAL CRYOPROTECTANTS	
Reasoning for NMR experiments: similarities of LTA and poly(A)	55
Equipment, materials, and methods	58
Results	64
Discussion	70

Conclusions	73
CHAPTER 6: OVERVIEW OF SPORE-FORMING BACTERIA AND SPORULATION	75
Introduction	75
Spores: structure, process of sporulation, germination	76
Spores: significance	82
Nature of water in the core of bacterial spores	83
<i>Bacillus pumilus</i> SAFR-032: novel spore isolate with enhanced resistance	85
Conclusion	88
CHAPTER 7: DEUTERIUM SOLID-STATE NMR EXPERIMENTS ON BACTERIAL SPORES—INSIGHTS INTO THE NATURE OF WATER INSIDE THE SPORE CORE	89
Introduction	89
Materials	89
Experimental Procedure	92
Preparation of sporulation medium	92
Preparation of LB media	93
Preparation of media—deuterium-labeled media	94
Sterility of media transfer	94
Growth protocol— <i>B.subtilis</i> species	94
Growth protocol— <i>B.pumilus</i> SAFR-032	95
Spore purification	96

Additional samples	98
NMR experiments	98
Results	100
Variable-temperature deuterium NMR of deuterium oxide	101
Solid-state deuterium NMR of bacterial spores	103
Deuterium NMR of bacterial spores: exchange experiments	105
Deuterium NMR of deuterated bovine serum albumin and crystalline calcium dipicolinate trihydrate	112
Discussion	115
Deuterium NMR of spores: lineshape comparisons	115
Peak assignments of spore immobile deuterium signals	117
Accessibility of spore core to external water	119
Future research aims	122
Conclusions	122
CHAPTER 8: TREATMENT OF BACTERIAL SPORES WITH OXINE®, A PROPRIETARY CHLORINE DIOXIDE-BASED BIOCIDAL AGENT	125
Introduction	125
Structure, mechanism of action, and uses of chlorine dioxide	125
Experimental protocol	131
Spore preparation	131
Preparation of chlorine dioxide	132
Exposure of dried spores to chlorine dioxide	133
Evaluation of spore damage with electron microscopy	134

Results	135
Spore preparations	135
Preparation of chlorine dioxide	135
Dried spores' exposure to chlorine dioxide	136
Discussion	138
Conclusions	146
REFERENCES	151

LIST OF TABLES

	Page
Table 5.1 (opposite). Peak height times line width values from -25°C to 0°C from S2PUL deuterium VT NMR experiments for various molecules of interest, with percent change between temperatures and cumulative percent change. n.d. = not detectable; N/A = not applicable.	69
Table 7.1. List of distance (in kHz) between immobile Pake doublets for various ² H NMR samples. N/A = not applicable (sample had only one identifiable doublet).	114
Table 8.1. Viable results after spraying Oxine® onto dry microscope cover slips coated with <i>B.subtilis</i> ATCC 6051 and <i>B.pumilus</i> SAFR-032 spores.	137
Table 8.2. Plate countings of post-exposure <i>B.pumilus</i> SAFR-032 spores exposed on aluminum coupons, 1 hour exposure time, 24 hour incubation time. Inactivated Oxine® concentration = 108.5 ppm ClO ₂ ; activated Oxine® concentration = 70.4 ppm, 39 ppm free. Numbers are colonies counted on TSA plates for the given serial dilution. TNTC = too numerous to count (>300 colonies, or >100 colonies in one quarter of the plate). * = agar plate appeared damaged or potentially contaminated. A and B are duplicate platings.	138
Table 8.3. Plate countings for post-exposure spores of <i>B.pumilus</i> SAFR-032 spores on Al coupons, 24 hour exposure time, 24 hour incubation time. Concentrations are identical to Table 8.2. * = potential contamination or plate damage.	138

LIST OF FIGURES

	Page
Figure 3.1. Teichoic acids are classified by where they are attached in the Gram-positive cell: to the peptidoglycan for WTA, or to the lipid bilayer membrane for LTA. Figure 1 from ref 21, reprinted with permission.	29
Figure 3.2. Lipoteichoic acid, left, has a polyglycerol phosphate backbone (A), whereas wall teichoic acids can have either polyglycerol phosphate (B) or polyribitol phosphate (C) depending on the bacteria. Figure 1 from ref 20, reprinted with permission.	30
Figure 3.3. This sequence of ^{31}P CPMAS spectra of LTA (<i>S.aureus</i>) dissolved in D_2O shows a total lack of phosphorus signal at -40°C and only minimal signal at -50°C , indicative of the presence of liquid water. Figure 2 from reference 26, reprinted with permission.	31
Figure 3.4. In contrast the VT spectra of bulk cell wall (peptidoglycan with teichoic acid) only protects liquid water down to between -10°C and -20°C via phosphorus CPMAS. Figure 4 from reference 26, reprinted with permission.	32
Figure 3.5. A Jablonski diagram showing the different electronic and vibrational states, and the pathways for fluorescence and phosphorescence (nonradiative decay pathways are not shown).	33
Figure 3.6. Structure of Rhodamine B, as the cation, with Cl^- counterion.	34
Figure 3.7. Rhodamine B's fluorescence emission is evident in a water solution at room temperature conditions but is quenched (with the appearance of	

spectral features related to ice scattering) at -20°C. Rice Lab, unpublished data.	34
Figure 3.8. At -20°C, rhodamine B fluorescence is quenched even with the addition of 1M NaCl or 5% w/v DNA solution, but is maintained after addition of 5% w/v LTA solution. Rice Lab, unpublished data.	35
Figures 3.9 and 3.10. Figure 3.9, left, shows structures of <i>B.subtilis</i> WTA and LTA (figure 2 from ref 21, reprinted with permission); Figure 3.10, right, is a structure of polyadenylic acid. The similar backbones led to the idea that poly(A) might possess similar liquid-water preservation properties under fluorescence spectroscopy.	36
Figure 3.11. Experimental setup for the fluorescence of rhodamine B solution with and without addition of polyadenylic acid (5% w/v) solution.	37
Figure 3.12. Comparison of fluorescence of rhodamine B dye (1×10^{-4} M) at room temperature and at 1 hour after cooling the sample holder to -15°C.	39
Figure 3.13. Comparison of fluorescence intensity of rhodamine B + poly(A) over a period of time chilling the sample to -20°C.	40
Figure 3.14. As shown by fluorescence live-dead assay, lipoteichoic acid serves as a potent cryoprotectant for cells of <i>B.subtilis</i> 1A578, performing comparably to addition of glycerol. (Rice Lab, unpublished data, courtesy A. Middaugh.)	42

- Figure 4.1. A positively charged nucleus with spin (and angular momentum) causes a magnetic dipole which precesses about an external magnetic field. 44
- Figure 4.2. NMR-active nuclei of spin $\frac{1}{2}$ A) degenerate under normal conditions B) split into two states in the presence of external magnetic field with associated ΔE . 45
- Figure 4.3. The magnetization of a sample is perturbed by an RF pulse away from the z-axis; the relaxing nuclei induce a free induction decay in the detector; Fourier transformation of the signal yields a spectrum. 46
- Figure 4.4. The powder lineshape of a molecule experiencing heteronuclear dipolar coupling, where D is both the dipolar coupling constant and the distance between the two peaks of the spectrum. 48
- Figure 4.5. The result of anisotropy and homonuclear dipolar coupling: deuterium NMR of deuterated DNA, at 0°C (A) and -15°C (B); while the area under the peak is identical, it is broadened to where the peak is unrecognizable. 50
- Figure 4.6. The transitions and spectra for liquid deuterium NMR, for the cases where the sample is in an isotropic system (a, left) or anisotropic system, as in a liquid crystalline state (b, right). 52
- Figure 4.7. The Pake pattern spectrum for solid-state deuterium NMR (in this case, frozen D_2O), with the characteristic two horned peaks; notice the broadness of the peak, a trademark of solid-state NMR. 53

- Figure 5.1. The structure of lipoteichoic acid, with side-chain units listed at right. The lipid tails are at bottom right, followed by the disaccharide moiety and the polyglycerolphosphate (PGP) backbone. 56
- Figure 5.2. ^{31}P VT CPMAS NMR of *S.aureus* LTA dissolved in D_2O indicates due to the absence of the phosphorus lineshape that some molecular motion exists as a result of liquid D_2O present as low at between -50 and -60°C ; LTA thus provides cryoprotectant effects. Figure 2 from Rice *et al* 2008¹⁶, reprinted with permission. 57
- Figure 5.3. Schematic representation of the equipment setup for the variable-temperature deuterium NMR experiments performed. 60
- Figure 5.4. Temperature-arrayed sequence of spectra of D_2O using the S2PUL pulse sequence, at 5°C increments from -45°C , at left. The distorted signals at $+5$ and $+10^\circ\text{C}$, right, are due to saturation of the detector by liquid deuterium signal above the melting point of D_2O . 65
- Figure 5.5. The temperature-arrayed spectra of D_2O using the SSECHO pulse sequence, at 5°C increments from -45 to 0°C . The decreasing set of Pake doublets are indicative of the immobile deuterium, which fades as the sample is warmed, with the appearance of a mobile deuterium signal within the frozen sample at right. 66
- Figure 5.6. The temperature array (in $^\circ\text{C}$) of the S2PUL experiment with 5% w/v lipoteichoic acid. 66
- Figure 5.7. The temperature array (in $^\circ\text{C}$) of the 5% w/v LTA SSECHO experiment. 67

- Figure 5.8. Graphical chart of the data points of Table 5.1 less the LTA; the ribosomal RNA comes from baker's yeast (*Saccharomyces cerevisiae*). 68
- Figure 5.9. Poly(A) compared with D₂O and LTA using data from Table 5.1. The LTA is present in this figure and not in Figure 5.8 due to LTA being at 5% w/v and all other samples at 2.5% w/v. 70
- Figure 6.1. Representative schematic of the general structure of a bacterial spore (not to scale). 76
- Figure 6.2. Diagram of the steps of sporulation, and the addition of germination to form a cyclical trend. 78
- Figure 6.3. Spores of *B.pumilus* SAFR-032 shown under phase contrast microscopy; dormant spores have a phase-bright core, while germinating spores with hydrated cores would show as phase dark. 79
- Figure 6.4. The structure of dipicolinic acid (pyridine-2,6,-dicarboxylic acid); in the spore core the molecule is negatively charged and associated with a Ca²⁺ cation. 81
- Figure 7.1. Schematic representation of VT NMR system for experiments. 92
- Figure 7.2. Phase contrast microscopy image of *B.pumilus* SAFR-032 spores grown in LB media and subsequently purified (1000x magnification). Spores exhibit a characteristic phase-bright center surrounded by phase-dark coat material. 97
- Figure 7.3. The schematic of the solid-state echo (SSECHO) pulse sequence, using parameters defined for Varian VNMR and VNMRJ software. The

initial 90° pulse is <i>p1</i> , the second 90° pulse is <i>pw</i> . <i>p180</i> and <i>d2</i> are optional properties and were ignored (<i>p180</i> , <i>d2</i> =0).	100
Figure 7.4. Solid-state VT ² H NMR spectrum of D ₂ O at -45°C.	101
Figure 7.5. Same sample of D ₂ O using VT ssNMR, at 0°C.	101
Figure 7.6. The temperature array (labeled with temperature, in °C) from which Figures 7.4 and 7.5 were taken; Figure 7.4 is at left (-45°C), Figure 7.5 at right (0°C).	102
Figure 7.7. Deuterium solid-state NMR spectrum of 25% D ₂ O <i>B.subtilis</i> ATCC 6051 spores (17.0 mg). Note the change in the scale from figure 7.4 and 7.5.	103
Figure 7.8. ² H NMR spectrum of 25% D ₂ O-labeled <i>B.subtilis</i> 1A578 spores, 19.7 mg, vs (vertical scale)=500k.	104
Figure 7.9. ² H NMR spectrum of 25% D ₂ O <i>B.pumilus</i> SAFR-032, 19.7 mg. vs=500k.	104
Figure 7.10. Overlays of Figures 7.7-7.9 on the same axis, all at vs=500k. Red = Figure 7.9, the 25% D ₂ O-labeled <i>B.pumilus</i> SAFR-032; blue = 25% D ₂ O-labeled <i>B.subtilis</i> 1A578 (Figure 7.8); green = 25% D ₂ O-labeled <i>B.subtilis</i> ATCC 6051 (Figure 7.7).	105
Figure 7.11. A flowchart comparison of the two exchange experiments, H-D and D-H exchange, respectively.	106
Figure 7.12. ² H NMR spectrum of the H-D exchanged spore sample of <i>B.subtilis</i> ATCC 6051, 13.3 mg.	107

Figure 7.13. ^2H NMR spectrum of H-D exchanged <i>B.subtilis</i> 1A578 spores, 13.6 mg.	107
Figure 7.14. ^2H NMR spectrum of H-D exchanged <i>B.pumilus</i> SAFR-032 spores, 14.2 mg.	107
Figure 7.15. Overlaid spectra of Figures 7.7 and 7.12 (<i>B.subtilis</i> ATCC 6051 spores, 25% D_2O label (red) and post-H-D exchange (green), respectively) scaled to equal mass.	108
Figure 7.16. Comparison of <i>B.subtilis</i> 1A578 spores (25% D_2O labeled, orange; post-1-week H-D exchange, teal) via ^2H NMR.	108
Figure 7.17. Comparison spectra of <i>B.pumilus</i> SAFR-032 (25% D_2O , blue; 1- week H-D exchange, red) spores via ^2H NMR.	109
Figure 7.18. Compared spectra of 40% D_2O <i>B.pumilus</i> SAFR-032 spores (red) with spores soaked in water (H-D exchange) for four weeks (green).	110
Figure 7.19. The overlaid spectra of <i>B.subtilis</i> ATCC 6051 spores by ^2H NMR; 25% D_2O spores (made in deuterated media), red; spores grown in media and deuterated post-sporulation (D-H exchange), light blue.	111
Figure 7.20. The comparison of 25% D_2O spores of <i>B.subtilis</i> 1A578 (red) and the post-sporulation deuterated spores of the same species (D-H exchange, light blue), similar to Figure 7.18.	111
Figure 7.21. The comparison of 25% D_2O <i>B.pumilus</i> SAFR-032 spores, red, and D-H exchanged (post-sporulation) spores of SAFR-032, blue.	111

- Figure 7.22. Two samples of deuterated bovine serum albumin studied via ^2H NMR: after 5 days' lyophilization, red (30.7 mg); after 19 days' lyophilization, blue (33.7 mg). 113
- Figure 7.23. The solid-state deuterium NMR spectrum of amorphous (powder) calcium dipicolinate. 113
- Figure 7.24. The solid-state ^2H NMR spectrum of crystallized deuterated calcium dipicolinate (70.0 mg). 114
- Figure 7.25. The crystal structure of calcium dipicolinate trihydrate, in this case a dimer, as determined by X-ray crystallography (courtesy Doug Powell). 115
- Figure 7.26. The peak features of *B.subtilis* ATCC 6051 spores (25% D_2O , red) are not attributable to the peak width of bulk frozen water (D_2O , blue). 117
- Figure 7.27. Overlaid spectra (not to scale) of: 25% D_2O *B.subtilis* ATCC 6051 spores, red; deuterated bovine serum albumin (19-day lyophilization), blue; deuterated calcium dipicolinate trihydrate crystal, black. 119
- Figure 7.28. External water is not able to exchange with immobile deuterium bound in the spore core during H-D exchange experiments. 120
- Figure 7.29. External deuterated water is unable to deuterate the spore core, as shown in D-H exchange experiments. 121
- Figure 8.1. Structure of chlorine dioxide. 126
- Figure 8.2. SEM image of pre-treatment dried *B.subtilis* ATCC 6051 spores on glass cover slips, magnification 10,000x. The spores appear oval in shape, in line with the expected size and shape of bacterial spores. 140

Figure 8.3. Post-Oxine®-treatment *B.subtilis* ATCC 6051 spores as seen via SEM, 10,000x magnification. A number of spores appear to have collapsed, a ring of outer material surrounding a nearly-hollow center; other spores are more intact but smaller and with a halo of material affected by the chemical treatment occurring at the interface between the spores and the glass cover slip. 141

Figure 8.4. Enhanced-magnification (25,000x) and tilted (45°) SEM image of post-Oxine®-treated *B.subtilis* ATCC 6051 spores. From this image it appears that the Oxine® has degraded the spore core material, causing the cortex to collapse; the cortex and coat appear mostly intact. 143

Figure 8.5. Pre-treatment *B.pumilus* SAFR-032 spores as seen on glass cover slips via SEM (10,000x magnification). There appears to be an unknown material, possibly exosporium, connecting some of the spores together. The overall shape of the spores is still oval, though slightly smaller in size versus the *B.subtilis* ATCC 6051. 144

Figure 8.6. Post-Oxine®-treated *B.pumilus* SAFR-032 spores as seen via SEM at 10,000x magnification. Several spores appear similarly affected to those of *B.subtilis* with a ring of material surrounding a dissolved/collapsed center; some of that material has leaked from the spores onto the surface of the glass cover 146

Figure 8.7. SEM image of *B.pumilus* SAFR-032 spores on an aluminum coupon, 10,000x magnification. The spores are normally-shaped, though there are unusual structures underneath the topmost layer of

spores, which may be overhangs and crevasses in the surface of the metal coupon. 147

Figure 8.8. SEM image of aluminum coupon, initially covered in *B.pumilus* SAFR-032 spores, after treatment with 3.5% w/v hydrogen peroxide (magnification 10,000x). No spores are apparent in this image, and there are unusual crystal-shaped structures visible on the lower surface of the coupon; what these shapes are is unknown. The lack of spores is possibly the result of the peroxide entirely dissolving the spores. 148

Figure 8.9. SEM image of *B.pumilus* SAFR-032 spores on an aluminum coupon, after treatment with inactive Oxine®, magnification 10,000x. Spores are present throughout the image, though it is obvious there are large pits and other structures, from the left side of the image. The spore bodies appear intact and oval in shape. The unknown crystal structures are visible underneath the top-most layer. 149

Figure 8.10. SEM image of an aluminum coupon coated in *B.pumilus* SAFR-032 spores treated with activated Oxine®, magnification 10,000x. Few spores were present in the observations of this coupon, though the collapsed spore body at center of this figure is one of them. The spore appears to be collapsed similarly to those in Figures 8-3 and 8-6. There does not appear to be as much layering as in previous figures, though the crystal-shaped bodies are more obvious even on the surface layer. 150

ABSTRACT

Water is the fundamental chemical molecule of life, and the nature of how water interacts with living organisms and how living organisms can maintain liquid water for metabolic function below freezing (cryoprotection) is of interest. In addition to psychrophilic microorganisms, the nature of water in the core of dormant bacterial spores is not clearly understood. If such mechanisms can be determined, they can be used for numerous methods, such as biocidal applications, or for preservation of tissue under freezing conditions. Such functions and cryoprotectant molecules may also have relevant implications for the theories of the origin of life on Earth which imply that such an origin occurred in colder conditions than exist today and the conditions oft theorized to occur on early Earth.

After an introduction into the RNA World hypothesis and its potential implication of a cold origin of life, and a discussion of extremophilic bacteria and their niches, this work will discuss previous research done in the Rice Group that determined the possibility that the Gram-positive cell wall component, teichoic acid, may possess cryoprotectant behavior, both in water by itself via NMR and fluorescence studies, but also *in vitro* with living bacteria. The similarity of the backbone of polyribonucleic acids, in particular poly(adenylic) acid, to the polyglycerolphosphate backbone of teichoic acids, led to research to determine if poly(A) also possessed cryoprotectant function based on this backbone structure. These experiments with rhodamine B-based fluorescence

spectroscopy and variable-temperature deuterium NMR spectroscopy indicate the possibility that it may have similar cryoprotection effects with water.

The bacterial spore is able to protect its vital contents from chemical lysis, antimicrobial agents, heat damage, UV radiation, and dehydration. The role of spore components in spore protection remains in dispute; nevertheless, water molecules are important in each process. Water in the spore can be found free or bound in two different areas, core and non-core. Bound water in the spore has come under recent scrutiny; it is suggested the core water is mobile, rather than bound, based on analysis of deuterium relaxation rates. After background material on the structure of bacterial spores and the sporulation cycle, a set of experiments are discussed with the goal of using solid-state deuterium NMR spectroscopy to locate water inside of the spore and to determine its mobility through the spectral lineshape. Using this approach, we are able to distinguish between mobile and immobile deuterated water molecules inside of the spore. Deuterium NMR spectra of bacterial spores reveals three distinct features: a narrow line of water in rapid motion, a broad immobile signal associated with coat proteins, and an intermediate signal associated with core molecules such as dipicolinic acid. The immobility of the core-bound water associated with dipicolinic acid indicates that the core water is not mobile but is in an amorphous, glassy state.

In addition, the extreme viability of bacterial spores, including certain spore isolates, makes identifying sporicidal agents and their mechanisms of action also of relevance. Preliminary research will be presented on the effects

of a proprietary stabilized chlorine dioxide-based biocidal agent, Oxine®, on bacterial spores. From SEM imagery of spores treated on glass cover slips, it appears that the mechanism of action of Oxine® is to penetrate the spore, possibly through chemical attack of the spore coat layers, and to dissolve the spore core, causing collapse of the spore structure.

CHAPTER 1: THE RNA WORLD HYPOTHESIS AND A COLD ORIGIN OF LIFE

Introduction

This present dissertation will deal with various portions of my research, predominantly involving bacterial spores, but also touching on preservation of life under extreme conditions and the molecules, such as lipoteichoic acid, that living organisms might use to ensure life in extreme environments. However, in order to properly address these matters, some sort of introduction into relevant principles is necessary. In these introductory chapters, I will present background material on one theory of a cold origin of life with relevance to cryoprotection, as well as background on the ability for bacteria to adapt to environments previously thought to be entirely inhospitable to life in any format.

An intriguing question in biology and biochemistry is how life came into existence in the early Earth. Before the first fossil record, approximately 3.5 billion years ago, and the time which the Earth cooled from its formation and initial impact events to be capable to support life, around 4 billion years ago, life began—but how did a random assortment of chemicals become a self-replicating cellular life? There are many competing theories that attempt to answer this question. We must be reminded, at the outset of any exploration of this topic, that “[since] the prebiotic era left no direct record, *we cannot hope to determine exactly how life arose. Through laboratory demonstration, however, we can at least demonstrate what sorts of abiotic chemical reactions may have*

led to the formation of a living system”¹ (Voet and Voet 29, emphasis added).

One theory that has gained support is the “RNA World” hypothesis.

The RNA World

The term “RNA World” was first introduced in 1986, in a letter to *Nature* journal by Walter Gilbert², referencing then-recent discoveries of catalytic activity in RNAs (dubbed ‘ribozymes’), including a letter referenced that was published in the preceding week’s issue which summarized those developments³. Gilbert proposed that “...if there are activities among these RNA enzymes, or ribozymes, that can catalyse [sic] the synthesis of a new RNA molecule from precursors and an RNA template, then there is no need for protein enzymes at the beginning of evolution. One can contemplate an *RNA world*, containing only RNA molecules that serve to catalyse [sic] the synthesis of themselves” (Gilbert 618, emphasis added). However, the initial explorations of the theme that would become the RNA World hypothesis date back to two similarly-themed papers published simultaneously in the *Journal of Molecular Biology* in 1968 by Leslie Orgel and Frank Crick^{4,5}. Orgel, in particular, posited that while (at the time) no nucleic acid with catalytic activity existed, that did not preclude the possibility, stating that it was “...quite possible that polynucleotide chains could make a primitive selection among organic molecules such as amino acids” (Orgel 1968, 387)⁴. Crick, also, was of the opinion that prebiotic life consisting of nucleic acids without proteins was at least possible: “It is thus not impossible to imagine that the primitive machinery had no protein at all and consisted entirely of RNA” (Crick 1968, 372)⁵.

But where did the organic molecules which would be necessary for RNA formation—or for that matter sugar and purine/pyrimidine base formation—come from? There has already been a great deal of speculation as to a ‘pre-RNA world’ where there were systems of nucleic acids which preceded RNA, including peptide nucleic acids or threose nucleic acids, as summarized by Orgel in a review in 2004⁶. Even if this were the case, this merely pushes the question of where the organic molecules come from further down the road into a ‘pre-RNA’ time rather than the RNA World. However, several possible theories exist for how organic molecules may have come into being on the prebiotic Earth. One theory, advocated by Wächtershäuser in 1988⁷, was that the first organic molecules were created near deep-sea vents, under high temperature conditions, and instead of being free-floating in solution, these early organic molecules, like formic acid, were bound and ‘grew’ on pyrite crystals, showing a potential exothermic reaction involving pyrite/iron, hydrogen sulfide, and carbon dioxide. A classic theory revolves around the Miller-Urey experiment, where the two scientists it is named for detected organic compounds, including amino acids, formed when a potential primitive reducing atmosphere of methane, ammonia, water and hydrogen was subjected to prolonged electric sparks meant to simulate lightning or other electrical discharges. (In 1959, the two reviewed their original findings and announced additional organic compounds had been detected, including glycine, alanine, aspartic and glutamic acid, urea, formic acid, and acetic acid⁸.) Still another theory, which can be found in several articles (most notably, if not as recently,

Chyba and Sagan's 1992 article in *Nature*⁹), suggests that organic carbon could have been delivered through accretion of interstellar dust, or by impacts by high-carbon-containing asteroids, and that organic compounds may have been synthesized (depending on the atmosphere of early Earth) through impact shock synthesis, electrostatic discharge, or ultraviolet irradiation.

The next step would be to find plausible prebiotic synthesis reactions for the three major compounds of ribonucleotides: purine and pyrimidine bases (adenine, cytosine, guanine, and uracil, or their derivatives), and a sugar (mainly ribose). Ribose synthesis can occur as a minor product of the Bulerow synthesis, as outlined in Orgel's review⁶, wherein formaldehyde self-polymerizes to form sugars (through the formation of glycoaldehyde and, later, glyceraldehydes). Purines have been shown to be synthesized through heating of formamide solutions, and in higher quantities when those solutions are irradiated with UV ($\lambda=254$ nm) radiation, including guanine and adenine¹⁰. Similarly, pyrimidines can be synthesized in prebiotic conditions; specifically, activated pyrimidine nucleotides can be synthesized without ribose at all, and with feedstock chemicals that could plausibly exist in prebiotic conditions, such as cyanoacetylene and cyanamide, glyco- and glyceraldehydes, and inorganic phosphate¹¹.

However, a drawback to these syntheses is that they are dependent on warm conditions, especially the purine synthesis described above. The 'warm and wet' model of the prebiotic origin of life is contrary to the requirement for the products of the synthesis, the organic compounds, to accumulate to sufficient

concentrations for reactions to form RNA to occur. This has been demonstrated in several papers. For instance, a paper in *PNAS* in 1995 by Larralde, Robertson, and Miller determined that the half-life of ribose was extremely short at 100°C and pH of 7.0 (73 minutes), and even at 0°C, short on geologic time scales (44 years)¹². Similarly, a 1998 paper showed that the ribonucleobases had similarly short half-lives at 100°C (ranging from 19 days for C to around 12 years for U), though the half-lives at 0°C are significantly larger ($\geq 10^6$ years for all except C, which is 17,000 years)¹³. Therefore under warm conditions, it is doubtful that ribonucleotides would be able to form.

RNA World and a cold origin of life

This leads to the concept of the 'cold origin' of the RNA World, where the early Earth was very cold and potentially covered by a thick layer of frozen ice over ocean. A cold origin would resolve the problem of hydrolysis of organic molecules, including sugars and the RNA bases, by shifting the equilibria of such processes away from hydrolysis (since, as Voet and Voet put it in their textbook, "...the rates of synthesis of these complex polymers would have had to be greater than their rates of hydrolysis...the 'pond' in which life arose may have been cold rather than warm, possibly even below 0°C...since hydrolysis reactions are greatly retarded at such low temperatures"¹ (Voet and Voet 32)). A *PNAS* paper by Bada *et al* in 1994 also provides support for a colder origin, as the Sun was less luminous at that time, giving a planetary ocean covered by an ice sheet which was hypothesized to be around 300 meters thick¹⁴. This was in the context of the likelihood of major impact events in the time frame of

the origin of life (~3.5-4 billion years ago) which would have locally melted the ice layer, allowing for exchange of gases and simple organic molecules between the ocean and the early atmosphere. Further, such a thick ice layer would have provided another benefit: "...[protecting] organic molecules dissolved in the unfrozen ocean below the ice layer from destruction by ultraviolet light"¹⁴ (Bada *et al* 1994, 1250).

Another potential synthetic method to form adenine was first described by Oro in 1961, through the polymerization of hydrogen cyanide¹⁵. A recent paper in 2002 by Miyakawa *et al* determined that the concentrations of HCN and its first catalytic product, formamide, would be too low in a warm primordial ocean for such polymerizations to occur (on the order of 10^{-13} to 10^{-15} M)¹⁶, suggesting that a cold origin would be more plausible. A second paper by Miyakawa *et al* reported a variety of ribonucleobases, both pyrimidines and purines, that were formed in a solution of ammonium chloride (formed by a mixture of gaseous hydrogen cyanide and ammonia) that was stored at -78°C for 27 years, including adenine, guanine, uracil, and other derivatives¹⁷. In a separate experiment published in the same article, Miyakawa showed that the adenine synthesis likely occurred under eutectic conditions by detecting adenine in a dilute ammonium cyanide solution held at -20°C for three months.¹⁷

Cold origin can also be supported for polymerization of RNA into oligomers. A 2003 paper in *JACS* by Monnard *et al*¹⁸ reported detecting RNA oligomers of varying length synthesized from activated ribonucleobases

(phosphoimidazolide-activated bases) with Mg^{2+} and Pb^{2+} in a concentrated, eutectic ice-water mixture held at $-18^{\circ}C$ for varying durations (up to 38 days). They reported that the synthesized products were "...at least 17 units long, with traces of longer products", and that "[the] ice eutectic synthetic conditions produced almost equimolar incorporation of each monomer"¹⁸ (Monnard *et al* 2003, 13738 and 13737). The implication of these results was made clear in a line from their paper: "Our working hypothesis is that the eutectic phases in ice concentrate, order, and preserve the activated nucleobases and products, allowing for a much more efficient polymerization to take place"¹⁸ (Monnard *et al* 2003, 13739).

Cold origin also does not prohibit RNA catalysis reactions. An article by Vlassov *et al*¹⁹ in 2005 dealt with a hairpin ribozyme from tobacco mosaic virus, which can ligate and cleave RNA strands. The ribozyme's rates of catalysis and ligation were monitored under various conditions, including at $37^{\circ}C$ in a Tris-HCl buffer and $MgCl_2$, and at $-10^{\circ}C$ with the same buffer except with NaCl instead. The results indicated that, while cleavage was dominant at the high temperature conditions, ligation dominated when the solution was in low-temperature conditions (though all reactivity stopped when the sample was cooled to $-20^{\circ}C$, presumably when the sample was frozen entirely). Vlassov indicated that at low temperatures and in the presence of monovalent cations (such as sodium), "...the ribozyme can effectively function in the absence of magnesium ions"¹⁹ (Vlassov *et al* 2005a, 208). The paper also showed that freezing enhances the catalytic activity through dehydration, as demonstrated

by improved ligation rates when in increasing percentage solutions of alcohols.

In a review of cold origin for the *Journal of Molecular Evolution* in 2005, Vlassov stated the best conditions for catalytic activity in a cold-origin scenario:

“...temperatures slightly below freezing, with fluctuations creating frequent cycles of freezing and melting...would result in dissociation and redistribution of primordial ribozyme and ligation substrates as well as in refolding of the ribozymes”²⁰ (Vlassov *et al* 2005b, 269).

RNA World and compartmentalization

Once the origin of organic molecules, the potential synthesis of ribonucleobases, and the potential synthesis of RNA oligomers and RNA catalytic activity (under the concept of cold origin) began, the next hurdle to the origin of life using the RNA World hypothesis is how to compartmentalize RNA molecules, catalytic products, and building blocks for synthesis in rudimentary ‘cells’. Such a process would be required, as described by Szostak *et al* in *Nature* in 2001, since there would be no impetus for ‘evolution’ to better and more efficient RNA molecules and ribozymes in solution: “...better replicases would replicate other RNA molecules more efficiently, but would have no advantage themselves, and would not increase in relative abundance”²¹ (Szostak *et al* 2001, 387). Another view towards the necessity of compartmentalization was stated in 2006 by Müller, focusing on why any small molecule synthesis would take place, as such synthesis “...is of evolutionary advantage to the respective catalysts and genome only if the metabolites are prevented from diffusing away”²² (Müller 2006, 1285). A rather more succinct

view was summarized in Orgel's 2004 review: "Molecules that stay together evolve together"⁶ (Orgel 2004, 117). While a cold origin might also be able to fulfill compartmentalization as eutectic ice-water mixtures will hold many small self-contained pockets of liquid water which will concentrate molecules and organic compounds, it is necessary to consider molecular methods of compartmentalization, from which primordial 'cells' could form.

It has been proposed that lipid bilayer membranes, just as they do in biological systems at present, served as the means through which compartmentalization took place in the RNA World hypothesis, since they "...fulfill all requirements...and because they are most relevant to biology"²² (Müller 2006, 1285). However, two arguments exist against this theory. First, as Müller himself admits, fatty acids are not stable enough in the same conditions that allow for ribozyme catalysis²². Second, as stated by Joyce in a 2002 paper on the evolution of the RNA World²³, "[the] notion of cellular compartmentalization should not be taken too literally...there are other ways to achieve the preferential association of an ensemble of compounds" (Joyce 2002, 219). One unique theory of non-lipid compartmentalization was provided in 2005 by Spirin²⁴ who claimed that colleagues of his had shown "...that RNA molecules can form *molecular colonies* on gels or other moist solid media when the conditions for their replication are provided" (Spirin 2005, 469, emphasis original), where RNA differentiation led to RNAs specializing in catalysis, genomic preservation, and acquiring needed substrates from the external environment.

Still, lipids form a starting point for the potential development of prebiotic membranes; a comprehensive review of the stability of lipid and other amphiphilic membranes and their implications for the origin of life can be found in *The Anatomical Record* in an article by Monnard and Deamer in 2002²⁵. Müller's paper, after admitting that pure lipid bilayer membranes would not be stable enough, provided an out for lipid membrane formation; "...incorporation of fatty acid alcohols stabilizes fatty acid vesicles against divalent cation precipitation"²² (Müller 2006, 1286). This could allow for amphiphilic 'cellular' membranes to form in prebiotic conditions, allowing for the compartmentalization of RNA sequences and ribozymes and the potential for diffusion of catalytic substrates and other desired small ions or molecules through the membrane. As RNA replication and catalytic activity progresses in such an early 'cell', the membrane will, according to Müller's theory, be compelled to grow due to osmotic pressure, absorbing neighboring vesicles and free-floating fatty acids²². Eventually, the 'cell' would divide, perhaps due to shear forces; in an article in *Nature* in 2001, Szostak *et al* suggested that this "...could lead to a primitive cell cycle controlled entirely by the biophysical properties of the membrane and environmental forces"²¹ (Szostak *et al* 2001, 389). One point that still has not been adequately addressed is how the RNA would incorporate the necessary genomic coding to ensure adequate cellular growth, as both the RNA replication cycle and the membrane growth/division cycle need to be in sync with each other, but once RNA control of membrane growth and structure could be established, this would "...facilitate growth of the

membrane compartment...to alter and control the properties of the vesicle membrane"²¹ (Szostak *et al* 2001, 389).

Evolving beyond the RNA World

Once this point in the development of 'life' consisting of replicating (and evolving) RNA inside of some form of membrane for compartmentalization was reached, Orgel surmised, "...everything that followed [was] in the realm of natural selection"⁶ (Orgel 2004, 100). This included the eventual end of the RNA World and its transition to the DNA/RNA/protein world that is the basis of all life today. The question, then, is how could the RNA World have transitioned to the DNA/protein world? Joyce's 2002 review suggests that such an evolution was necessary, as RNA was not the ideal molecule for adapting to changing environmental conditions, and therefore it would be necessary to develop "...a separate macromolecule that would be responsible for most catalytic functions, even though that molecule contained subunits that were poorly suited for replication"²³ (Joyce 2002, 219). Since RNA is capable of protein synthesis, it would not be hard to imagine RNAs synthesizing proteins with higher catalytic rates than it itself could achieve through ribozymes. This would, however, inevitably lead to RNA being supplanted for catalysis and other enzymatic reactions by the better-suited proteins. Indeed, as Joyce put it, "The invention of protein synthesis...was the crowning achievement of the RNA world, but also began its demise"²³ (Joyce 2002, 219).

With catalytic function no longer a necessary feature for RNA, leaving it with solely the function of preserving and replicating the genetic code for

procreation, natural selection would then tend to promote the best material that would help to preserve and replicate the genetic information most effectively. While RNA had the advantage of being able to be synthesized (hypothetically) in prebiotic environments, its structure was less stable than other potential nucleic acids, such as DNA. Joyce theorizes that DNA may have started as a backup 'failsafe' where RNA was reverse-transcribed to DNA, "...then read back to RNA by a DNA-dependent RNA polymerase. Eventually the DNA molecules became the objects of replication"²³ (Joyce 2002, 220). With DNA becoming the basis for genetic replication, the transition was complete: "The lower reactivity but greater stability of DNA makes it a better choice for the genetic material, whereas the greater chemical diversity of the subunits of proteins...makes protein a better choice as the basis of catalytic function"²³ (Joyce 2002, 220). While RNA's dual ability to both serve as genetic code and enzyme via the ribozyme made it quite useful in prebiotic conditions, Müller argues that "[from] our biological perspective, the rise of a DNA/protein world over the RNA world may seem inevitable"²² (Müller 2006, 1289).

Cold origin of life: when?

The last question, then, is less one of 'how?' and more a question of 'when?'. Orgel, in his 2004 review, stated towards the beginning that "...the problem of the origin of life is the problem of the origin of the RNA World..."⁶ (Orgel 2004, 100). Therefore, the origin of the RNA World is necessarily the origin of life on Earth. While the earliest known fossils of life are about 3.5 billion years old¹, and it is generally accepted that life could not have formed in

the first couple hundred million years after the formation of the Earth, there is a broad range of when the RNA World could have arisen. Joyce, for his part, gave a range in his review of the RNA World of between 4.2 and 3.6 billion years ago²³, while Orgel, in an earlier 1998 paper for *Trends in Biochemical Sciences* suggests "...a window of a few hundred million years that opened about four billion years ago"²⁶ (Orgel 1998, 491). A 1998 paper by Lazcano and Miller seems to suggest a smaller time frame of origin of 300 million years, between 3.8 and 3.5 billion years ago²⁷. Further, they suggest that life developed very quickly: "...there is no reason to assume that the self-organization of prebiotic compounds into a system capable of undergoing Darwinian evolution involved extended periods of time. We envision a maximum upper limit of 5×10^6 years"²⁷ (Lazcano and Miller 1998, 796). A paper published in 2002 in *Geology* makes a suggestion that liquid water oceans were present at even earlier times than that, between 4.4 and 4.0 billion years ago²⁸, but the possibility that life formed in that time is offset by the existence of a late heavy bombardment which likely sterilized any life that might have formed.

The intriguing nature of how the RNA World may have been synchronous with the origins of life ensure that, over 40 years since the Crick and Orgel papers^{4,5} which began the theorization of a pre-DNA life, and nearly 25 years since the Gilbert letter stating the term 'RNA world'², there is still much to be learned about this theory and the conditions of early Earth that might make it more or less plausible, specifically the 'cold origin' RNA World. Indeed, a recent paper in the online-only journal *Nature Communications*²⁹ suggests

that not only would eutectic ice channels in ice be viable for RNA synthesis and catalytic activity, but that (for certain ribozymes which most model the likely prebiotic RNA structures) catalysis was increased in frozen conditions. The paper also suggests that catalytic activity was also dependent on ions (which conveniently follow the Hofmeister series) and that ice allowed for higher-fidelity RNA replication.

Conclusion

While, to rephrase the initial quote of this paper from Voet and Voet, we will never know with certainty how life developed, as there is no evidence or fossil record to show which theory or hypothesis was correct, it seems plausible that the RNA World hypothesis could have been the origin of prebiotic life on Earth. Even with the apparent necessity for a cold origin, the plausible prebiotic synthesis of RNA precursors and bases, coupled with the advantages of synthesis, catalytic function, and compartmentalization provided by a cold/frozen origin, and the prospect of natural selection driving the genesis of proteins and DNA, the RNA World hypothesis is an intriguing concept that deserves attention.

The RNA World hypothesis is intriguing for this present work due to the possibility, if correct, that life on Earth formed in a colder origin than previously thought, and which would encourage the development of organisms and strategies for protection against that cold, anoxic environment. Also intriguing is the 'evolutionary' aspect of the RNA World: that as RNA may have 'evolved' into DNA and proteins as an adaptive strategy for better synthesis and more

reliable genetic replication, so too can, and have, bacteria and other organisms proven that they can adapt to environments that would otherwise be hostile to unadapted life. The next section of the introduction deals with the different extremes of conditions that bacterial life has evolved to survive within.

CHAPTER 2: EXTREMOPHILIC ORGANISMS

Introduction

The diversity of life is astounding, driven by the need for adaptation to the particular climate that the organism is in and the filling of different niches. That life, in all of its forms, has adapted to survive and thrive in all of the varied ecosystems of Earth is a testament to evolutionary pressure and the idea that life will find a way to survive harsh conditions. However, for many years there were some areas of our planet that, even with such diversity of life, were believed inhospitable to any organisms. The Dead Sea, for instance, was named such owing to its high salinity and lack of marine life such as fish; there are many large vast deserts which, at initial glance, seem utterly barren; and the polar regions were thought sterile due to the permanent sub-freezing temperatures. Modern science has, however, shown that even in these desolate regions bacteria are able to survive—and not just in those areas, but also against much more extreme conditions, such as thousands of meters underwater or underground, in extremely hot or cold or desiccated environments, and others. These organisms are generally referred to, as a class, as *extremophiles*—organisms that not only tolerate but can grow and thrive in ‘extreme’ conditions.

Extremophiles: definitions and significance

‘Extreme’ is a relative term that requires further definition for a proper assessment of extremophilic bacteria. One well-worded way to define it is described as follows: “By extreme conditions we mean those which are far from

the normal conditions used to describe the origins of physiological biochemistry...these kinds of extreme microbial growth conditions are found in exotic environments which appear limited today but which were thought to be much more widespread on primitive Earth”¹ (Lowe *et al* 1993, 453). What may be considered ‘extreme’ for human life, or life for the majority of higher organisms, has become (through adaptation and evolution) suited to bacterial life. Canganella and Wiegel in *Naturwissenschaften*² state this point thusly: “Any environment is likely to contain living organisms—one just has to know how to recognize their presence” (Canganella and Wiegel 2011, 254). Thus as more of the Earth has become accessible for exploration, and as scientific techniques for isolation, identification, and culturing bacteria have improved, we have found novel bacterial adaptations to a wide variety of conditions—extremes of temperature, of pH, of affinity for saline or metallic environments, or of resistance to harmful conditions such as pressure or radiation.

Extremophiles are of importance to science both due to the potential biological and biotechnological applications^{1,2} but also with respect to astrobiological applications. For instance, the evidence of water (in some state) on several bodies in the Solar System, such as the Jovian moon Europa³, the Saturnian moon Enceladus^{4,5}, and the planet Mars^{6,7} provides impetus for study of cold-adapted (psychrophilic) bacteria, while others suggest that, in addition, study of sulfur-dependent or acidophilic microorganisms may be fruitful due to the abundant tectonic and volcanic activity on the Jovian moons and evidence of ancient volcanic activity on Venus and Mars⁸. In this section I shall briefly

describe several different types of extremophiles and provide examples of species for each, to demonstrate the variety of adaptations that bacteria have undergone to fill in specific 'extreme' niches.

Psychrophiles

One of the first review papers on psychrophilic bacteria used a definition that psychrophiles were "...organisms having an optimal temperature for growth at about 15°C or lower, a maximal temperature for growth at about 20°C, and a minimal temperature for growth at 0°C or below"⁹ (Morita 1975, 144).

Psychrophilic bacteria, then, would be expected to be found across the globe, given the large parts of the planet (in the Arctic/Antarctic and in most of the ocean water) are near or below 0°C¹⁰. These conditions provide several problems with biological function, including the freezing of the cytoplasm, loss of flexibility of the lipid membranes, and other conditions; some psychrophilic bacteria have adapted to these problems through increased unsaturated lipids, production of antifreeze proteins and cryoprotectants, and enzymes which are adapted to have increased activity at cold temperatures when compared to moderate-temperature-tolerant (mesophilic) bacteria¹¹.

There are a diverse number of psychrophilic bacteria; the first such bacteria to have its genome sequenced was *Colwellia psychrerythraea*¹².

Psychrophilic species also exist that are methanogens, such as *Methanogenium frigidum*, which was isolated from Antarctica¹³. It is suggested that there are much larger numbers of psychrophilic Gram-negative bacteria, and in more diverse genera, than there are of Gram-positive psychrophiles².

Psychrophilic and psychrotolerant bacteria can survive and be metabolically active in different environments. One possible environment to enable bacterial survival in cold conditions is for bacteria to be present in eutectic water:ice channels in sea ice, either free-floating in the channels or adhered to particles trapped in the ice, and observed to be metabolically active down to -20°C ¹⁴; these results were expanded upon through study of tritium-labeled leucine uptake in chilled/frozen artificial sea water¹⁵. Another environment is in subglacial lakes, where the pressure of the glaciers has created pockets and lakes of liquid water, such as beneath Lake Vostok^{16,17} or other large ice sheets in Antarctica¹⁸. One paper, measuring CO_2 emission rates of permafrost soil, suggested that biologically-generated CO_2 (indicative of metabolic activity) is produced at temperatures as low as -39°C ¹⁹.

Thermophiles

Traditional definitions of thermophilic bacteria were those having optimal temperature for growth between 45 and 80°C ; however, with the characterization of bacteria that can, in some cases, have optimum or even minimal growth temperatures at or above 90°C ²⁰, a division of thermophiles into hyperthermophiles ($T_{\text{opt}} \geq 80^{\circ}\text{C}$), extreme thermophiles (70 - 80°C), and moderate thermophiles (45 - 70°C) has been suggested². These bacteria can be found in both terrestrial environments, such as volcanic hot springs²⁰ or in subterranean environments²¹, or in marine settings, most commonly associated with hydrothermal vents on the ocean floor²⁰. Thermophilic bacteria are

diverse, such bacteria being found in a variety of genera, including *Bacillus*, *Clostridium*, *Thermus*, and other bacterial genera²².

Thermus thermophilus is being analyzed with a view towards it being used as a laboratory standard thermophilic strain, with a recent paper showing it can be used with plasmids for genetic manipulation; the well-known properties of *Thermus* bacteria in their thermophilic growth temperatures and no need for specific amino acids or vitamins in media being advantages in laboratory cultivation²³. *Thermus thermophilus* is considered a “model system” for the study of natural transformation of genes with other thermophilic species due to being found in habitats with other thermophilic bacteria and archaea²⁴ (Averhoff and Müller 2010, 510). Other thermophilic and hyperthermophilic species can exhibit higher T_{opt} or T_{max} ; for instance, some bacteria isolated from marine hydrothermal vents, such as *Pyrococcus furiosus*, have a T_{opt} of 100°C and a T_{max} of 105°C²⁰; these temperatures can be reached due to the increased atmospheric pressure in deep ocean vents, such as for *M.kandleri* with a T_{max} reported at 122°C². Many *Bacillus*, *Thermus*, and *Clostridium* species are moderate thermophiles².

The practical importance of thermophiles is from the enzymes and proteins they carry. Thermophilic enzymes and proteins, while being thermostable, are more rigid as a result and easier to crystallize²². In addition to their thermostability, they can also exhibit resistance to chemical denaturation²². Perhaps the most important enzyme isolated from thermophilic bacteria is the DNA polymerase enzyme from *Thermus aquaticus*, whose high

thermal stability allowed for more rapid genetic amplification through polymerase chain reaction (PCR) techniques. As a review from 1990 indicates, “[t]he single most important development has been the purification and commercial distribution of a heat-resistant DNA polymerase from the thermophilic bacteria *Thermus aquaticus* (*Taq*)”²⁵ (Gibbs 1990, 1203). Another interest is in the possibility that thermophilic bacteria may have been the first life on the planet², with their putative ancient origin one explanation for their small genomes (the other being the possible difficulties in high-temperature DNA replication)²³. Some industries’ work in identification and characteristics of thermophilic and thermotolerant bacteria is related to the risk of food contamination, for instance the possibility of thermotolerant/thermophilic bacilli to either survive Pasteurization or to form biofilms inside of milk and dairy processing equipment²⁶.

Halophiles

Halophilic bacteria, as with the thermophilic and psychrophilic bacteria, can generally be divided between those that are simply tolerant of higher than physiological salt levels, and true obligate halophiles that require higher levels of salt to grow. A reasonable definition that has been given is that obligate halophiles require $\geq 3.0\%$ w/v NaCl in solution for growth². Other definitions determine halophilicity by the molarity of NaCl that the organism is able to grow in, with halophilic bacteria growing best above 0.2M NaCl (with moderate halophiles best between 0.5 and 2.5M and extreme halophiles above 2.5M and up to saturated NaCl solutions)²⁷. It is interesting that most extreme halophiles

are not bacteria, but archaea, while the majority of moderate halophiles are in bacterial genera²⁷.

The challenge of high salt content is the regulation of osmotic pressure, which generally occurs either by allowing cytoplasmic salt concentration to equalize with the extracellular concentration, or the synthesis of molecules that can replace salts in cytoplasmic solution and which do not interfere with the cellular metabolism, such as sugars or amino acids²⁴. It is suggested that extremely halophilic bacteria may have evolved for the former option, which is "...energetically cheaper...[but] requires extensive adaptations of the intracellular machinery, and these can be achieved only in a long and complex evolutionary process"⁸ (Pikuta *et al* 2007, 193). Most halophiles require active control of sodium content, as it is necessary for (for example) ATP synthesis but excessive amounts of sodium in the cytoplasm can be toxic²; however, some species have different requirements, such as *Halobacillus halophilus* which depends on Cl⁻ exclusively for growth²⁴. An additional adaptation strategy occurs through reduction of hydrophobic interactions in proteins to counteract the increase in those interactions in halophiles which adapt the 'salt-in' strategy of having high cytoplasmic salinity²⁸.

Halophilic bacteria can also provide potential biotechnological applications. While the study of these has progressed slower than the study of similar applications from halophilic archaea (notably *Halobacterium* sp.), there are some notable examples, such as the possibility for the production of plastic-like extracellular polysaccharides^{27,29}. In addition, halophilic archaea and some

bacteria are able to produce and store the class of polyester compounds known as polyhydroxyalkanoates, which are biocompatible and easily recovered from lysed halophilic cells; however, no attempts have been yet made on production or use of these biopolymers on any commercial or industrial scale^{27,29}.

Radiation resistance

While there are no bacteria that require radiation for growth, there are known species that are able to tolerate and survive high levels of radiation. The most prominent of those are part of the *Deinococcus* genus, chief among those being the first to be identified, *Deinococcus radiodurans*, which is able to resist high levels of ionizing radiation and repair double-strand breaks in its DNA without any observed lethality up to and in some cases beyond 5,000 Gy^{30,31} (1 Gy = 1 J ionizing radiation/kg of matter). This genus contains 20 species, while some species in other genera exhibit radiation resistance, including *Acinetobacter*, *Hymenobacter*, *Kineococcus*, *Kocuria*, *Methylobacterium*, *Thermococcus*, and *Pyrococcus* species⁸. These species, unlike the method of radiation resistance found in spore-forming (*Firmicutes*) bacteria in forming the endospore and becoming dormant, are able to highly resist ionizing radiation and repair DNA damage, including double-strand breaks, while remaining viable vegetative cells².

The mechanisms in which a species such as *Deinococcus radiodurans* can resist ordinarily lethal radiation levels are not clear, but research has identified several avenues that it has at its disposal for that purpose. One recent article suggests that an increased concentration of manganese cations in

the cytosol of *D.radiodurans* is a likely possibility, as it is less likely than other cations such as Fe^{2+} to react with peroxides formed from radiolysis of water to form reactive oxygen species and free radicals³⁰. Other described possibilities involve a high number of duplicate sets of DNA/chromosomes (high ploidy), since *D.radiodurans* has never been reported to have less than four genome copies; tight coiled nucleoids which limit ionizing radiation damage; and the possibility that the DNA in *D.radiodurans* is sterically prevented from separating after a double-strand break so that the repair of the lesion is essentially already templated³². Some have speculated that there is a correlation between radiation resistance and desiccating environments, as some species of *Deinococcus* have been isolated from desert environments^{2,22}; other extremophilic bacteria, such as *Pyrococcus furiosus*, have also been found to have moderate levels of ionizing radiation resistance³⁰.

Piezophiles/Barophiles

Pressure-tolerant or pressure-requiring bacteria are not as well-defined in the terminology as other extremophiles, with piezophile and barophile seemingly used interchangeably to define the same types of organisms. Some definitions of piezophilic or barophilic bacteria simply require optimal growth at a pressure greater than atmospheric ($\sim 0.1 \text{ MPa}$)^{33,34}; others require the optimal growth to be at or above certain higher pressures, such as 40 MPa ^{8,32}. Most all known piezophiles are deep-sea bacteria owing to the high pressures of marine trenches and the depths of the oceans (with pressures as high as 110 MPa in the Marianas Trench²); the vast majority of piezophiles are from the *Shewanella*

and *Moritella* genera, with other species in the *Colwellia*, *Psychromonas*, and *Photobacterium* genera³⁴. Many piezophiles are also psychrophiles, as the ocean temperatures are generally quite low at those depths, but some are thermophiles as well through adaptation to conditions near hydrothermal vents².

High pressures have many effects on bacteria. Lipid membranes, as in cold-temperature conditions, become less flexible and more impermeable; protein conformational changes and difficulty in DNA transcription become apparent³⁶. Motility also becomes impaired as pressure increases, and pressure induces upregulation of both heat- and cold-shock proteins³³. Piezophiles adapt to these changes through many methods, such as increasing unsaturation of fatty acids in the lipid bilayer^{33,37}; in addition, upregulation of certain genes at increased pressures may produce 'chaperones' that aid protein folding and enzyme function at higher pressures, mainly in piezotolerant organisms³⁶. While the applications of piezophilic adaptations such as these are not as well-known or studied as, perhaps, the thermo-/psychrophilic bacteria, continued study of these adaptations may prove fruitful at some point, given the known effects of high pressure on selective gene expression and protein function³⁸.

Acidophiles and alkaliphiles

Bacteria can also adapt themselves to different pH environments. Bacteria have been found that can grow and tolerate extremely acidic and fairly alkaline environments. Acidic environments are associated with high metal contents, usually from mine runoff³⁹ and can vary wildly depending on their

energy source, whether autotrophic (as in *Acidithiobacillus ferrooxidans*), heterotrophic (*Ferromicrobium acidophilus*), or 'mixotrophic', that is, able to operate in either regime, mainly the domain of sulfur-using bacteria². (Bacteria are, of course, not the only living organisms to be adapted to acidic environments; algae, fungi, and archaea have all been found that are able to grow near pH of 0²² with two particular archaea, *Picrophilus oshimae* and *Picrophilus torridus*, able to tolerate pH -0.2⁸.) Most acidophilic bacteria have pH values in their cytoplasm closer to neutral than their external environments, indicating adaptation to reduce proton influx and actively transport excessive protons out of the cytoplasm². Enzymes from acidophiles have been used in several industries, such as in desulfurization of coal, starch processing, and feedstock production⁸.

Alkaline environments, such as soda lakes, are present on Earth, and mainly consist of cyanobacteria⁸ though alkaliphilic bacteria are present in most bacterial orders^{2,40}; they typically require high levels of Na⁺ similar to that of halophiles² but must contend with low levels of H⁺, which can constrain ATP synthesis²². This is overcome through increased acidic polymers in the cell wall and the peptidoglycan producing a negative charge to repel cations and reduce the pH on the cell surface and antiporters to remove excess sodium cations while concentrating protons in the cytoplasm⁴⁰. Alkaliphiles are useful to industry in the enzymes they are able to produce, such as catalases and proteases, that are stable at high pH and used in detergents and other cleaning solutions^{40,41}.

Conclusion

Everything above, while merely a brief summary of a few categories of extremophiles (not having mentioned bacteria adapted to high metal concentrations or low-moisture environments, such as a novel bacteria found in the hyperarid Atacama Desert of Peru that tolerates and oxidizes arsenic, for instance⁴²), and having mainly confined these to bacteria rather than archaea, fungi, and other microorganisms, shows the adaptability of bacteria to varied and harsh climates and environments. Adaptation has proven to be one viable method of survival for these particular species. However, it is not the only method of survival. As my research work and background in the main chapters of this dissertation will show, some bacteria take a different tack towards survival of extreme conditions, in the form of sporulation.

CHAPTER 3: RHODAMINE-B FLUORESCENCE STUDIES OF POLY(ADENYLIC) ACID, A POTENTIAL CRYOPROTECTANT, IN RELATION TO LIPOTEICHOIC ACID

Introduction

There are many organisms, micro- and macro-, that have adapted to survive in extreme conditions¹, especially in extreme cold conditions². There are some larger organisms that are able to survive in cold environments, for example the Himalayan snow midge, which at the time of its discovery was the coldest insect species to show activity³. Also, evidence of bacterial metabolic activity has been found at temperatures as low as -20°C ⁴. These conditions frequently require either conditions that ensure the presence of liquid water in some form, such as high saline or brine concentrations⁵ or other physical forces providing liquid water such as ice-mineral boundary layer interactions⁶, or the presence of antifreeze proteins or other extrapolymeric substances in the organism⁷.

Such cryoprotecting agents could have many applications, such as better methods of food preservation by reducing freezing damage, and other methods⁸. A relatively recent review indicates 'antifreeze proteins' (AFPs), called varying terms other than that, have been found in numerous types of fish, plants, insects, and bacteria; the methods these proteins use for cryoprotection were explained and potential applications for food preservation, cryoprotection of proteins, embryos, and living tissue, and cryosurgery were described⁹. As

such identifying other biomolecules that possess some sort of cryoprotectant effect is of importance.

Structure and function of teichoic acids

Teichoic acid (TA) is a polymeric macromolecule that is found in the cell walls of Gram-positive bacteria in association with the lipid bilayer membrane and the cell wall peptidoglycan¹⁰. The general structure of teichoic acid is a polyglycerol- or polyribitol-phosphate repeating backbone with side chains which vary according to the species of bacteria; they are further differentiated by whether they contain lipid tails to interact with the lipid bilayer membrane (lipoteichoic acid, LTA) or are covalently bound to the cell wall peptidoglycan (wall teichoic acid, WTA)^{10,11}. The existence of teichoic acids has only been known for less than sixty years^{12,13} but their functions are varied.

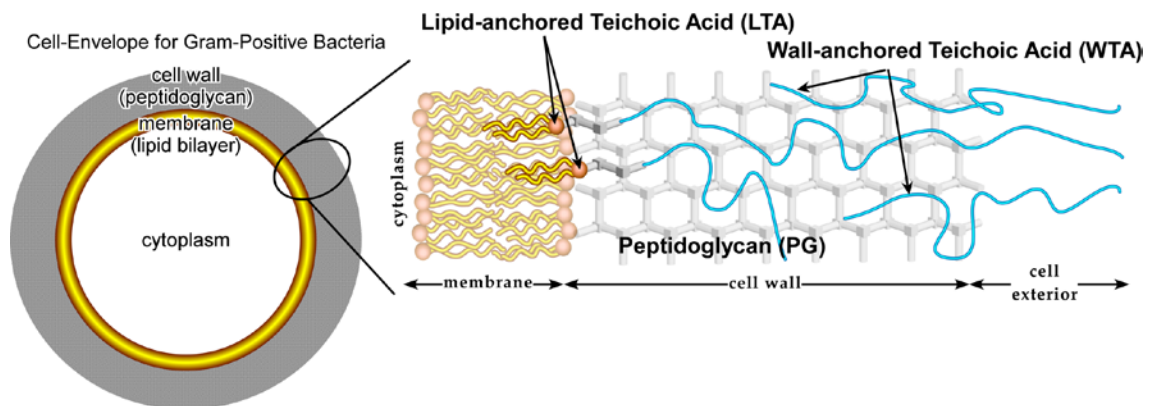


Figure 3.1. Teichoic acids are classified by where they are attached in the Gram-positive cell: to the peptidoglycan for WTA, or to the lipid bilayer membrane for LTA. Figure 1 from ref 21, reprinted with permission.

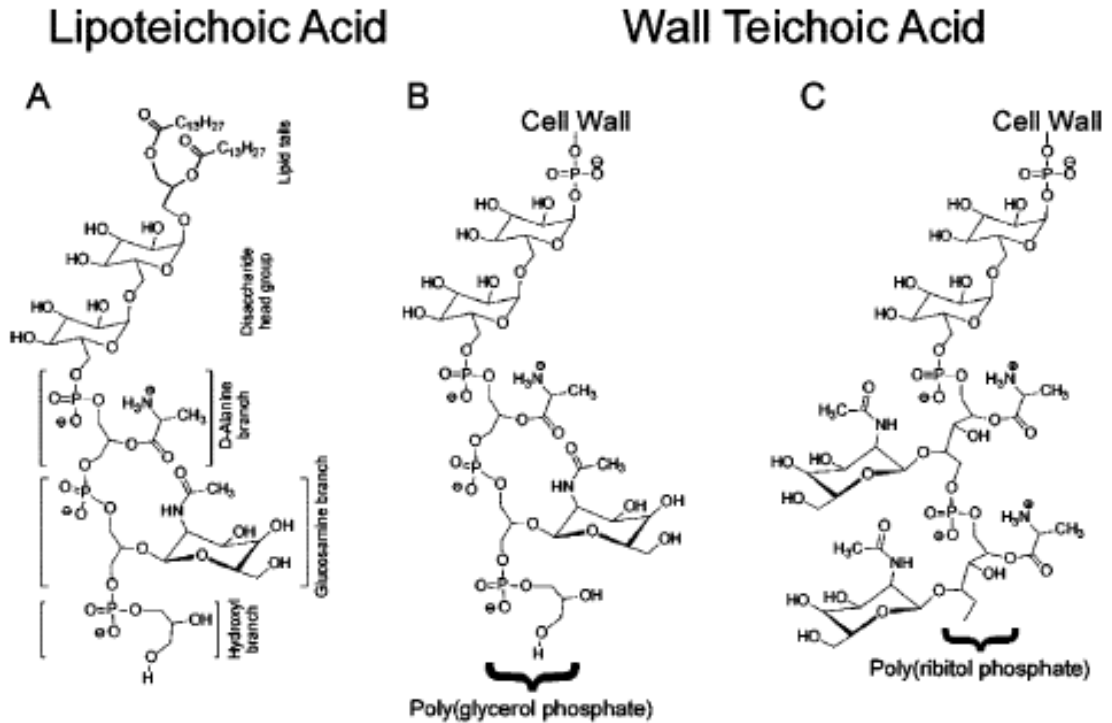


Figure 3.2. Lipoteichoic acid, left, has a polyglycerol phosphate backbone (A), whereas wall teichoic acids can have either polyglycerol phosphate (B) or polyribitol phosphate (C) depending on the bacteria. Figure 1 from ref 20, reprinted with permission.

Teichoic acids are necessary for cell growth and division; while viable deletion mutants without LTA¹¹ or WTA³⁵ exist, loss of both LTA and WTA was fatal in *B.subtilis*¹¹. LTA in particular has been associated with immune system response and cytokine induction¹⁴⁻¹⁹. Teichoic acids are also implicated as being essential for metal binding and transport into the cell, primarily in a bidentate fashion²⁰, and teichoic acids with D-alanine moieties are also involved in giving a partial positive charge to the cell wall facilitating repulsion of cationic antimicrobial peptides (cAMPs)^{21,22}. LTA has been considered as a similar molecule to the Gram-negative lipopolysaccharide (LPS) in its nature as a

virulence factor and immunostimulatory agent²³. Teichoic acids are also associated with biofilm formation and bacterial adhesion²³⁻²⁵.

In the course of solid-state NMR experiments to determine the metal binding mechanisms of teichoic acids^{20,21,25}, it was discovered that pure LTA from *Staphylococcus aureus*, when dissolved in deuterium oxide and run on a ³¹P CPMAS ssNMR instrument with variable-temperature (VT) capabilities, that the characteristic phosphorus chemical shift anisotropy (CSA) tensor does not appear until below -40°C²⁶. This is indicative of there being sufficient molecular motion to prevent cross-polarization from occurring, and therefore of the likely presence of liquid water even at temperatures much below freezing. Similar experiments with bound cell wall peptidoglycan and wall teichoic acid showed ³¹P signals not present until -20°C, indicating that the antifreeze potential is reduced but not removed by the teichoic acids being bound in the peptidoglycan.

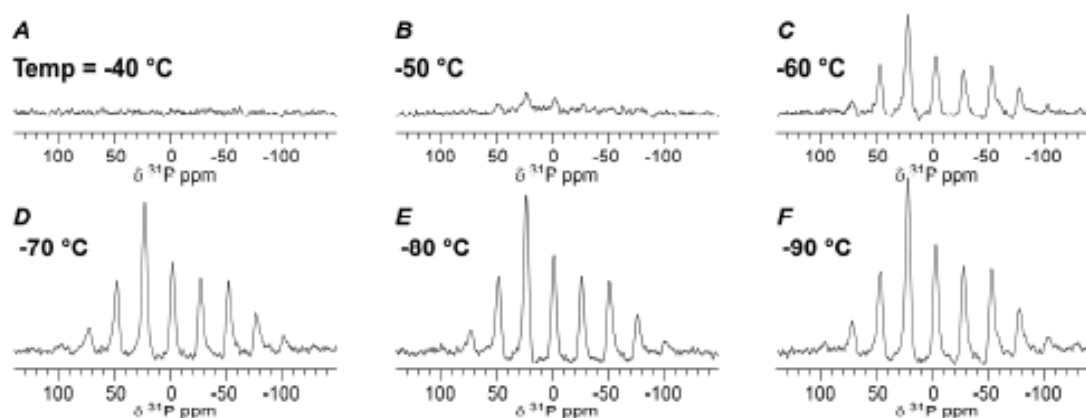


Figure 3.3. This sequence of ³¹P CPMAS spectra of LTA (*S.aureus*) dissolved in D₂O shows a total lack of phosphorus signal at -40°C and only minimal signal at -50°C, indicative of the presence of liquid water. Figure 2 from reference 26, reprinted with permission.

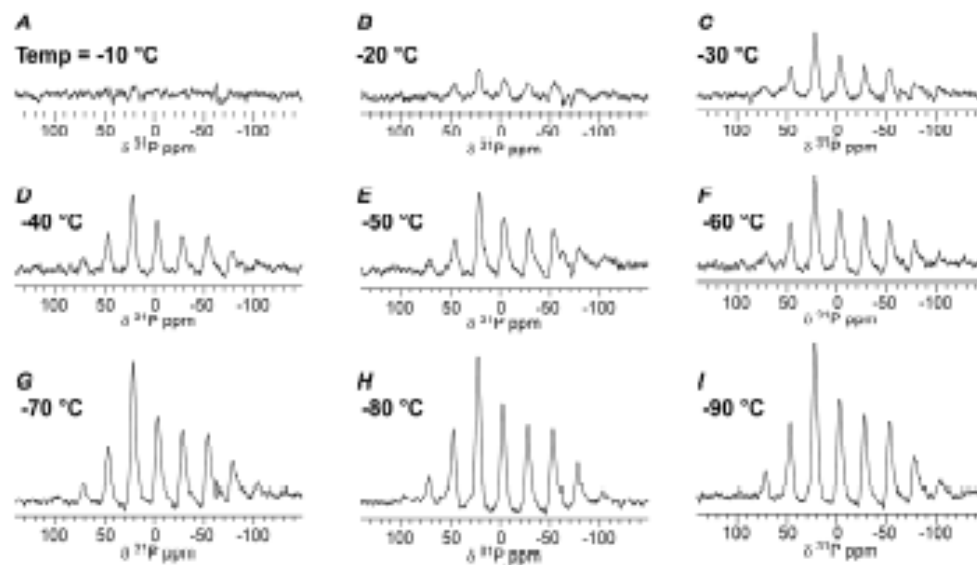


Figure 3.4. In contrast the VT spectra of bulk cell wall (peptidoglycan with teichoic acid) only protects liquid water down to between -10°C and -20°C via phosphorus CPMAS. Figure 4 from reference 26, reprinted with permission.

These results seemed to suggest that teichoic acids, and lipoteichoic acid in particular, may be cryoprotectants. To further study this, additional experiments were necessary. These experiments would both verify the NMR data as well as examine structural aspects of why teichoic acids would exhibit cryoprotectant effects. These experiments would be based on the interactions of teichoic acids and other molecules on the fluorescence behavior of rhodamine-B dye at room temperature and sub-freezing temperatures.

Principles of fluorescence; structure and function of rhodamine B

Fluorescence and phosphorescence are spectroscopic properties of some molecules for the relaxation of those molecules from an excited state to a lower energy excited state or the molecule's ground electronic energy state via radiative processes²⁷. Fluorescence is attributed to relaxation in the same state

(the singlet state, S); phosphorescence is attributed to the excited molecule undergoing conversion to a different state (the triplet state, T) before relaxation²⁸. These conversions can be described through the use of a Jablonski diagram to illustrate the various pathways of excitation and emission or decay of the excited states of the molecule. Fluorescence and phosphorescence are not novel phenomena, although until the 19th century the terminology of fluorescence and phosphorescence had not been developed²⁹.

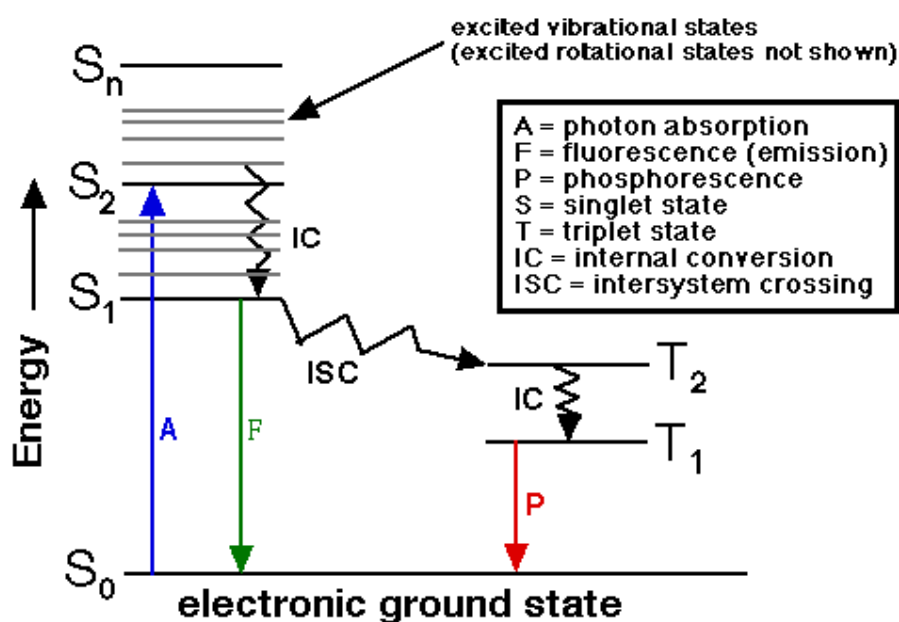


Figure 3.5. A Jablonski diagram showing the different electronic and vibrational states, and the pathways for fluorescence and phosphorescence (nonradiative decay pathways are not shown).

Rhodamine B is a fluorescent dye belonging to a class of dye molecules with structures based on xanthene³⁰. Rhodamine B (and the rhodamines in general) have been used as laser dyes^{31,32}. From the conjugated structure it is obvious why rhodamine B is a fluorescent dye.

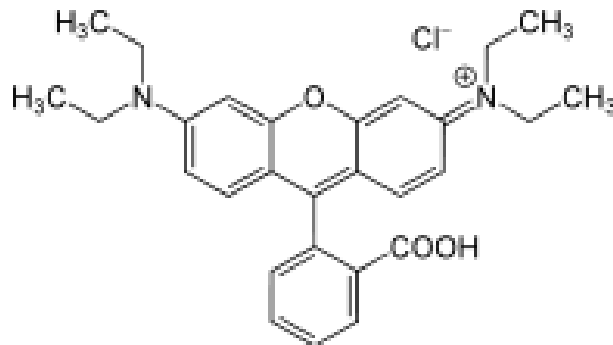


Figure 3.6. Structure of Rhodamine B, as the cation, with Cl⁻ counterion.

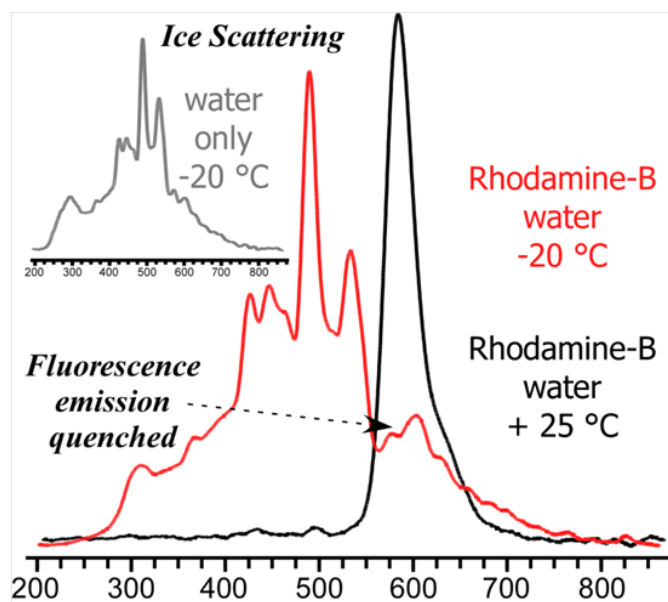


Figure 3.7. Rhodamine B's fluorescence emission is evident in a water solution at room temperature conditions but is quenched (with the appearance of spectral features related to ice scattering) at -20°C . Rice Lab, unpublished data.

When a solution of rhodamine B is frozen, the fluorescence of the dye is quenched, as observed in Figure 3.7; this is suggested to be a result of the freezing causing the dye to preferentially undergo intersystem crossing to the triplet state and undergoing phosphorescence rather than fluorescence. In addition, the fluorescence spectrum shows many broad peaks as opposed to a single peak for the rhodamine B due to the source light being scattered by ice

crystals diffracting the light. However, when a rhodamine B dye solution was doped with a 5% LTA solution, the fluorescence remained apparent at sub-freezing temperatures; other adulterants such as DNA and NaCl did not provide such an effect, as seen below in Figure 3.8.

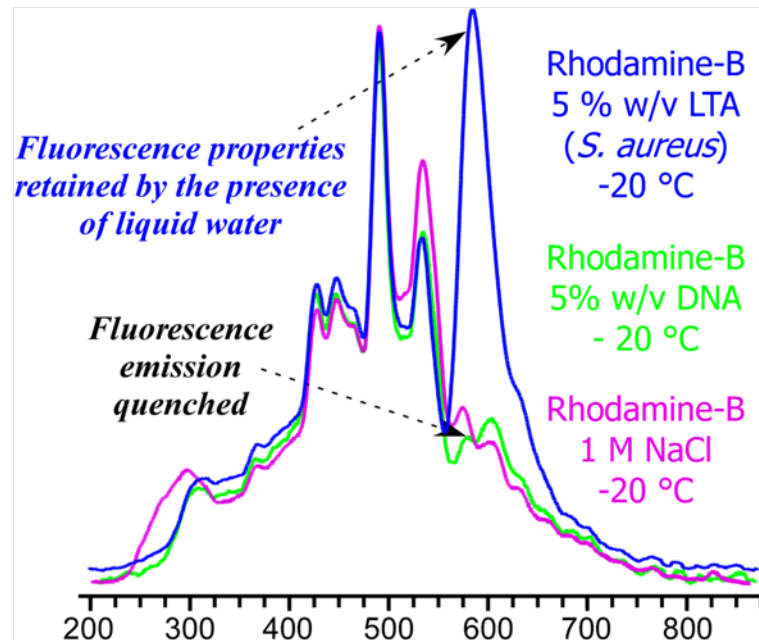
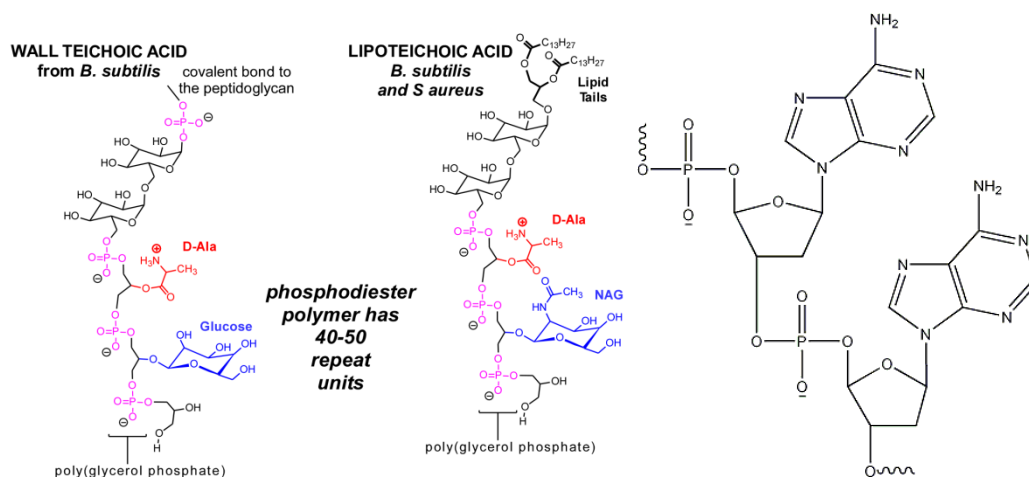


Figure 3.8. At -20°C, rhodamine B fluorescence is quenched even with the addition of 1M NaCl or 5% w/v DNA solution, but is maintained after addition of 5% w/v LTA solution. Rice Lab, unpublished data.

It was hypothesized that other biological molecules with similar backbone structures as lipoteichoic acid may have cryoprotectant effects as determined by fluorescence spectroscopy, i.e. that the cryoprotectant effect is structure-based. One such molecule is polyadenylic acid (poly(A)), a poly-ribonucleotide with a phosphodiester backbone similar to the backbone of lipoteichoic acid. (It was thought that perhaps, since poly(A) is itself fluorescent³³, that the use of

rhodamine B would not be necessary, but the emission wavelength of fluorescence of poly(A) was below the range of the instrument being used.)



Figures 3.9 and 3.10. Figure 3.9, left, shows structures of *B. subtilis* WTA and LTA (figure 2 from ref 21, reprinted with permission); Figure 3.10, right, is a structure of polyadenylic acid. The similar backbones led to the idea that poly(A) might possess similar liquid-water preservation properties under fluorescence spectroscopy.

In order to test this theory, the experimental procedure that was performed previously in the Rice Group for the fluorescence spectroscopy of rhodamine B solution, doped with various chemicals, was used for the tests with polyadenylic acid.

Experimental Procedure

Rhodamine B (Sigma-Aldrich, St. Louis, MO, USA) was dissolved in Milli-Q doubly-distilled water to a concentration of 1.0×10^{-4} M. 25 mg of polyadenylic acid potassium salt (Poly(A), Sigma-Aldrich, P9403) was dissolved with 500 μ L of distilled water to form a 5% w/v solution. Solutions were held in borosilicate tubes (4mm ID, 4cm length) capped with rubber stoppers.

Fluorescence measurements were made using an Ocean Optics USB2000-FLG fluorescence spectrometer hooked up via fiber-optic cables to

the side of a Quantum Northwest TLC50 cuvette holder perpendicular to the entrance of the light source, an Ocean Optics PX-2 xenon arc lamp. The cuvette holder was hooked up to a Quantum Northwest TC-125 temperature controller to set and hold the temperature of the cuvette holder, and had tubing connecting it to a Neslab Endocal RTE-110 water pump filled with a 1:1 mixture of water and ethylene glycol to serve as the chilling fluid. The cuvette holder had an adapter allowing for use of the borosilicate tubes, which were smaller than standard cuvettes in size. The USB2000-FLG was connected via USB cabling to a computer running Ocean Optics SpectraSuite software for data collection purposes, with the data transferred to Excel for graphing.

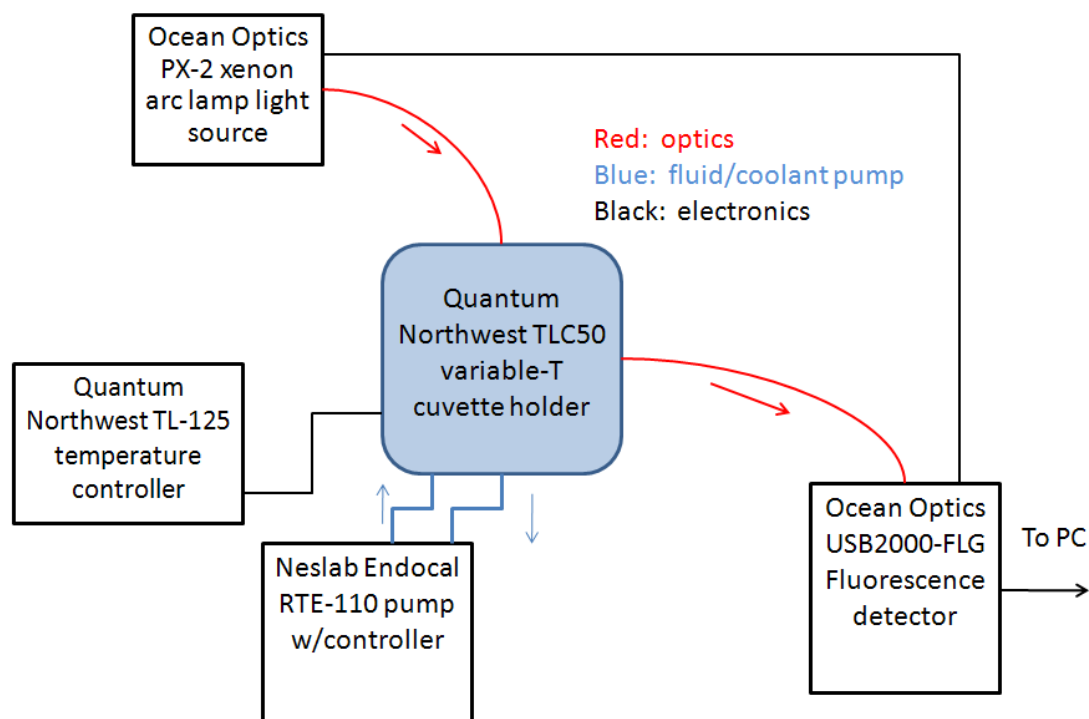


Figure 3.11. Experimental setup for the fluorescence of rhodamine B solution with and without addition of polyadenylic acid (5% w/v) solution.

Samples were prepared by mixing, in the borosilicate tubes, 35 μL of the 1×10^{-4} M rhodamine B solution either with 15 μL of distilled water or 15 μL of the

dissolved poly(A) solution. This resulted in an effective rhodamine B concentration of 7×10^{-5} M and an effective concentration of poly(A) of 1.5% w/v. The aliquots were scanned for their fluorescence spectra over a range of 370-1050nm, initially at room temperature ($\sim 20^{\circ}\text{C}$) and then at various temperatures until the sample holder temperature reached the desired temperature of -20°C , and then for various times after that as the sample itself cooled towards -20°C over the course of an hour (with t_0 being the time that the cooling began). Emphasis was put on taking spectra at the maximal fluorescence intensity prior to sample freezing and at the point where fluorescence intensity decreases coupled with backscattering due to presence of ice crystals.

Results

The results are shown as Figures 3.12 and 3.13 below. Figure 3.12 shows the quenching of fluorescence of rhodamine B when the sample freezes, as a result of a transition of rhodamine B from fluorescence (in the singlet state) to phosphorescence (in the triplet state) via inter-system crossing. It also shows the scattering of the xenon arc source light by frozen water (ice crystals) apparent across the entire spectral range. From this we can determine whether liquid water is maintained in the experimental sample with the poly(A), as a frozen sample will have both a quenched rhodamine B fluorescence and the presence of ice scattering-associated peaks.

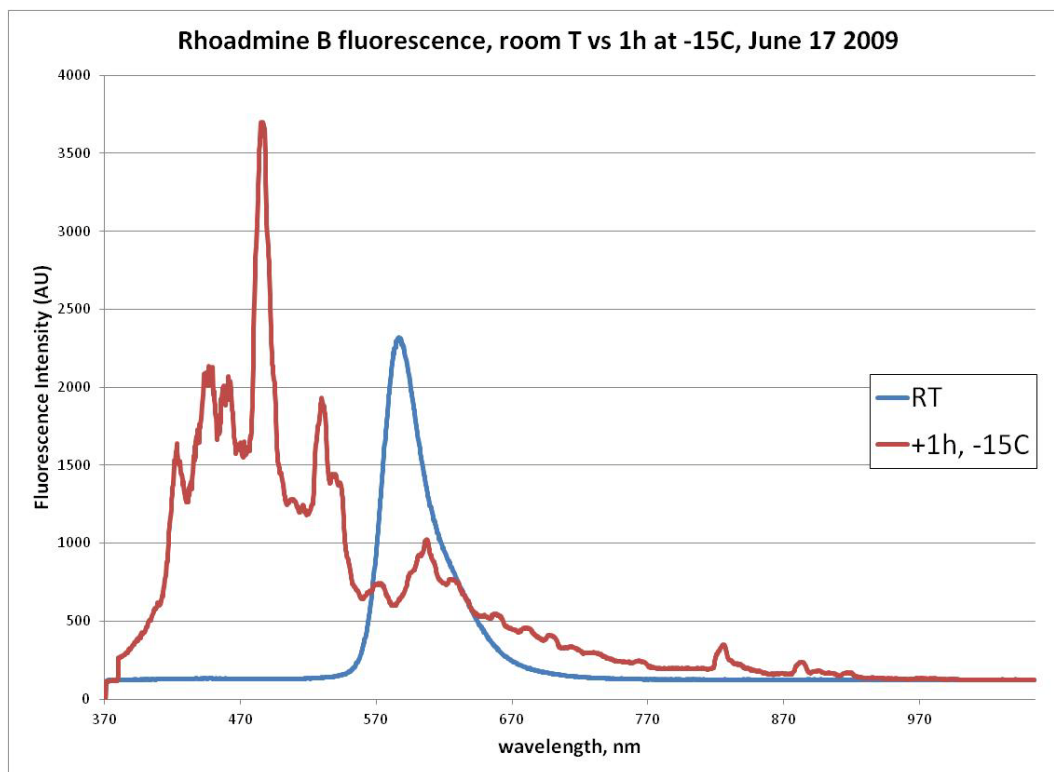


Figure 3.12. Comparison of fluorescence of rhodamine B dye (1×10^{-4} M) at room temperature and at 1 hour after cooling the sample holder to -15°C .

Figure 3.13 shows the raw data results of the cooling of the mixed rhodamine B/poly(A) solution, prepared as described above. As occurred in the rhodamine B/distilled water sample (data not shown), the fluorescence intensity of the rhodamine B increases initially as the sample is cooling; this is a result of rhodamine B's quantum yield being temperature dependent³⁶. The intensity, in fact, goes off-scale high on the USB2000 detector in the readings immediately prior to the cuvette holder reaching $\sim -15^{\circ}\text{C}$. After this point the intensity drops dramatically along with the first appearance of light scattering by ice formation. However, the fluorescence intensity increases again, redshifting, along with more light scattering, indicating that there is both ice formation and liquid solution still present at the same time.

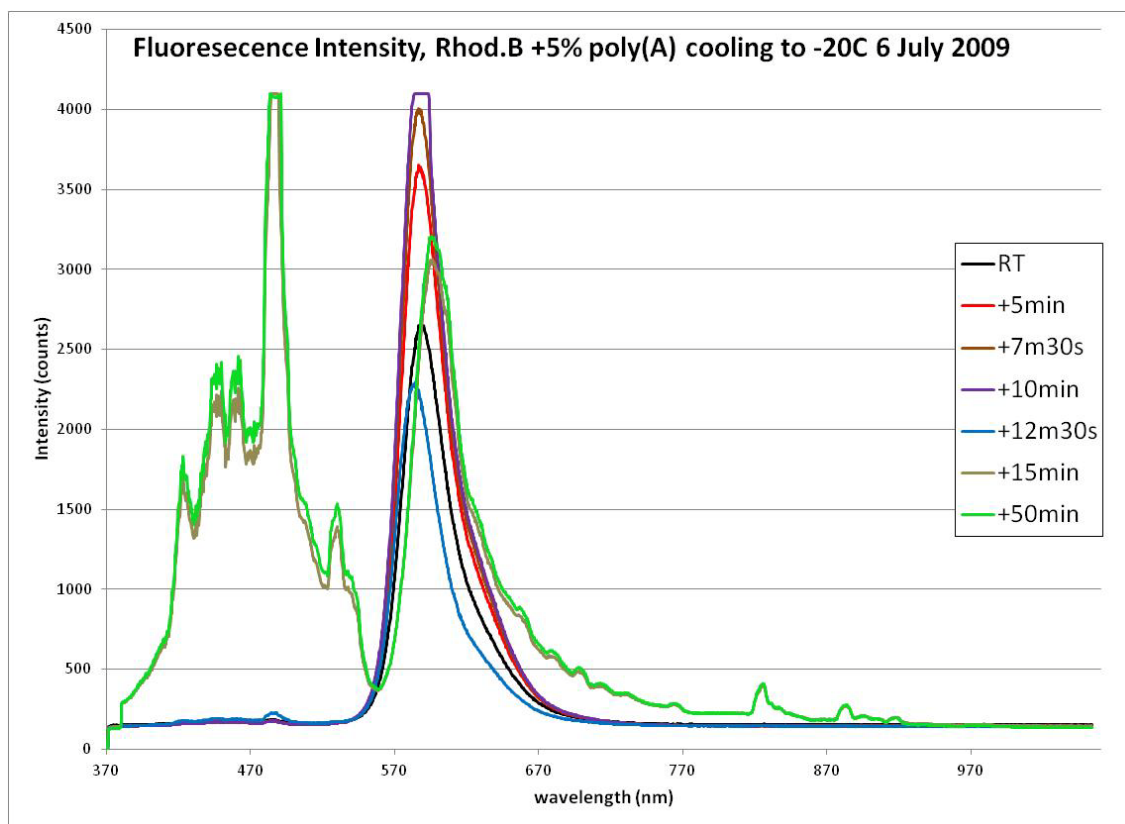


Figure 3.13. Comparison of fluorescence intensity of rhodamine B + poly(A) over a period of time chilling the sample to -20°C .

The increased fluorescence intensity despite the presence of ice crystals and concomitant light scattering can be explained in either of two ways. Either the light scattering is caused by ice crystals forming on the exterior of the borosilicate glass tube, leaving the liquid sample, or the scattering is the result of pure water freezing out of the solution, leaving the rhodamine B dye in a smaller volume and increasing its effective concentration. The loss of fluorescence intensity in the rhodamine B-only sample would seem to indicate that the former is unlikely. Thus the figures suggest that poly(A) does serve to maintain the presence of liquid water down to around -20°C .

Conclusions

Since poly(A) appears to act as a cryoprotectant, similar to teichoic acid, further experiments were necessary. In this instance, our experimentation would return to the arena of variable-temperature deuterium solid-state NMR, since it had already been performed with the teichoic acids (as shown above in Figures 3.3 and 3.4). These experiments would be performed along with other experiments in the Rice Group that would continue examination of lipoteichoic acid's cryoprotectant behavior. While these other experiments are outside of the scope of this work, in the strict sense, one can see from the data below (obtained by a fellow member of the Rice Group, Amy Middaugh) that LTA provides cryoprotectant effects to vegetative cells at sub-freezing temperatures, in this case at -20°C , for periods of time up to a month. The effect is comparable to the addition of glycerol to preserve bacterial cells, demonstrating an LTA cryoprotectant effect on living organisms in addition to the previous studies done both in this dissertation and earlier in the Rice Group on bulk water.

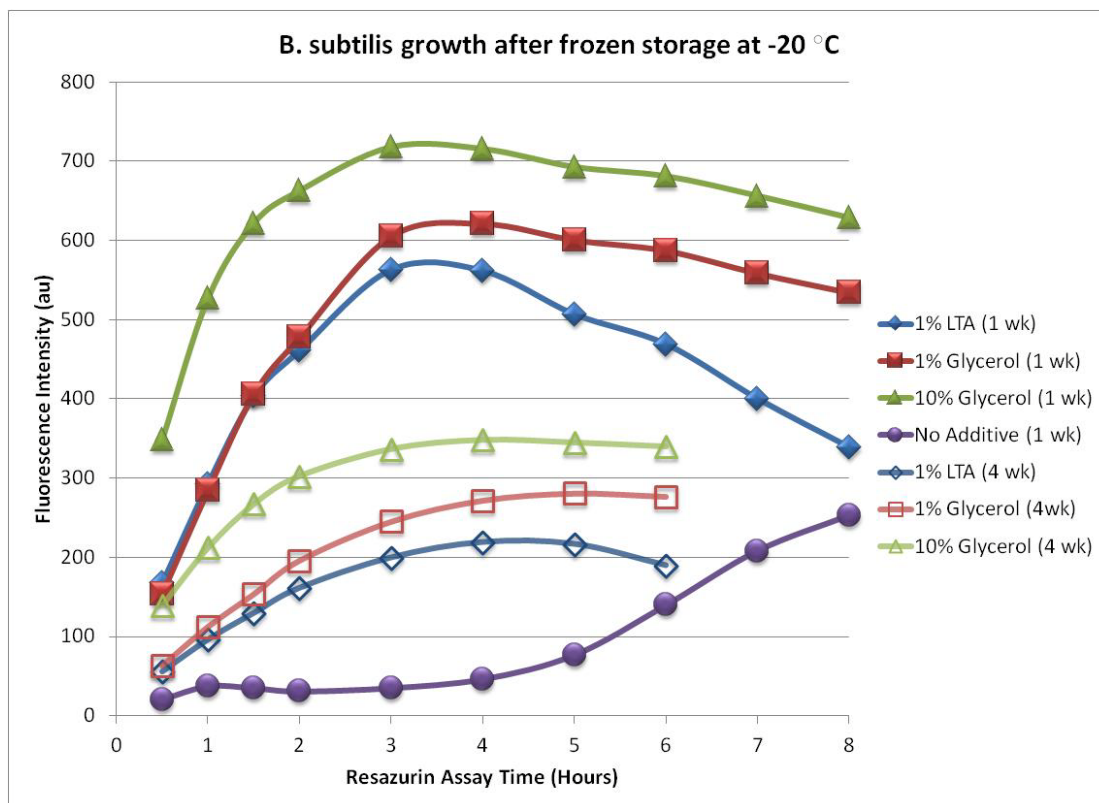


Figure 3.14. As shown by fluorescence live-dead assay, lipoteichoic acid serves as a potent cryoprotectant for cells of *B.subtilis* 1A578, performing comparably to addition of glycerol. (Rice Lab, unpublished data, courtesy A. Middaugh.)

While that data demonstrates LTA's cryoprotectant behavior as applicable to *in vitro* systems, it does not answer a key question suggested by the rhodamine B fluorescence work described earlier in this section: could poly(A) and other such molecules serve as potential cryoprotectants at similar temperatures as had already been shown to occur with teichoic acids? Through the use of variable-temperature deuterium NMR experiments, as previously performed on the teichoic acids, we intended to discover the answer to that question.

CHAPTER 4: GENERAL PRINCIPLES OF DEUTERIUM NUCLEAR MAGNETIC RESONANCE SPECTROSCOPY

Nuclear magnetic resonance (NMR) spectroscopy is a well-known and widely used technique for determination of spectroscopic and structural information in molecules. Despite having a fairly short history of only ninety years or so since the first papers indicating the theoretical background was possible¹ and only being less than seventy since the first papers describing what we would recognize as NMR¹⁻³, it has become ubiquitous for many reasons. As such, and as it is used in several experiments described in this dissertation, it is necessary to describe the basic concepts of NMR theory. This has been described in several journal articles and books, which are included for reference and further reading here⁴⁻¹¹.

Nuclear spin and degeneracy; RF pulses and free induction decay

Nuclear particles—protons and neutrons—possess spin, similarly to electrons. The protons and neutrons, both spin = $\frac{1}{2}$, will pair with each other in a fashion much like electrons, such that the nucleus as a whole will have a net spin if there is an odd number of either neutrons or protons (an odd atomic number or an odd mass number); these nuclei are of interest due to their interactions with magnetic fields, whereas nuclei with even numbers of protons and neutrons have no net spin and do not have any interactions with magnetic fields. For instance, carbon-12 is not 'active' in the NMR sense, whereas carbon-13 is considered active. This is similar to how paramagnetic oxygen can be confined through magnetic fields whereas diamagnetic oxygen cannot.

Since all nuclei are positively charged (from the protons), nuclei that possess spin establish a magnetic dipole with an associated dipole moment μ . The nuclei have an angular momentum as well, S , and each nucleus has a distinct gyromagnetic (or magnetogyric) ratio, γ , defined as:

$$\gamma = \mu / S.$$

In the presence of an external magnetic field (defined as B_0) the nuclei will align themselves in the field such that they will precess around the axis of the magnetic field, which is generally defined as being along the z-axis. The rate of precession is defined as the Larmor frequency, ω_0 :

$$\omega_0 = -\gamma B_0$$

which can be converted to Hertz by division by 2π as the angular momentum has the Planck constant (\hbar) in its term. These frequencies are in the range of RF transmissions, luckily for scientists, and thus the precessing magnetic moment can be perturbed by application of RF signals at the Larmor frequency.

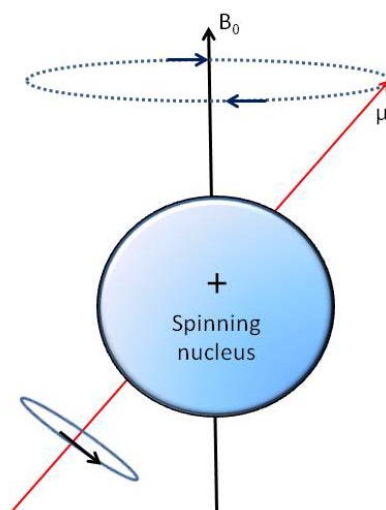


Figure 4.1. A positively charged nucleus with spin (and angular momentum) causes a magnetic dipole which precesses about an external magnetic field.

This occurs because the nuclei, in a magnetic field, align in $(2 I + 1)$ ways with the magnetic field (where I is the spin number of the nucleus in question; NMR-active nuclei have $I > 0$). In the simplest case, where $I = \frac{1}{2}$, there are two ways to align the nuclei: either with the magnetic field (spin-up, α) or against it (spin-down, β). These two states are degenerate when the nucleus is not in an external magnetic field but split in the presence of B_0 producing a difference in energy levels:

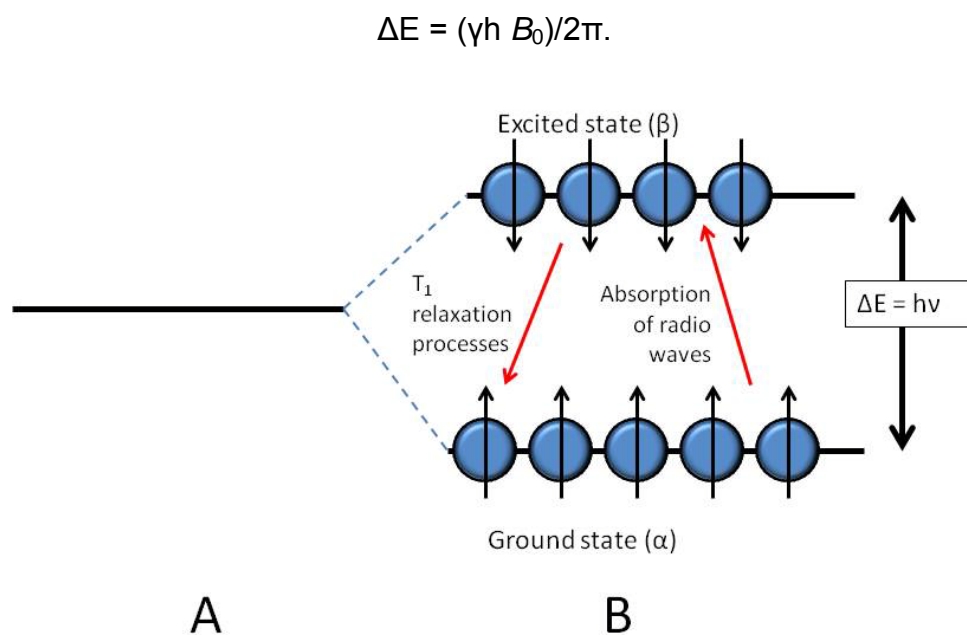


Figure 4.2. NMR-active nuclei of spin $\frac{1}{2}$ A) degenerate under normal conditions B) split into two states in the presence of external magnetic field with associated ΔE .

Application of an RF pulse at the Larmor frequency serves to perturb the bulk magnetization (by causing a change in the population of the two states) causing it to change orientation from the z-axis (along B_0), ideally to where the spins will face detectors placed perpendicular to B_0 . When the RF pulse is removed, the spinning magnetic field induces a signal in the detectors, which

decays as the nuclei both return to the z-axis and, due to slight perturbations in the nuclei, fan out and rotate about the xy-plane. These are known as spin-lattice (transverse, T_1) and spin-spin (longitudinal, T_2) relaxation respectively. This induced signal is known as the free induction decay (FID), which appears as a sinusoidal curve (as the magnetization still precesses about B_0 and the z-axis, just along the xy-plane instead of closer to the z-axis) that decays as the bulk magnetization returns towards the z-axis.

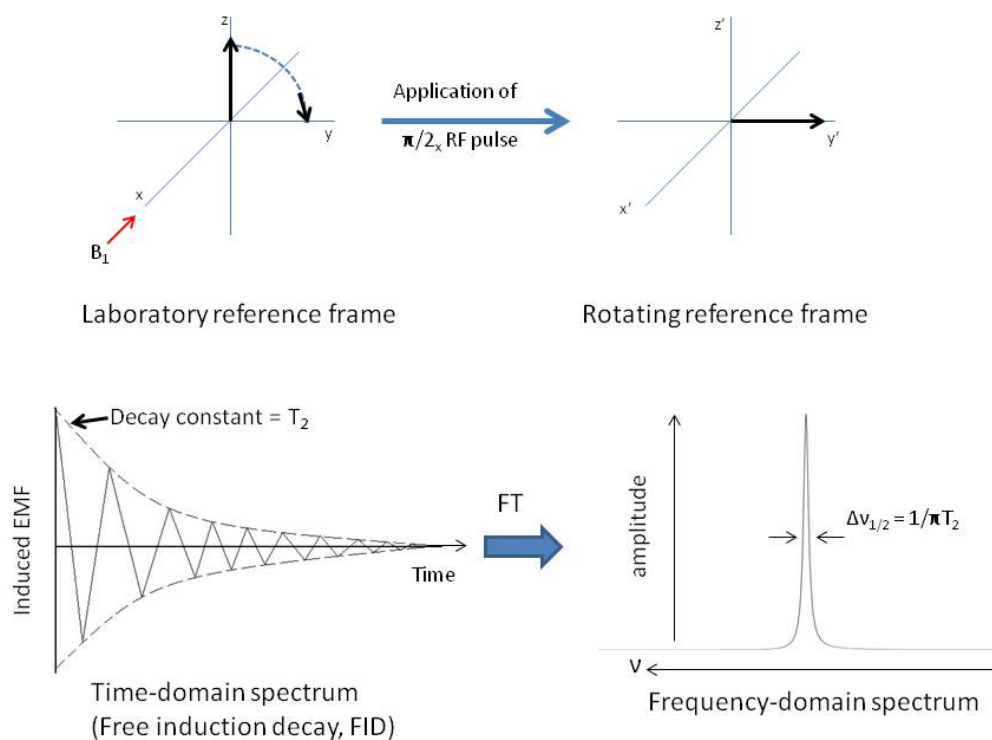


Figure 4.3. The magnetization of a sample is perturbed by an RF pulse away from the z-axis; the relaxing nuclei induce a free induction decay in the detector; Fourier transformation of the signal yields a spectrum.

When the FID is Fourier transformed from a time domain to a frequency domain, a spectrum is generated, where the signals of the nuclei involved

appear as peaks, the intensity of the peaks depending on the number of nuclei (and the amount of sample) and the linewidth being determined in part by T_2 by the equation

$$\Delta\nu_{1/2} = 1/\pi T_2.$$

The main draw of NMR is that it is not as simple as that; in B_0 the electrons of atoms also are perturbed, which causes an induced magnetic field (B_{ind}) which interacts with other NMR active nuclei. This interaction causes variations in the local magnetic field felt by the nucleus:

$$B_{loc} = B_0 + B_{ind}$$

which results in slight variations in the Larmor frequency per nucleus, depending on the local environment around it. This local environment includes structural features of the molecule, such as functional groups, or electron-donating or electron-withdrawing groups or other functionalized features that would affect B_{loc} . Thus when the FID is Fourier transformed the spectrum will show slight differences in peak strength and location that can be related to the structure of the sample molecule, the chemical shift.

Dipolar coupling and chemical shift anisotropy effects

In addition, interactions between the magnetic dipoles of NMR-active nuclei can occur in a through-space, distance-dependent manner which can also result in line broadening effects, known as dipolar coupling. The dipolar coupling constant, D , is given as

$$D = (h/2\pi)(\mu_0/4\pi)(\gamma^I\gamma^S/r^3)$$

where I and S refer to the two nuclei in question, respectively, and r is the distance between the two nuclei. This coupling can be divided into two groups: homonuclear dipolar coupling, where I and S are equal, and whose main effect is line broadening; and heteronuclear dipolar coupling, where I and S are different nuclei, and the main effect is forming a characteristic lineshape (the Pake pattern) where the twin horns of the pattern are separated by D, as shown below.

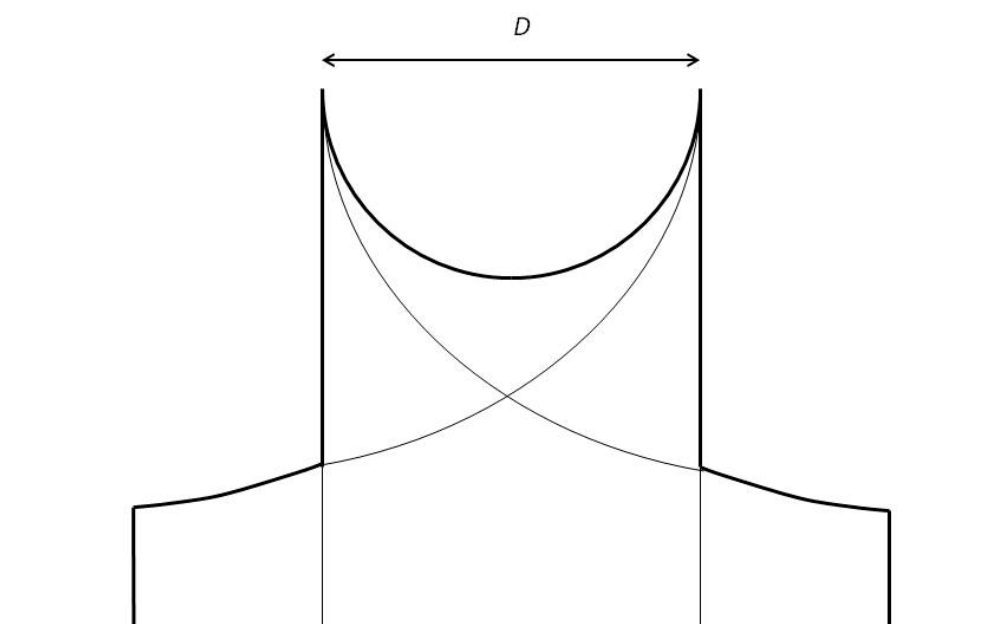


Figure 4.4. The powder lineshape of a molecule experiencing heteronuclear dipolar coupling, where D is both the dipolar coupling constant and the distance between the two peaks of the spectrum.

The two couplings are described by their characteristic Hamiltonians, with homonuclear dipolar coupling

$$H^{\text{homo}} = -D (0.5) (3\cos^2\theta - 1) (3I_z S_z - I \cdot S)$$

and for heteronuclear dipolar coupling

$$H^{\text{hetero}} = -D (3\cos^2\theta - 1) (I_z S_z).$$

In solid-state NMR, the sample is not a solution but some sort of solid substrate, either a powder or crystal. This results in differences in the spectra due to the difference between liquids and solids dealing with the molecular motion of the sample. In liquids, while at any given moment a molecule may be in any number of orientations with respect to the magnetic field, on the NMR timescale the ability of the molecules to move about (rotational and vibrational motions) results in averaging of the signals from all orientations into a single isotropic chemical shift, σ_{iso} . For solid samples with hindered molecular motion, there is no averaging of the signal and different chemical shifts arise depending on the orientation of the molecule relative to the magnetic field, leading to anisotropy and an orientational dependence on the chemical shift. The intensity of the signal depends on how many nuclei are perpendicular to B_0 ; for a molecule shaped like an ellipsoid with the major axis along z, the peak intensity along z (with a chemical shift of σ_{zz}) will be lower than those along the other two axes because along the x and y axes there are more molecules perpendicular to the magnetic field (when the field is aligned with x or y) and thus in line with the detector. When $\sigma_{xx} = \sigma_{yy}$, the resulting peak pattern has a single sharp peak with a long single-sided tail from $\sigma_{xx} = \sigma_{yy}$ towards σ_{zz} , then rapidly declines to zero signal past σ_{zz} . When $\sigma_{xx} \neq \sigma_{yy}$, the solid-state peak shape will have a maximum at σ_{yy} which tails off on both sides, to σ_{xx} and σ_{zz} . The calculated isotropic shift then is defined as the average of the three anisotropic shifts, and the chemical shift anisotropy tensor (Δ_{CSA}) is defined as

$$\Delta_{\text{CSA}} = \sigma_{\text{zz}} - \sigma_{\text{iso}}$$

The chemical shift anisotropy is responsible for part of the line broadening effect in solid-state NMR spectra (along with the dipolar coupling). The line broadening can be very large, on the order of tens or hundreds of kHz for protons, making it implausible to run (as seen in Figure 4.5 below); other nuclei are commonly used instead.

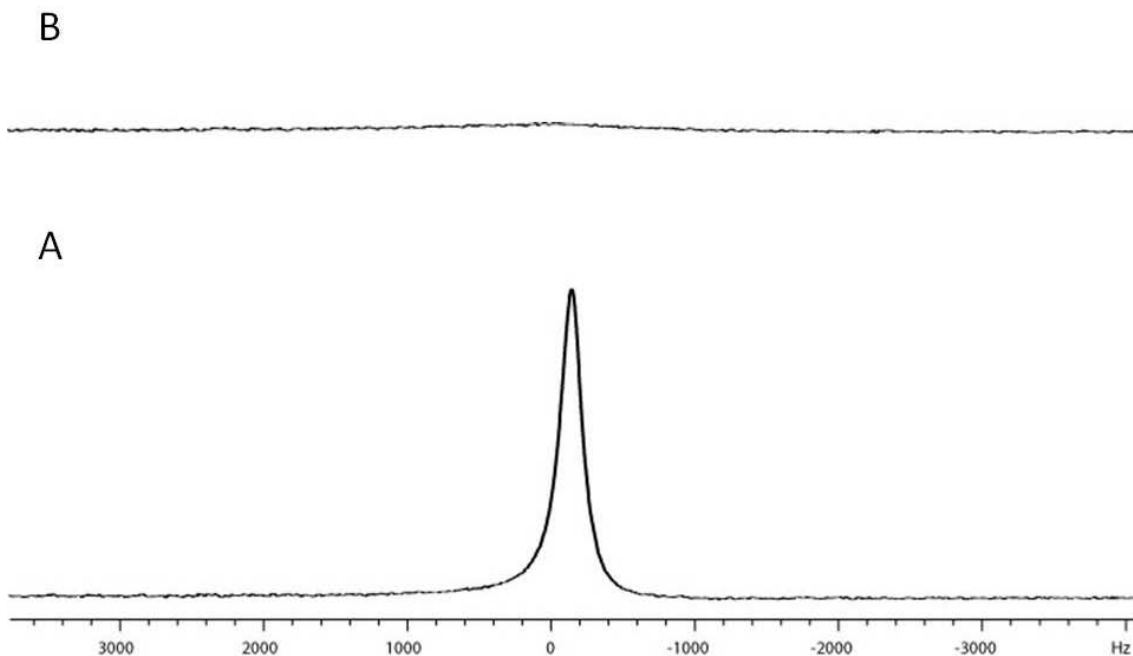


Figure 4.5. The result of anisotropy and homonuclear dipolar coupling: deuterium NMR of deuterated DNA, at 0°C (A) and -15°C (B); while the area under the peak is identical, it is broadened to where the peak is unrecognizable.

As the strength of a sample's signal is dependent on the strength of the magnetic field it is subject to, modern NMR spectrometers use superconducting magnets to induce stronger magnetic fields that can be produced through permanent magnets. In order to allow the magnets to function it is bathed in a sealed dewar with liquid helium (at 4 Kelvin), surrounded by a second dewar filled with liquid nitrogen (at 77 K) to prevent boil-off of the helium. Samples are

put into a probe (containing the RF coil and receiver circuitry, as well as tuning equipment) which is introduced into the magnetic field and is connected to the electronics to generate the RF pulses as well as to detect the signal from the receiver and to perform the Fourier transformations and other data analyses.

Deuterium NMR spectroscopy

NMR spectra can be collected for NMR-active nuclei with spins other than $\frac{1}{2}$ as well; for instance, deuterium (^2H) NMR is a known phenomenon despite having a spin of 1. This (by the $2I + 1$ equation) gives three states and two allowed transitions; for solid-state deuterium NMR, this yields spectra similar to the Pake pattern but with the distance between the two peaks equivalent to some fraction of the quadrupolar coupling constant. (The liquid state deuterium spectra will either present singlets, if isotropic, or non-Pake doublets for liquid anisotropic samples¹², as shown below in Figure 4.6.)

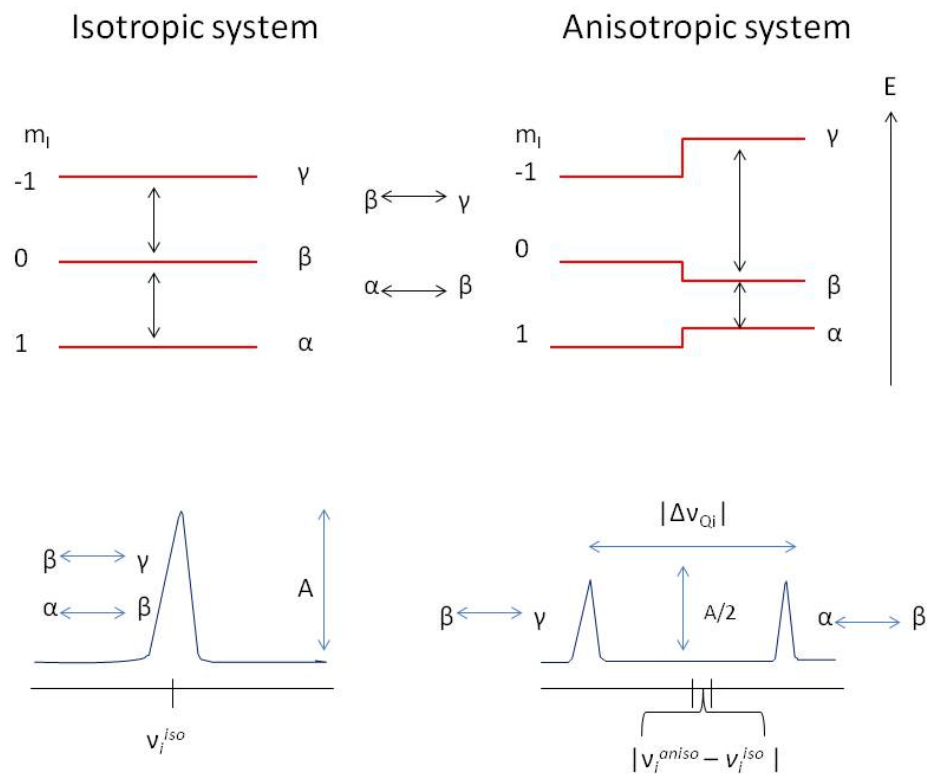


Figure 4.6. The transitions and spectra for liquid deuterium NMR, for the cases where the sample is in an isotropic system (a, left) or anisotropic system, as in a liquid crystalline state (b, right).

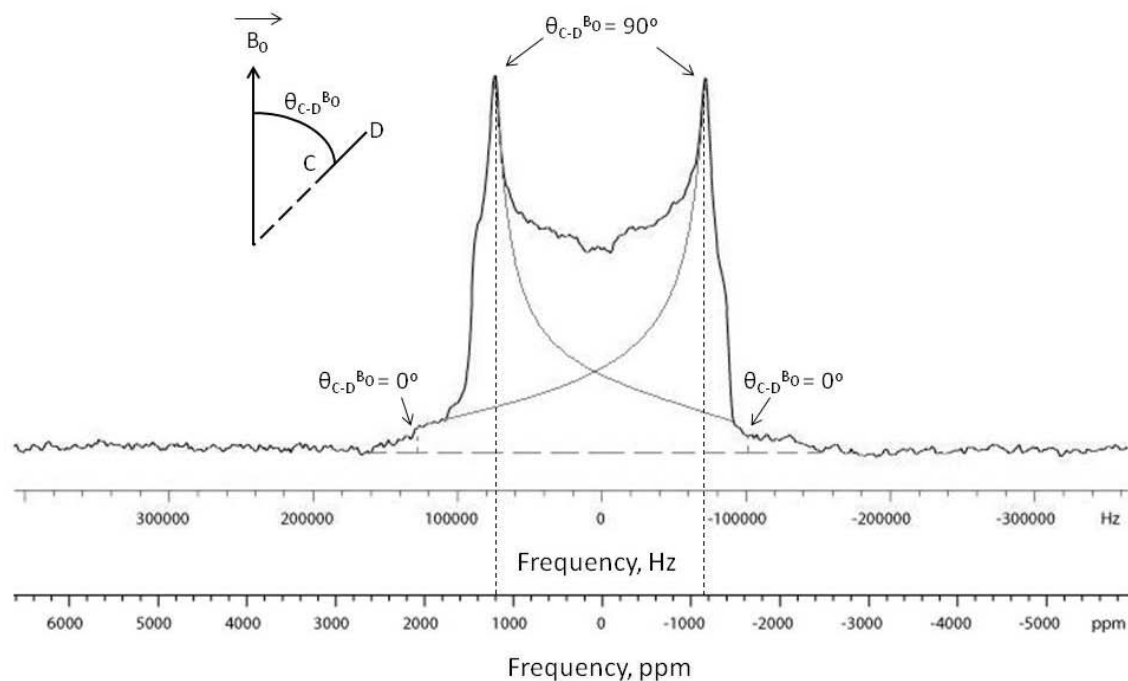


Figure 4.7. The Pake pattern spectrum for solid-state deuterium NMR (in this case, frozen D_2O), with the characteristic two horned peaks; notice the broadness of the peak, a trademark of solid-state NMR.

At first glance deuterium would not seem to be a viable nuclei for solid-state NMR experiments. This would be due to the quadrupolar nature of the nucleus which causes very fast relaxation, T_2 , and thus broad lines of hundreds of ppm in width that cannot be observed without specialized equipment along with its low natural abundance (0.015%), though natural abundance deuterium NMR (in both liquid and solid-states) have been performed¹². However, the large quadrupolar moment allows for justification of treating 2H as an isolated nucleus, ignoring dipolar and chemical shift interactions and simplifying analysis of the spectrum¹⁴, and labeling/deuteration of molecules is fairly inexpensive

and easy to perform, relative to enrichment of other nuclei¹⁵. As such it has been used in many experiments dealing with structure or molecular motion¹⁶⁻¹⁹.

CHAPTER 5: VARIABLE-TEMPERATURE DEUTERIUM NMR OF POLY(ADENYLIC) ACID AND OTHER POTENTIAL CRYOPROTECTANTS

Reasoning for NMR experiments: similarities of LTA and poly(A)

Lipoteichoic acid is a component of Gram-positive bacterial cell walls, comprised of glycolipid tails stretching back into the lipid bilayer membrane of the cell while a repeating polyglycerolphosphate (PGP) backbone protrudes into the cell wall and extracellular space with varying side chains¹⁻⁶. It is associated with Gram-positive bacteria and in particular with species containing low levels of guanine and cytosine². In *B.subtilis*, LTA-lacking mutants have been grown, though they exhibit defects in cell division and are sensitive to Mn²⁺; LTA is however necessary for *B.subtilis* sporulation and has been found to be essential for vegetative cell function in *S.aureus*⁷. The synthesis appears to start with the formation of the lipid anchor followed by linking of the glycolipid moiety to a phosphate through a glycerol linkage, then polymerization of the glycerolphosphate ester into a phosphodiester linkage (the PGP backbone)².

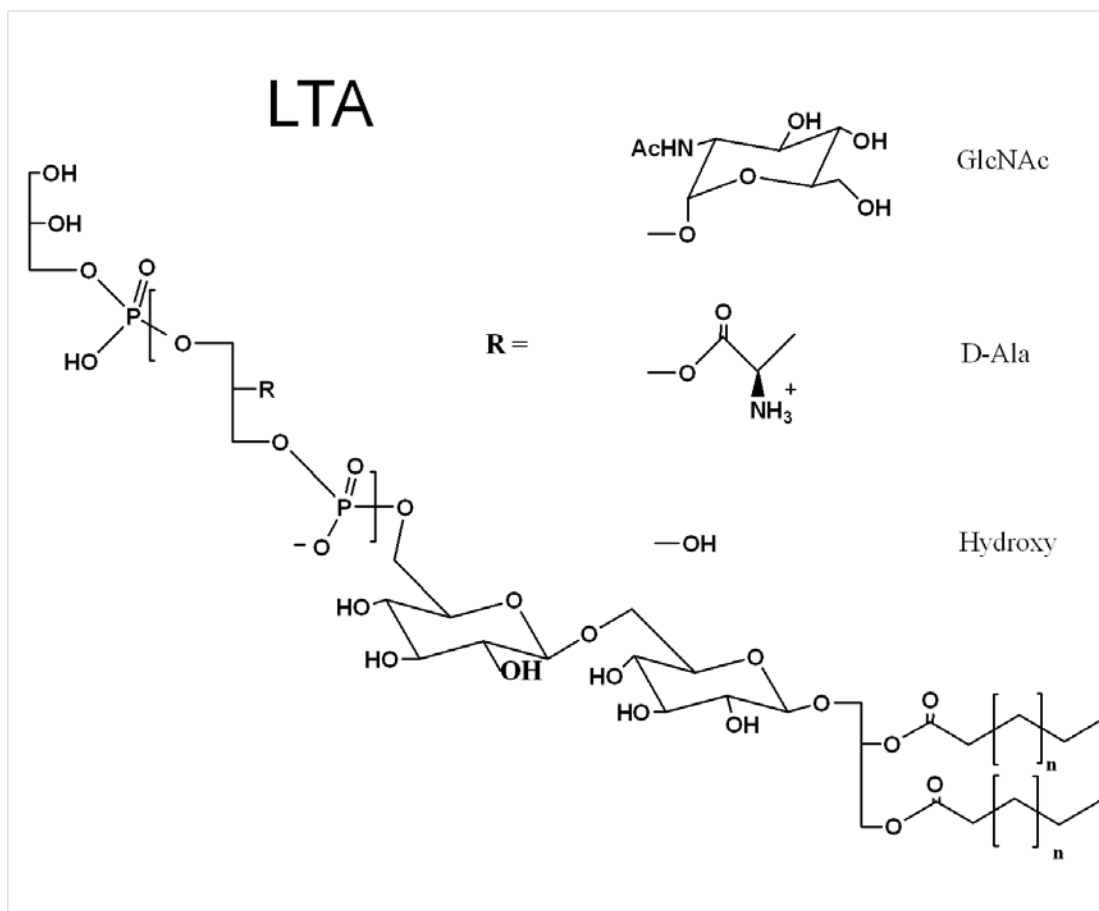


Figure 5.1. The structure of lipoteichoic acid, with side-chain units listed at right. The lipid tails are at bottom right, followed by the disaccharide moiety and the polyglycerolphosphate (PGP) backbone.

Lipoteichoic acid is known to serve a purpose in scavenging metal cations from the extracellular space due to the negatively-charged phosphate groups comprising the backbone of the molecule^{8,9}. It is also known to be a pyrogenic agent and an inflammatory agent towards the immune system¹⁰⁻¹².

Previous research in the Rice Group has focused on different aspects of LTA's properties. Published research has been based on solid-state NMR research on the nature of metal cation binding to the phosphate (PO_4^-) groups of the teichoic acid polyglycerolphosphate backbone, using cadmium and magnesium, both divalent cations^{13,14}. Additional prior research was based on

teichoic acids in general providing a cryoprotectant effect on liquid water at subfreezing temperatures based on both variable-temperature ^{31}P CPMAS NMR and fluorescence experiments with rhodamine B^{15,16}.

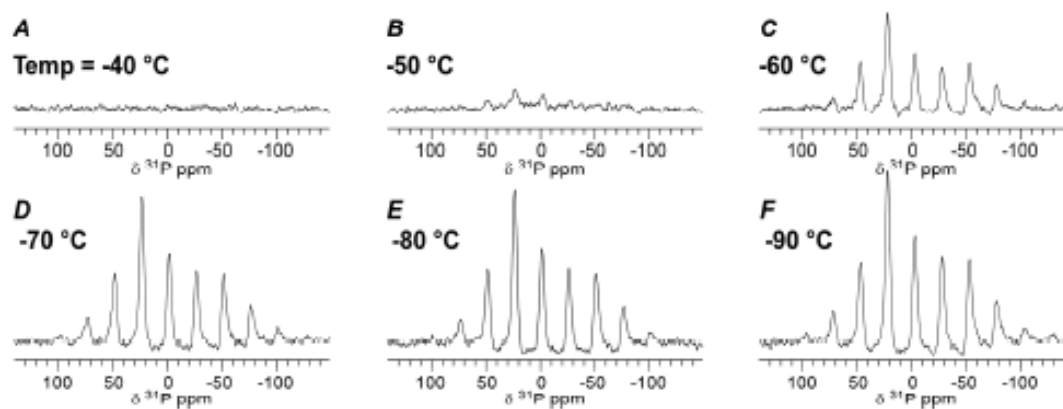


Figure 5.2. ^{31}P VT CPMAS NMR of *S.aureus* LTA dissolved in D_2O indicates due to the absence of the phosphorus lineshape that some molecular motion exists as a result of liquid D_2O present as low as between -50 and -60°C ; LTA thus provides cryoprotectant effects. Figure 2 from Rice *et al* 2008¹⁶, reprinted with permission.

It was suggested that, based on these results, LTA having cryoprotectant properties may be a result of the structure of the LTA, and indeed of teichoic acids in general since WTA provided a lesser, but still noticeable, freezing point depression based on VT ^{31}P CPMAS NMR experiments¹⁶. This would explain, at least partially, some older work which indicated in its results (though it was not the intent to study that facet) that Gram-positive bacteria are more viable after rapid freeze-thaw cycles than Gram-negative bacteria¹⁷. If other molecules which possess similar features could be shown to have cryoprotectant properties as well it would suggest that perhaps *all* biomolecules which have a PGP backbone could have some cryoprotectant effects. Most notably among these molecules are, obviously, the polynucleic acids, which

bind through ester linkages between phosphate groups and have PGP backbones in large-scale structures such as RNA and DNA, one of which, poly(adenylic) acid (poly(A)) was shown earlier in this work to have some cryoprotectant effect by use of rhodamine B dye fluorescence.

In order to examine this theory, an experiment was devised utilizing deuterated biomolecules to examine the deuterium solid-state NMR spectra of these molecules at a range of temperatures, from above to well below the nominal freezing point of deuterium oxide (+3.8°C). By observing the spectra to see the appearance and disappearance of characteristic features of liquid and frozen D₂O, the validity of the hypothesis that biomolecules with polyglycerolphosphate backbones provide cryoprotectant properties to their host species could be tested.

Equipment, materials, and methods

Variable-temperature NMR experiments were performed using a 400-MHz (9.4 T) superconducting magnet (Oxford Instruments, Abingdon, Oxfordshire, UK) with a Varian Instruments (Palo Alto, CA, US) 400 MHz 5mm wideline probe (model RB968568) tuned to deuterium (*sfreq*= 61.424 MHz). The RF pulses and data collection were performed by a Varian *Unityplus* NMR console, controlled by the user with Varian *VNMR* software (version 6.1c) running on a Sun Microsystems SPARCstation 20 workstation using the Solaris operating system. The sample temperature was measured and controlled via software through an Oxford Instruments temperature controller and a Sorensen DCR-13B power supply for the probe heating element.

Sample temperature was additionally controlled with an FTS Systems Airjet chiller (model XRIIB51A00) and an FTS Systems temperature controller (TC-84, model XRTCA-0). The gas supply for all VT experiments was in-house nitrogen gas, spliced to feed room-temperature N₂ directly to the probe (as body air) and to the inlet of the FTS Airjet system; chilled N₂ was introduced to the sample via an insulated hose clamped onto a glass fitting protruding from the probe base. The desired temperatures of the chilled N₂ and of the sample were independently regulated; the former by the FTS TC-84 temperature controller, the latter by the Oxford temperature controller and the Sorensen power supply as controlled by the NMR console and the *VNMR* software (*vtype=1* enabling VT control in the software, using *temp=* to adjust desired sample temperature). An upper barrel assembly was attached to the top of the magnet barrel to funnel the chilled gas out and to minimize cooling and condensation on the interior of the magnet barrel. (An approximate representation of the experimental setup is replicated below.)

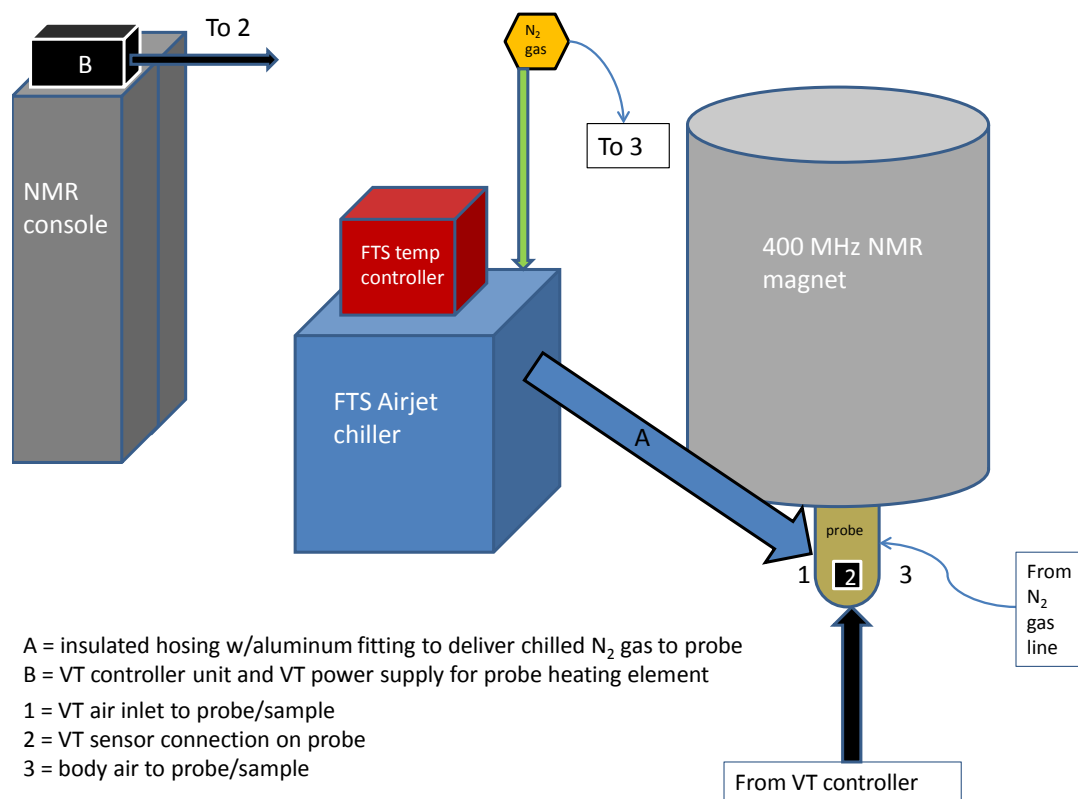


Figure 5.3. Schematic representation of the equipment setup for the variable-temperature deuterium NMR experiments performed.

Purified lipoteichoic acid from *S.aureus* was purchased from Invivogen (San Diego, CA, US; category code tlrl-pslta). DNA (sodium salt) from fish sperm was bought from AMRESCO (Solon, OH, US; product no. 0644). Various other chemicals were purchased from Sigma-Aldrich (St. Louis, MO, US): polyadenylic acid, potassium salt (“Poly{A}”, product no. P9403); polyadenylic acid-polyuridylic acid, sodium salt (“Poly{A:U}”, P1537); bovine serum albumin (BSA, A7966); and RNA from baker’s yeast (*Saccharomyces cerevisiae*) (R6750). Deuterium oxide, 99.9% purity, purchased from the stockroom of the Department of Chemistry and Biochemistry was acquired from

Cambridge Isotope Laboratories (Andover, MA, US) in both 25g (DLM-4-25) and 100g (DLM-4-100) sizes.

Weighed amounts of the above chemicals were dissolved in D₂O in Eppendorf tubes to obtain deuterated samples. The molecules studied were at either 2.5% or 5% weight/volume ratios, typically by dissolving 5 mg of the sample in 100 or 200 μ L of D₂O. Samples were then pipetted into cleaned ceramic or glass rotors, capped with an O-ring sealed top with a hole to allow air to escape and thus allowing the samples to expand when frozen in the VT experiments without breaking the rotor, particularly when using the glass rotors. The rotors were placed in the probe, which was then inserted into the magnet and screwed tight. The samples were chilled to the desired initial temperature through the VT system before tuning was performed. Due to the limitations of the VT power supply (it would trip an over-voltage protection at above 25 volts), experiments that required a temperature range starting lower than -45°C (by arraying the *temp* variable) were broken into two experiments to allow for a raising of the nitrogen gas temperature coming from the chiller. It was also determined that using the parameter *masvt='y'* to tell the instrument that a high-powered VT unit was in place allowed for unbroken experiments over a temperature range of -45°C to +10°C (with the chiller unit set to ~-60°C) without danger of tripping the power supply's overvoltage cut-off.

During these experiments, a pre-acquisition delay (PAD) of 900 seconds (15 minutes) was incorporated to allow the sample temperature to stabilize at the desired temperature for that spectrum. When a temperature array was set

up, the software and console would apply the PAD between each arrayed spectrum; however, the default setup is to interleave between arrayed spectra ($il='y'$) every block of saved data (the block size, bs). This would force the spectrometer to wait for the PAD each time between spectra every block size, which would greatly increase the time required to run the experiments and put a strain on the VT system. Therefore interleaving was disabled for these experiments ($il='n'$) so that the spectrometer would collect the complete spectrum at each arrayed temperature value before moving to the next value in the array (and thus invoking the PAD). As a rule, the temperatures in the array increased (starting at the coldest temperature), and were always adjusted in 5°C increments.

Two pulse sequences were used in these experiments. The S2PUL (standard 2-pulse) sequence was used to observe liquid deuterium signals only, with the characteristic being very short delay times between scans (~ 0.6 - 1.0 s) and very high numbers of scans (~ 2000 scans per spectrum) at each temperature. With this sequence the signal would be very small at very low temperatures, increasing as the sample warmed, until the sample was liquid and the very strong liquid D₂O singlet would emerge. The SSECHO (and SSECHO1) pulse sequence was used to detect the characteristic 'horns' (the Pake doublet) of frozen/immobile deuterium at low temperatures, which would decay as the sample was warmed up. However, due to the very long T_1 time of frozen deuterium (approx. 23 s) and the need for the delay time to be 5 times T_1 to ensure total relaxation of the deuterium before the next scan, the overall

delay time is much longer (120 s). The signal intensity was such, however, that well-defined Pake peaks could be seen at very low numbers of scans—for these experiments 64 scans was a common number. In this way, both sets of experiments could be performed with minimal or no intervention, although the experimental duration was shorter for S2PUL experiments (~10-13h) than SSECHO experiments (~24h) due to the shorter length of time to collect data for each spectrum (1200-2000s for S2PUL; ~7700s for SSECHO).

To determine a rough way of comparing data points from different spectra, a system was used by which the liquid water peak from the S2PUL experiments at each temperature of the array had its height (nl) and its linewidth (res , using the 50% line width for FWHM—'full width at half maximum'—as the linewidth) were measured, and then multiplied together to get an estimate of the peak's area. The height was measured at the location of the liquid deuterium peak. When using res , VNMR uses the largest peak in the spectrum, which under normal circumstances is the same as the liquid deuterium peak. In some cases, the signal at the peak location is too low (in the noise) and when using res the software (VNMR) cursor will jump to a different location in the spectrum. In that circumstance the peak signal was deemed to be undetectable and no value was determined for the peak area estimate. These data points were plotted against each other in Excel to graphically observe the strongest liquid deuterium signal at different temperatures. Where possible, spectral parameters (both for data collection and the display of said data e.g. Fourier

transformations) were held constant for all spectra to ensure compatibility between data sets.

Results

Below, two figures (5.4 and 5.5) are included showing the deuterium oxide temperature arrays in both the S2PUL and SSECHO pulse sequences to visually demonstrate the differences between the pulse sequences and what information can be gleaned from each. As mentioned above the S2PUL looks only at the purely liquid deuterium signal, whereas the SSECHO is primarily focused on the immobile/frozen deuterium signal. The central peak in this case is not only *liquid* deuterium that may still be present but also deuterium that is *mobile* within the frozen water (indicative of sudden flips or other motion within the frozen deuterium—which, as the frozen matrix begins to soften and thaw at warmer temperatures, becomes easier and thus a stronger signal).

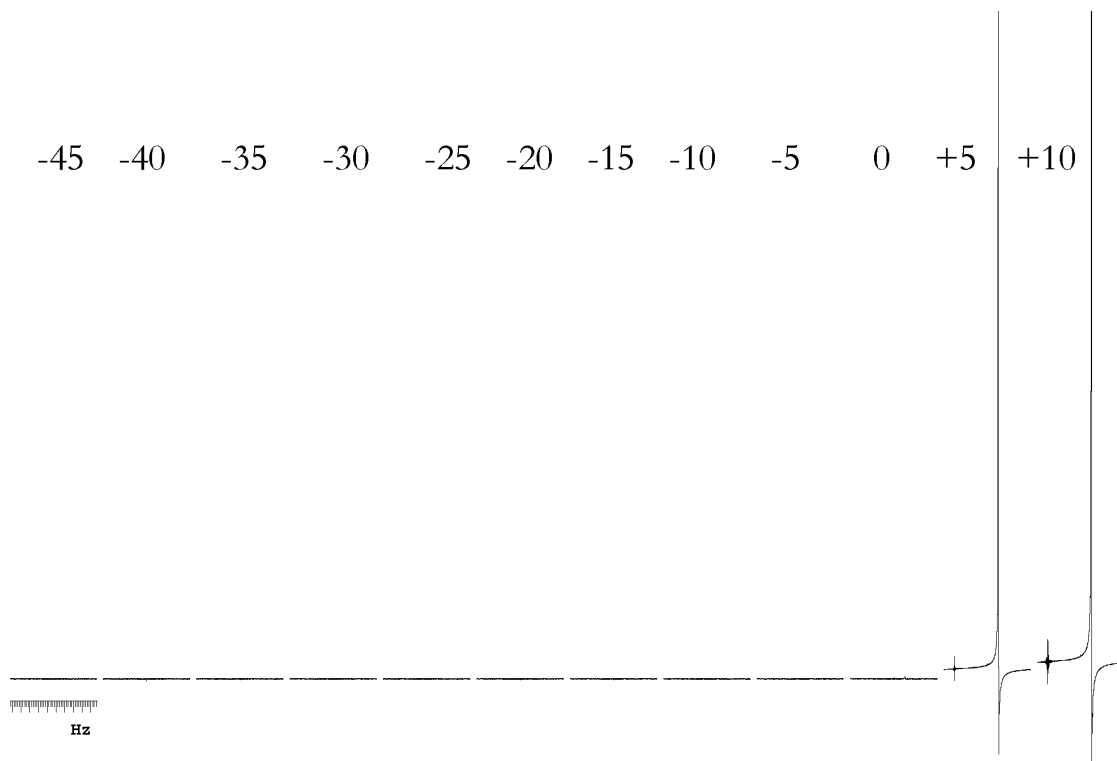


Figure 5.4. Temperature-arrayed sequence of spectra of D_2O using the S2PUL pulse sequence, at $5^\circ C$ increments from $-45^\circ C$, at left. The distorted signals at $+5$ and $+10^\circ C$, right, are due to saturation of the detector by liquid deuterium signal above the melting point of D_2O .

In comparison, the lipoteichoic acid temperature arrays indicate the LTA's ability to provide cryoprotection to the D_2O , based on the much colder spectrum in the S2PUL experiment in which the liquid deuterium signal appears and the larger size of the signal at warmer temperatures, as well as the more pronounced decrease of the Pake doublet and appearance of the mobile deuterium peak in the SSECHO experiment. This serves to demonstrate LTA's known cryoprotective effects from earlier experiments mentioned before.

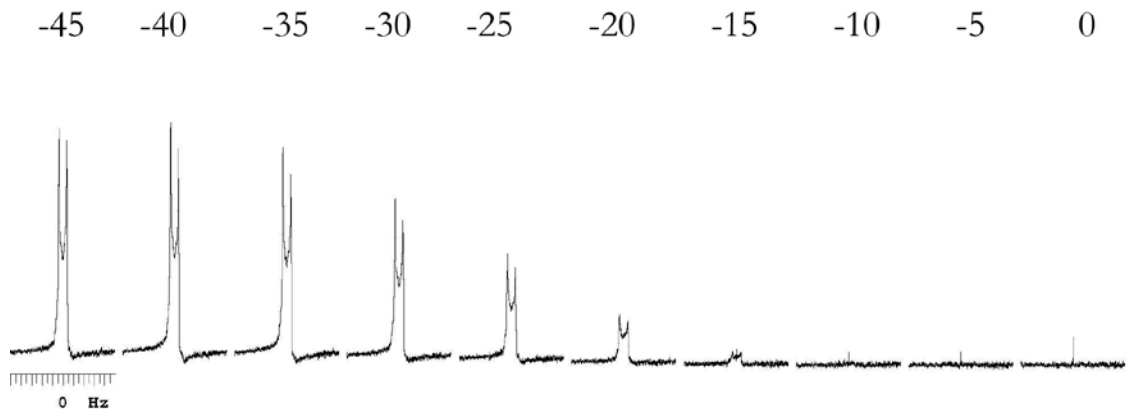


Figure 5.5. The temperature-arrayed spectra of D₂O using the SSECHO pulse sequence, at 5°C increments from -45 to 0°C. The decreasing set of Pake doublets are indicative of the immobile deuterium, which fades as the sample is warmed, with the appearance of a mobile deuterium signal within the frozen sample at right.

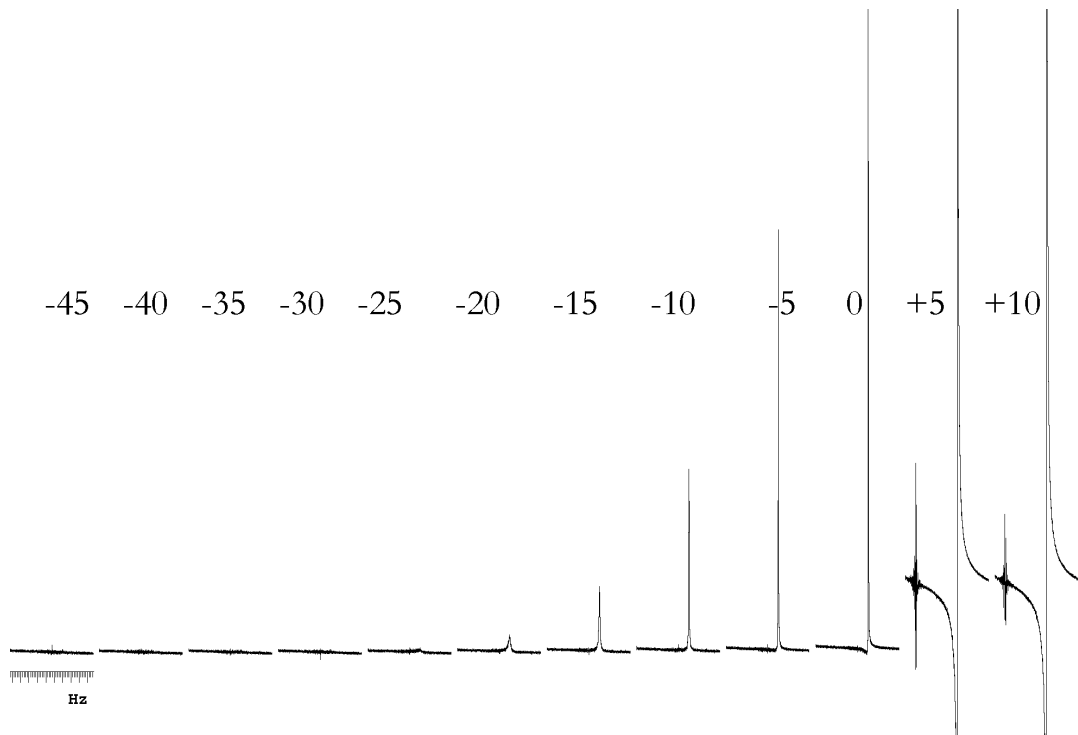


Figure 5.6. The temperature array (in °C) of the S2PUL experiment with 5% w/v lipoteichoic acid.

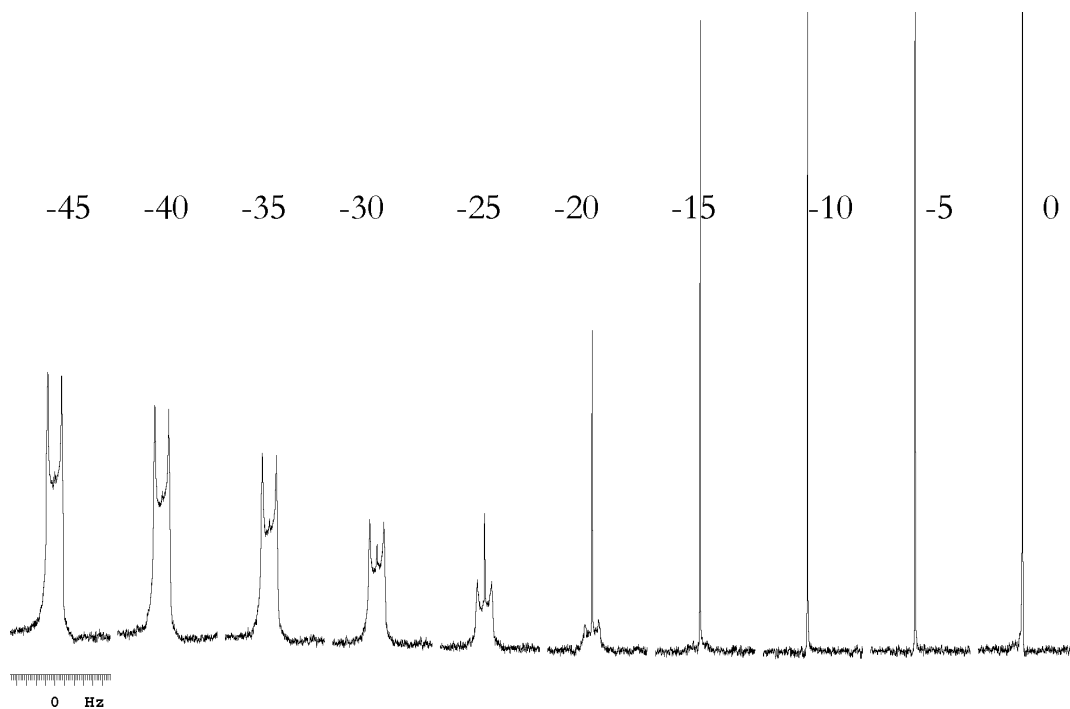


Figure 5.7. The temperature array (in °C) of the 5% w/v LTA SSECHO experiment.

A table of the quantitative S2PUL data (the peak height times line width) for each molecule is shown below. The data were taken from S2PUL experiments with a temperature array from -45°C to +10°C with 5°C steps; the shown data range (from -25°C to 0°C) was chosen due to all molecules but poly(A) showing no discernible signal at -25°C or below and all molecules showing massive signals above zero due to the melting of frozen D₂O and thus that deuterium being detected in the S2PUL experiments. This data is shown in a graphical format below in Figures 5.8 and 5.9; the LTA is put separately in Figure 5.9 owing to it being at a 5% w/v concentration compared to all other samples (at 2.5% w/v).

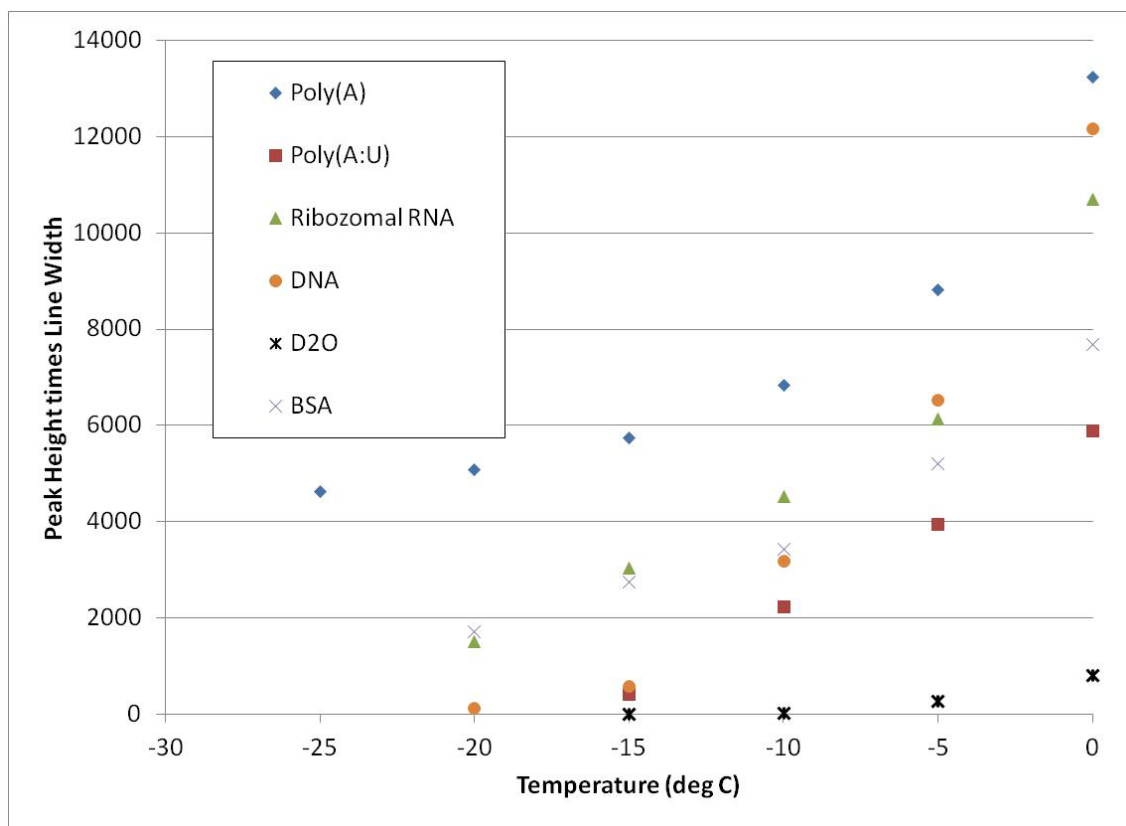


Figure 5.8. Graphical chart of the data points of Table 5.1 less the LTA; the ribosomal RNA comes from baker's yeast (*Saccharomyces cerevisiae*).

Table 5.1 (opposite). Peak height times line width values from -25°C to 0°C from S2PUL deuterium VT NMR experiments for various molecules of interest, with percent change between temperatures and cumulative percent change. n.d. = not detectable; N/A = not applicable.

Molecule	% w/v	-25°C	-20°C	-15°C	-10°C	-5°C	0°C	Cumul % chng
D ₂ O	Pure	n.d.	n.d.	9.42544	15.3766	263.95	802.713	8417
BSA	2.5%	n.d.	1716.30	2751.67	3433.65	5210.97	7694.46	348.3
Poly(A)	2.5%	4626.63	5094.78	5744.84	6850.47	8827.72	13246.9	186.3
Poly(A:U)	2.5%	n.d.	n.d.	408.566	2242.94	3941.68	5889.13	1341
DNA	2.5%	n.d.	128.470	589.784	3189.18	6537.60	12164.4	9369
RNA (baker's yeast)	2.5%	n.d.	1511.47	3038.07	4529.73	6140.26	10701.8	608.0
LTA	5%	n.d.	2585.04	9490.77	14831.8	21169.4	34251.1	1225

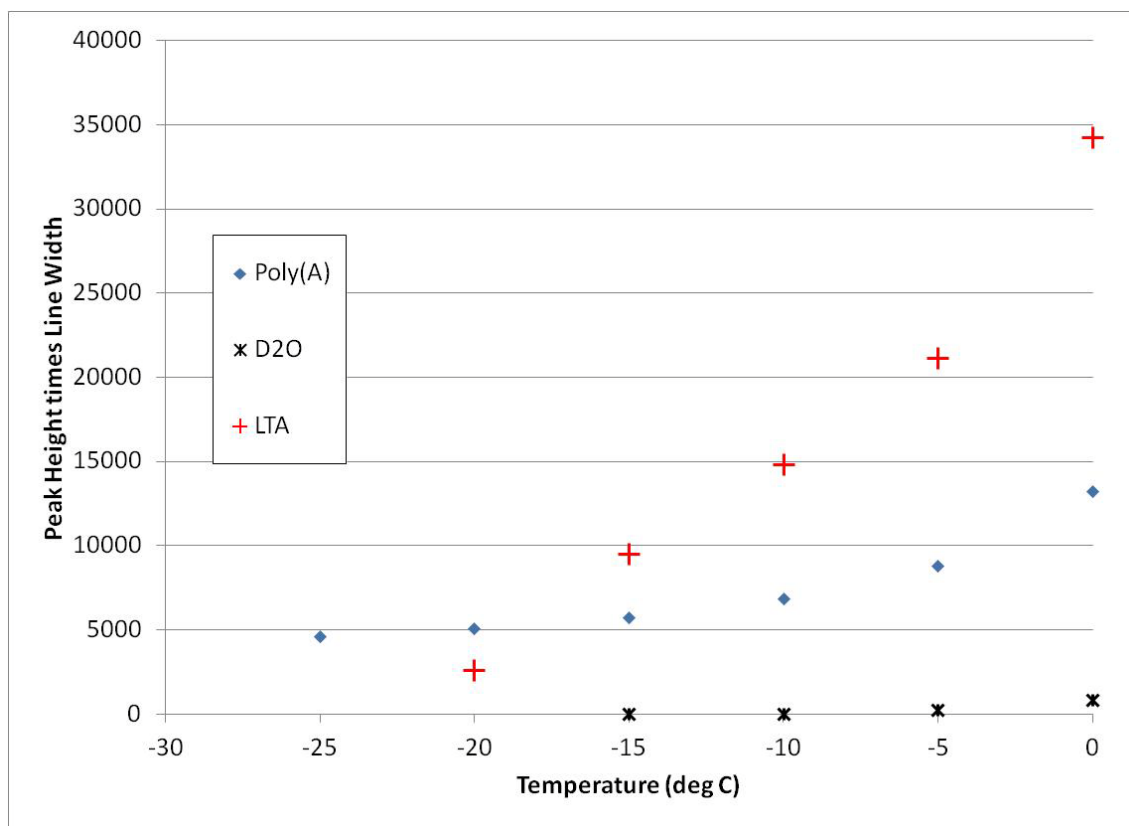


Figure 5.9. Poly(A) compared with D₂O and LTA using data from Table 5.1. The LTA is present in this figure and not in Figure 5.8 due to LTA being at 5% w/v and all other samples at 2.5% w/v.

Discussion

From the data, several things are apparent. First, LTA still possesses cryoprotectant abilities based on the SSECHO and S2PUL temperature arrays and the S2PUL quantitative data (the peak height times line width values), although the degree of cryoprotection is not as strong as it appeared in the other deuterium and ³¹P NMR experiments performed previously in the Rice Group. This could be due to the more indirect method of studying the cryoprotection, where the deuterium signal from the D₂O is used to observe the frozen/liquid state of the water whereas, for example, the determination of liquid water in the LTA ³¹P NMR was the appearance or lack of appearance of the

characteristic solid-state phosphorus tensor occurring only when the phosphorus-bearing species is immobile¹⁶.

Second, it is interesting to note in this experiment that the polyadenylic acid, poly(A) maintains some degree of cryoprotectant behavior at a lower temperature than all other molecules studied. The presence of cryoprotection by itself appears to prove the hypothesis that species with polyglycerolphosphate backbones might have cryoprotectant abilities, but it is unclear whether the extended cryoprotection can be interpreted to mean that poly(A) could be better as a cryoprotectant than LTA, given the extreme low temperatures that LTA has exhibited cryoprotection.

Third, it appears as though double-stranded species such as the DNA and the poly(A:U) do not have as strong a cryoprotectant effect as single-stranded species such as poly(A) and LTA. This could be explained by the cryoprotection being an effect of the molecular motion of the single-stranded species; when the ability of the molecule to have free motion is curtailed due to the hydrogen-bonding between the nucleotides, the motion is reduced and there is less liquid water. (³¹P NMR studies of poly(A), poly(A:U), and RNA from *Saccharomyces cerevisiae* indicate that the mixed RNAs of the baker's yeast are in an intermediate state of cryoprotection between the immobile poly(A:U) and the more mobile poly(A)¹⁸.)

Fourth, it is also interesting to consider poly(A) as a potential cryoprotectant species given the presence of poly(A) tails on the ends of messenger RNAs. However, the known function of the poly(A) tails is not to

provide cryoprotective benefits but to prevent degradation of the mRNA by exonucleases and enhance transcription¹⁹ and that it is obvious that not all organisms express cryoprotective behavior. As LTA's importance in Gram-positive bacteria and its already-determined cryoprotective effects have been mentioned above, it is tempting to think that perhaps, since poly(A) does exist in most cells and throughout all three domains of life, that it might have some ancillary role for cryoprotection. Perhaps poly(A) may have exhibited cryoprotectant effects in biological systems in the ancient past, maybe in the cold-origin of the RNA World or in other panglacial eras, and such action was evolved out of with the development of alternative cryoprotectant strategies and a warmer Earth.

Finally, there is the concern that results of cryoprotection may not be valid due to the possibility that the presence of any additive to water will affect the freezing point or cause some liquid water to still exist at the interface between the solute and the water²⁰. This might be the case considering that even non-PGP-bearing molecules such as bovine serum albumin exhibited some cryoprotective behavior. However, this concern may be mitigated because water is known to exist in a boundary layer between proteins and bulk solution. Moreover, I suggest that the magnitude of the cryoprotection exhibited by LTA and poly(A) indicates behavior above and beyond what might simply be associated with 'unfrozen' water bound or in such a monolayer around proteins or other biomolecules; in addition such behaviors would not

explain the much lower temperatures of mobile water as shown in the ^{31}P NMR experiments performed previously to this work.

As far as future lines of research, experiments have been underway to examine whether LTA provides cryoprotectant effects *in vivo* through addition of LTA or other antifreeze compounds to growing vegetative cells prior to a freezing process and then examining viability of the cells after thawing, with the assumption that cell death would be the result of freezing. Such a cryoprotection effect would also verify that the above results from the present experiment described were not due to simple physical effects but had biological relevance. As previously mentioned at the conclusion of the fluorescence chapter of this work, preliminary results from other members of the Rice Group indicate that addition of LTA to vegetative cells provides cryoprotectant effects enabling vegetative cell survival at -20°C comparable to addition of glycerol. However, studies comparing poly(A) to glycerol performed by others in the Rice Group suggest that poly(A) did not provide similar benefit *in vitro*.

Conclusions

In order to test whether similarly-organized biomolecules to lipoteichoic acids (containing a polyglycerolphosphate backbone) exhibit cryoprotective behavior as LTA exhibited, various molecules were dissolved in D_2O and frozen to study via variable-temperature deuterium solid-state NMR the liquid deuterium signal as the samples were gradually warmed up. Through data obtained using the S2PUL pulse sequence, it was determined that polyadenylic acid (poly(A)) exhibits cryoprotective behavior similar, though not as intense as,

lipoteichoic acids at temperatures close to that of the freezing point of D₂O, but which is greater than LTA at lower temperatures. These results suggest that poly(A) by itself may be a cryoprotection agent, although its applicability *in vivo* for biological systems is unclear.

CHAPTER 6: OVERVIEW OF SPORE-FORMING BACTERIA AND SPORULATION

Introduction

All living organisms have mechanisms to ensure their survival in harsh conditions; many species have evolved to be tolerant to extreme conditions. Some microorganisms have adapted to pressure extremes, such as in deep-sea environments¹, while others have diversified to extremes of high temperatures, salinities, or acidities². A widely studied area of bacterial extremophiles are the psychrophiles, species that are tolerant to sub-freezing temperatures³ and are persistent in conditions such as sea ice in the Arctic⁴. Microorganisms have also been found in conditions which would at first appearance be entirely inhospitable, such as the Atacama Desert of Chile, a hyperarid environment which yet contains viable microbial communities despite the harsh conditions⁵⁻¹⁰.

However, there are some conditions that are too harsh for actively-metabolizing organisms to tolerate; as a result some species of Gram-positive bacteria have developed a method for surviving periods of extreme stresses through metabolic dormancy and formation of a protective coating, which is known as sporulation. *Bacillus subtilis* is typically the microorganism which is studied with sporulation^{11,12}, although other Gram-positive bacteria form spores as well¹³, mainly from the *Bacillus* and *Clostridium* genii¹². This process allows bacteria to survive harsh environmental conditions or nutrient depletion for long

periods of time; one spore strain was recovered, cultured and sequenced after being encased in Dominican amber for millions of years¹⁴.

Spores: structure, process of sporulation, germination

The structure of spores is common to all spore-forming bacteria^{15,16}. The spore is an oval-shaped body, whose size varied by species but generally is about 1 to 1.5 μm in length and 0.5 to 1 μm wide¹⁷ with densities of approximately 1.2 g/mL wet and 1.4-1.5 g/mL dry¹⁸. The spore is layered, with an laminar coat layer^{19,20} surrounding a thick cortex which is comprised of peptidoglycan²¹ which is different in structure and cross-linking density from the peptidoglycan in the Gram-positive vegetative cell wall²². The spore core contains the genetic material of the bacteria, as well as water (though a low amount) and other molecules which serve to protect against damage to the spore's DNA from external factors such as UV radiation²³⁻²⁵.

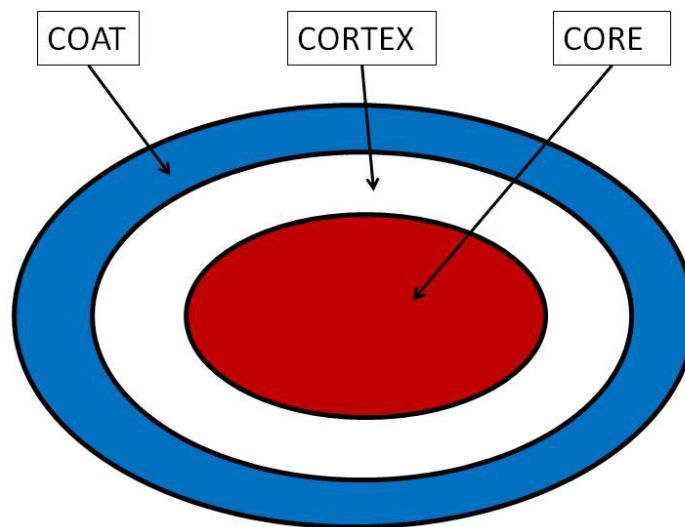


Figure 6.1. Representative schematic of the general structure of a bacterial spore (not to scale).

Sporulation occurs during periods of stress, as mentioned above, with particular attention to nutrient starvation. The sporulation process is well-regulated and can be divided into stages, as shown in Figure 6.2 below. In brief, the initial stimulation to sporulate (as the result of starvation, or any other factor which could act on the phosphor-relay Spo0A²⁶ or, even before that, kinases¹²) triggers the replication of the cell's nuclear material; one copy of this material is separated from the rest of the cell by the formation of an internal septum. The septum acts to engulf the nuclear material and forms an enclosed membrane, dividing the bacterium into a 'mother cell' and a forespore, each of which acts independently but cooperatively in the remaining stages of sporulation. In turn, the two produce various proteins and other material that forms a thicker core membrane, then the formation of the peptidoglycan cortex, and then the layers of the spore coat, until a fully-formed spore has been completed. The mother cell then lyses, releasing the spore into the environment. The spore is metabolically dormant until conditions around it indicate that it is 'safe' for the spore state to end, through the diffusion of nutrients or other materials into the spore, which stimulates the germination process.

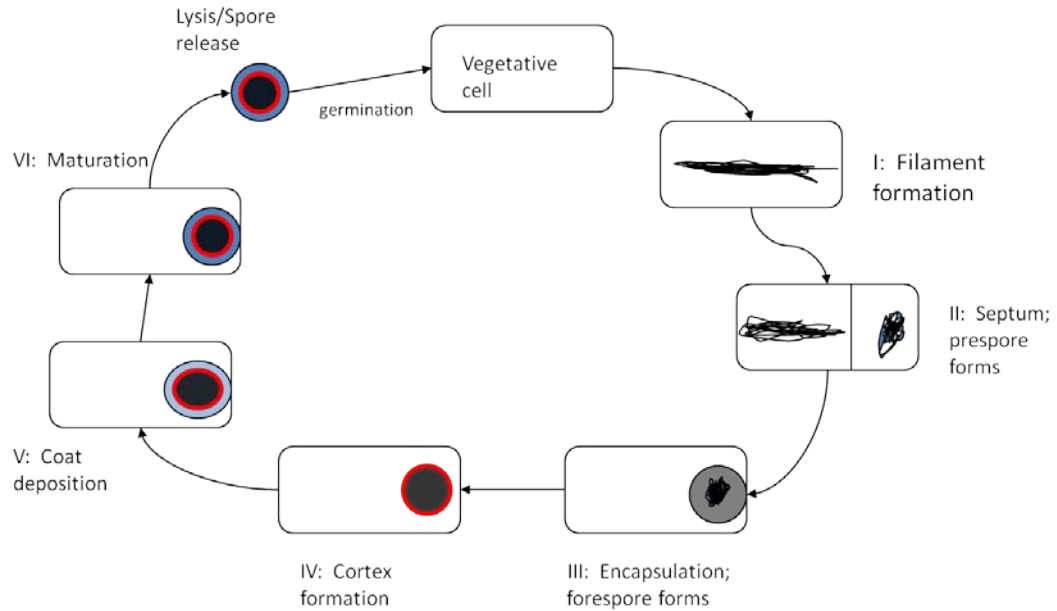


Figure 6.2. Diagram of the steps of sporulation, and the addition of germination to form a cyclical trend.

In the germination process^{27,28}, germination receptors are activated by reception of nutrients; in some cases, exogenous presence of a molecule associated with the spore core, dipicolinic acid, associated with a calcium cation²⁹, may induce germination even without the presence of nutrients. During germination, the calcium dipicolinate is released from the core, associated with rehydration of the spore core; this is then followed by hydrolysis of the cortex and the reactivation of metabolic processes, reformation of the cell wall, and then degradation of the spore coat to expose a vegetative cell. This process can be followed in real-time through the use of phase contrast microscopy techniques, since dormant spores have a distinctive phase-bright appearance of their cores due to the density of the material, which becomes phase-dark when the core is rehydrated³⁰.

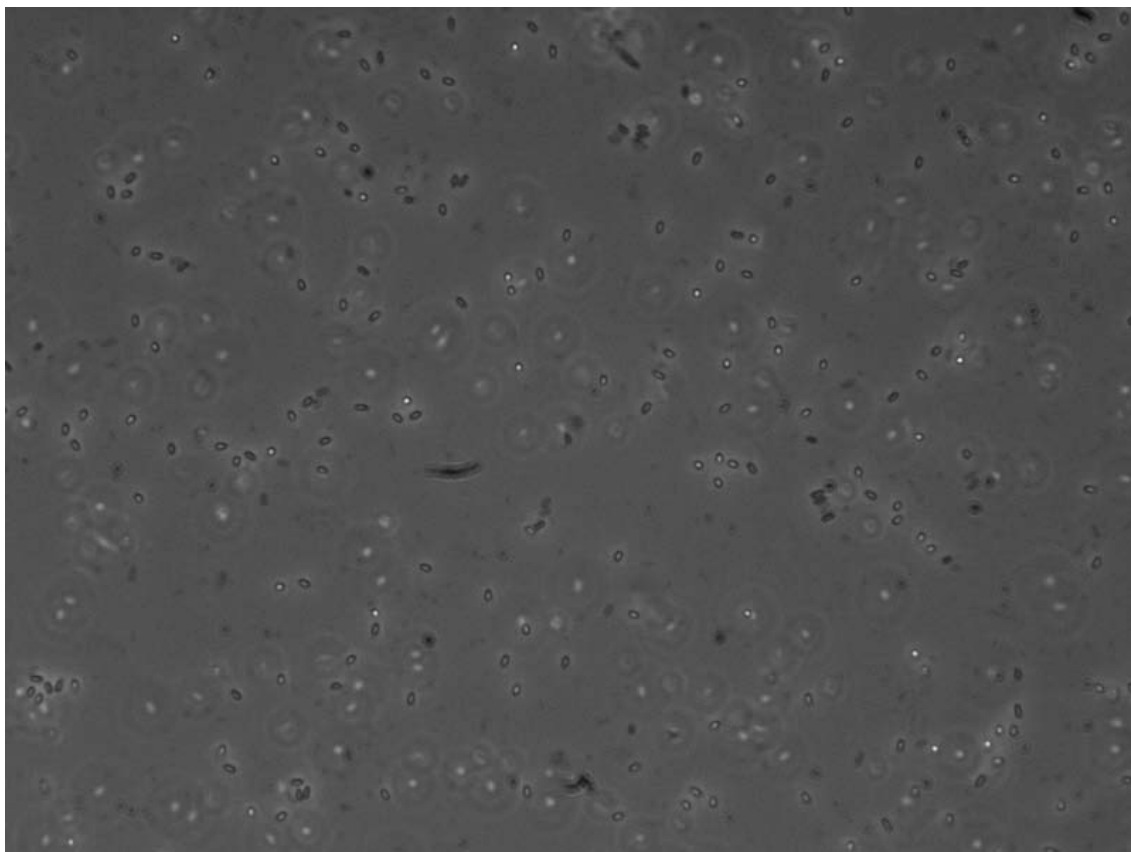


Figure 6.3. Spores of *B.pumilus* SAFR-032 shown under phase contrast microscopy; dormant spores have a phase-bright core, while germinating spores with hydrated cores would show as phase dark.

Each part of the spore provides its own contribution to the overall resistance against degradation:

Spore coat. The assembly and role of the spore coat has been described in detail¹⁹. In brief, coat assembly occurs as part of the defined sporulation program guided by coat assembly proteins formed in the mother cell and attached to the membrane of the forespore, most notably SpoIVA and CotE^{31,32}. The coat can be divided into distinct inner and outer layers, and is resistant to most attempts to solubilize it³³. Loss of the spore coat, either through chemical decoating or deletion mutants, has been shown make spores

highly sensitive to lysozyme and hydrogen peroxide treatment, and in most cases sensitizes them to UV radiation exposure³⁴. In addition, loss of spore coat layers also had negative effects on survival of spores in simulated Mars environments³⁵.

Cortex. The peptidoglycan cortex is implicated in spore dormancy and heat resistance³⁶. The primary theory is that the cortex is able to swell and contract in order to promote maintenance of a dehydrated core; strains with more crosslinking and thus less flexibility exhibited lowered heat resistance³⁷. In addition, the altered structure of the peptidoglycan shown above, with the muramic lactams, is necessary for spore germination, as the lactam is a target for site-specific cleavage of the peptidoglycan; mutants without the muramic lactam are unable to germinate as the cortex cannot be degraded³⁸. Interestingly, it appears that coat assembly is a requisite for cortex formation, as defects in coat assembly prevent cortex assembly in spores³⁹.

Core. The core contains numerous small molecules that are involved in various spore resistances. One of those is dipicolinic acid, as already mentioned above²⁹, which appears as a 1:1 chelate with Ca^{2+} . This molecule is essential for the stability of spores, as spores without DPA are described as being unstable and tended to spontaneously germinate⁴⁰. The dipicolinic acid (DPA) is in the core, comprises 5-15% of the total dry weight, and is synthesized in the mother cell¹⁵ and transported into the forespore by the SpoVAD protein⁴¹. DPA in the core (as calcium dipicolinate) is extremely concentrated, above its solubility, and more similar to a dry powder as

determined by Raman spectroscopy than a solution⁴²; spores without DPA have higher core water contents and as well as being more prone to spontaneous germination, are more susceptible to heat treatment and peroxide exposure²⁴. The DPA is released during germination⁴³; germination can be induced by exogenous calcium dipicolinate²⁹.

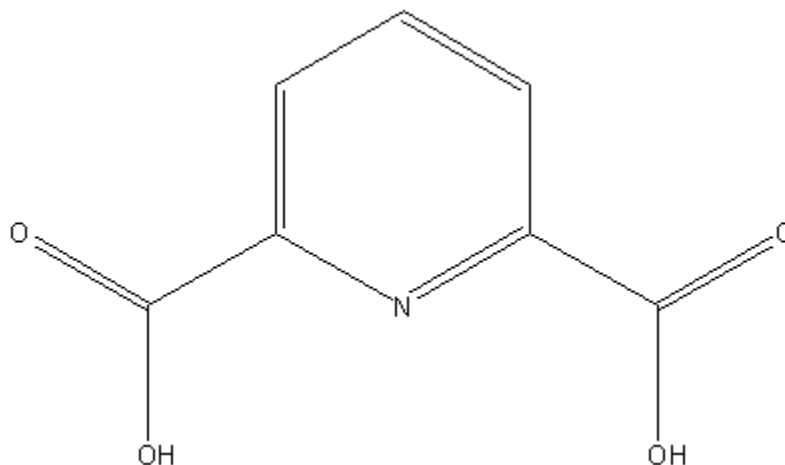


Figure 6.4. The structure of dipicolinic acid (pyridine-2,6,-dicarboxylic acid); in the spore core the molecule is negatively charged and associated with a Ca^{2+} cation.

Another set of core-associated molecules are the small acid-soluble proteins (SASPs). These molecules have been studied as well for some length of time⁴⁴⁻⁴⁶ due to their association with the spore core. These SASPs were originally thought of as a mechanism for producing amino acids for enzyme processes at the outset of germination⁴⁴, though they have since been found to be responsible for UV protection of the DNA in the spore core⁴⁶ through the reduction of UV damage and mutagenesis of the DNA and leaving any damage in the form of spore photoproduct, which is easily repaired in the initial steps of germination⁴⁵. SASPs are also indicated to provide resistance to dry heat inactivation, again by prevention of DNA damage⁴⁷, and DPA cooperates with

the SASPs to ensure, again, that most DNA damage by UV irradiation is as the easily-repaired spore photoproduct and not as more permanent damage⁴⁸.

Spores: significance

There are several reasons why studies of spores are of importance. The first is that spores are ubiquitous in our environment, found in soils, on rocks, and in other locations as well⁴⁹. Several review articles^{25,49} make the point that spores have been found in every ecosystem on the planet, and in addition to the 25-to-40 mya spores recovered from the Dominican amber, a paper in 2000 reported a novel species recovered from a salt crystal dating to 250 million years ago⁵⁰.

Another reason is that several spore-forming species are responsible for infectious diseases and other maladies. For example, *Clostridium difficile* is an anaerobic Gram-positive spore-forming bacteria that is responsible for recurring, nosocomal, and antibiotic-associated gastrointestinal disorders⁵¹ and which is infectious, especially in hospital environments⁵². Botulism is another disease caused by a spore-forming bacterium, *C.botulinum*⁵³. Anthrax, a considerably more studied organism due to the 2001 anthrax attacks, is caused by *B.anthraxis*⁵⁴, and apart from the disease itself, is difficult to properly sterilize out of some environments, such as office buildings⁵⁵.

A third reason is that spores can survive in extreme conditions, as mentioned before²⁵, which could cause problems in the field of space research. Specifically, the ubiquity of bacteria, even inside of 'clean room' facilities for spacecraft assembly⁵⁶, poses concerns about the ability of normal sterilization

and cleaning protocols to lower microbial loads on spacecraft. Current policies are defined in a way to limit the possibility of forward contamination by spacecraft missions⁵⁷; however, given the growing evidence that bacteria (and spore-formers in particular) could survive on Mars to some extent given tests using simulated environments⁵⁸⁻⁶⁰, there is a concern that unless better ways of sterilization are found that forward contamination might occur, or alternatively, that false positives might occur on any life-detection missions⁶¹.

Nature of water in the core of bacterial spores

A key question that has not been adequately explained in the literature is 'What is the nature of the water inside the core of a *Bacillus* spore?'. Core water, at least the lowered levels of it compared to vegetative cells, has been implicated in aiding the resistance to bacterial spores to wet heat treatment²⁵, and several papers have tried to determine the actual state of water in the spore core. Sapru and Labuza in 1993⁶² suggested that, among other reasons, the presence of dipicolinic acid at high concentrations leading to reduced motion of DNA by phosphorus NMR studies would lead to a core state where the contents—water, nucleic acids, dipicolinic acid, and other molecules—was not liquid, nor a well-defined crystal, but in an amorphous 'glassy' state. Ablett's work in 1999⁶³ using differential scanning calorimetry (DSC) and carbon-13 NMR indicated that it was likely, based on transition temperatures and the presence of a carbon signal for calcium dipicolinate only in a CPMAS (cross-polarization magic-angle spinning) spectrum (associated with a solid or immobile state) rather than an SPMAS (single-polarization magic-angle

spinning) spectrum (associated by the authors as being a mobile regime), that a glassy state was likely in an endospore core.

However, Sunde in 2009⁶⁴ seemed to reject that hypothesis. His work, using deuterium and oxygen-17 NMR on *B.subtilis* spores, suggested to him that the water in the core was more mobile than Sapru and Ablett were implying, and that while it was possible that the core water was 'bound', that would not necessarily imply a glassy state—"Core water is both bound and mobile, and there is no contradiction in this" (Sunde 2009, 19338). He suggested instead that the phenomenon of heat resistance being related to core water content was not due to a formation of a glassy state but rather to the prevention, due to low hydration, of thermal denaturation of proteins in the core, thus hindering any aggregation or irreversible conformational changes to enzymes and proteins necessary for metabolic function when the spore germinates.

In addition, there is a question as to other resistances are related to the state of water in the spore core. Ablett and Sunde's papers above were done using *B. subtilis* spores, and Sapru's paper reported glass transition temperatures from literature for mainly *B.stearothermophilus* and *C.botulinum*, though with references to *B.megaterium*, *B.subtilis*, and *B.cereus*. One question was whether a spore species with higher levels of resistance to methods of inactivation rather than heat treatment would have the same state of core water as well-studied species such as *B.subtilis*. A recently-isolated species of spore-forming bacteria proved to be worth a comparative study.

Bacillus pumilus SAFR-032: novel spore isolate with enhanced resistance

A strain of *Bacillus pumilus*, SAFR-032, was first reported in a partially-sequenced 16S ribosomal genome that was submitted to GenBank under accession # AY167879 on October 21, 2002 from the Jet Propulsion Laboratory⁶⁵ and first noted in publication in 2004 by Link and others⁶⁶ when discussing *B.pumilus* isolates from JPL's Spacecraft Assembly Facility and their resistance to UV radiation when compared to the type strain, *B.pumilus* ATCC 7061, as well as a biosimetry strain of *B.subtilis*, WN624. This paper noted that against 254-nm wavelength UV radiation, all of the isolates were more resistant than the type strain, and one, SAFR-032, was extremely resistant (~339 times more resistant relative to *B.pumilus* ATCC 7061); it was noted that, after reporting on LD₉₀ (lethal dose for 90% population) and D (dose producing one log of inactivation) for the spore isolates, SAFR-032 was "...the most highly UV-resistant spores yet to be discovered..."⁶⁶ (Link 2004 161). In addition, while attempting to relate the enhanced resistance to peroxide resistance, SAFR-032 was discovered to have enhanced resistance to 5% hydrogen peroxide compared to the type strain.

In a paper in the following year, various *Bacillus* species were tested for survival under simulated Mars UV conditions, including *B.pumilus* SAFR-032⁶⁷. Again, it was the most UV-resistant species of all tested, being the only species that was not totally inactivated during the limits of exposure (30 minutes) to full-spectrum (200-400 nm) UV exposure and which consistently showed higher LD₅₀ and LD₉₀ values than other species. The authors, reminding the reader

that SAFR-032 was isolated from the JPL Spacecraft Assembly Facility (as all of the *B.pumilus* isolates were), "...it is likely the *B.pumilus* strains adapted over time to the conditions present in the spacecraft assembly facilities, and this may explain their elevated levels of resistance⁶⁷" (Newcombe 2005 8155).

In 2007, the genome of SAFR-032 was sequenced to identify genes that could explain the UV and peroxide resistance apparent to that strain⁶⁸. The results were, as the paper's title put it, 'paradoxical' as there are several genes known in *B.subtilis* and *B.licheniformis* that serve oxidative stress response, peroxidase function, or UV protection/DNA repair that have no homologous gene in *B.pumilus*, yet there are novel genes in SAFR-032 that may be responsible for ensuring the UV/peroxide resistance. This is emphasized by results showing survival of SAFR-032 to greater extent than *B.subtilis* and *B.licheniformis* species in both UV and 5% hydrogen peroxide exposure (Figure 7, below). In addition, research last year showed that SAFR-032's peroxide resistance could stem from a combination of manganese catalases, one not present in the type strain, the tendency of these catalases to be concentrated in the coat, and for the product of the reaction of these catalases with peroxide to be oxygen which forms a physical gas barrier to further diffusion of the peroxide through the spore⁶⁹.

Last year, the first publication reporting results from long-duration exposure of *B.pumilus* SAFR-032 onboard the EXPOSE facility attached to the International Space Station were reported⁷⁰. In it, it was indicated that spores of SAFR-032 exhibited very high survival when shaded from solar radiation, both

in vacuum and in simulated Martian atmosphere. While exposure to direct solar UV radiation caused massive (~> 7log) reductions in the top-most exposed layer of spores, regardless of atmospheric conditions, spores on coupons shaded by being in middle or bottom trays exhibited comparable survival to their dark counterparts, and there were a small handful (<20) of viable spores that were recovered from the top layers which, when cultivated, produced a generation of highly UV-resistant spore variants of SAFR-032. The authors conclude that this demonstrates that spore species, at least SAFR-032, are capable of long-duration survival in space conditions.

Another reason why spores and spore survival are a topic of key interest lies in the topic of lithopanspermia, that is, the idea that microbes from one inhabited body could be transported to another habitable body inside of rocks. This topic has been mentioned in several recent reviews^{25,71-73}. The principle of lithopanspermia in these reviews is that microbes inhabiting interior surfaces of rocks could survive ejection from a planet's gravity as a result of spalling during an impact event, subsequently survive interplanetary transit protected from UV, desiccation, low temperatures, and vacuum, survive planetary re-entry, and colonize their new environment. These reviews indicate that certain bacteria and lichen species have been able to survive exposure to the acceleration forces that spalling would produce, and that it is possible for the environment in the interior of re-entering rocks or meteorites to not heat beyond tolerable levels. As previous research has shown the ability for some spores to survive

prolonged exposure to real-space conditions⁷⁰, hardy spores would be the most optimal biological candidates for lithopanspermia.

Conclusion

Bacterial spores are extremely hardy microorganisms capable of surviving extreme conditions and are ubiquitous through the biosphere. Their protective layered structure and metabolically-inactive core allow for long-term survival under desiccating conditions and conditions of low nutrients, and spores have been found in locations designed to prevent biological contamination. However, there are some aspects of spore resistance and function, such as the nature of the water inside the core of dormant spores and how it affects resistance, that are still not fully understood. Since deuterium NMR had been previously used in the Rice Group as mentioned earlier in this work to determine the state of water with cryoprotectants, it seemed natural to use that approach to study this particular problem of bacterial spores.

CHAPTER 7: DEUTERIUM SOLID-STATE NMR EXPERIMENTS ON BACTERIAL SPORES—INSIGHTS INTO THE NATURE OF WATER INSIDE THE SPORE CORE

Introduction

In order to perform the sorts of experiments needed to try to answer some of the questions introduced in the last chapter of this dissertation, a viable protocol for sporulation and for NMR analysis of the spores is required. This protocol must ensure that bacteria will make spores with both sufficient purity and amount for NMR analysis, and that the NMR experiments will provide useful structural information which can be used to find insights in the structure of the spore and the nature of the water inside of the spore cores. A proper experimental protocol may be able as well to determine if there are structural differences in *B.pumilus* SAFR-032 that can be related to and explain some of its increased resistance to UV radiation, peroxide exposure, and other nominally lethal hazards. As such, this chapter will describe the materials, methods, and other experimental protocols for spore experiments, as well as showing and discussing the results of those experiments.

Materials

Bacillus subtilis ATCC 6051 was obtained from the Bacillus Genetic Stock Center (BGSC, Columbus, OH), and is the wild type strain of *B.subtilis* as originally identified by Conn in 1930¹ as the Marburg strain.

Bacillus subtilis 1A578 is a chloramphenicol-resistant mutant of *B.subtilis* 168² obtained from Dr. Phillip Klebba (University of Oklahoma), itself a

tryptophan auxotroph of the *B.subtilis* type strain³ which had lost some behaviors of the wild-type bacteria through domestication⁴.

Bacillus pumilus SAFR-032 was provided by Dr. Parag Vaishampayan (Jet Propulsion Laboratory, California Institute of Technology, Pasadena, CA) and was isolated as described above.

Deuterium oxide, 99% purity, was used as purchased from the departmental stockroom from Cambridge Isotope Laboratories (Andover, MA).

MOPS buffer (3-(N-morpholino)propanesulfonic acid), Calbiochem brand, was used as purchased (EMD Millipore, Billerica, MA).

Yeast extract (Thermo Fisher Scientific, Waltham, MA) and tryptone (Bacto brand, Benton-Dickinson, Franklin Lakes, NJ) were used to prepare LB media.

Distilled water as needed was provided by a Milli-Q Reagent Buffer System (Millipore, Billerica, MA).

Chloramphenicol was purchased from Sigma (Sigma-Aldrich, St. Louis, MO).

New Brunswick Scientific Co. (now Eppendorf, Enfield, CT) incubators (floor-model Series 25 and benchtop G24 incubator-shakers) were used for bacterial growth.

Beckman (now Beckman Coulter, Indianapolis, IN) J2-HS centrifuge, along with Beckman JA-14 and JA-17 rotors, were used for centrifugation and purification steps.

Samples were freeze-dried using a Labconco (Kansas City, MO) FreeZone 1 lyophilizer (1L capacity).

Equipment for NMR analysis were used as previously described during the VT deuterium NMR of proteins and nucleic acids in this dissertation. In brief, NMR experiments were conducted on an Oxford 400 MHz (9.4T) superconducting magnet using a Varian Instruments 400 MHz 5mm deuterium wideline probe (*sfreq* = 61.424 MHz), with data collected using a Varian Unity*plus* console and displayed using Varian VNMR (v 6.1c) software on a Sun SPARCstation 20 workstation running the Solaris operating system. VT experiments were performed using in-house nitrogen gas controlled by an FTS Systems Airjet chiller (model XRIIB51A00), an FTS Systems temperature controller (TC-84, model XRTCA-0), an Oxford probe temperature controller and Sorenson DCR-13B power supply for probe heating. Sample temperature was regulated independently of nitrogen gas temperature, setting the latter cooler than the former and using the probe heater to maintain the sample at desired temperature (via *temp*). Software control of the temperature during experimentation was achieved using arrays of *temp* and the parameter *vttemp=1*. An upper barrel assembly directed the gas up through the bore of the magnet and out the top to prevent condensation inside the magnet bore or on the probe. A schematic is shown below as Figure 7.1; for non-VT experiments, the temperature controllers and chillers were disconnected and the sample was run at ambient temperature (~20-21°C).

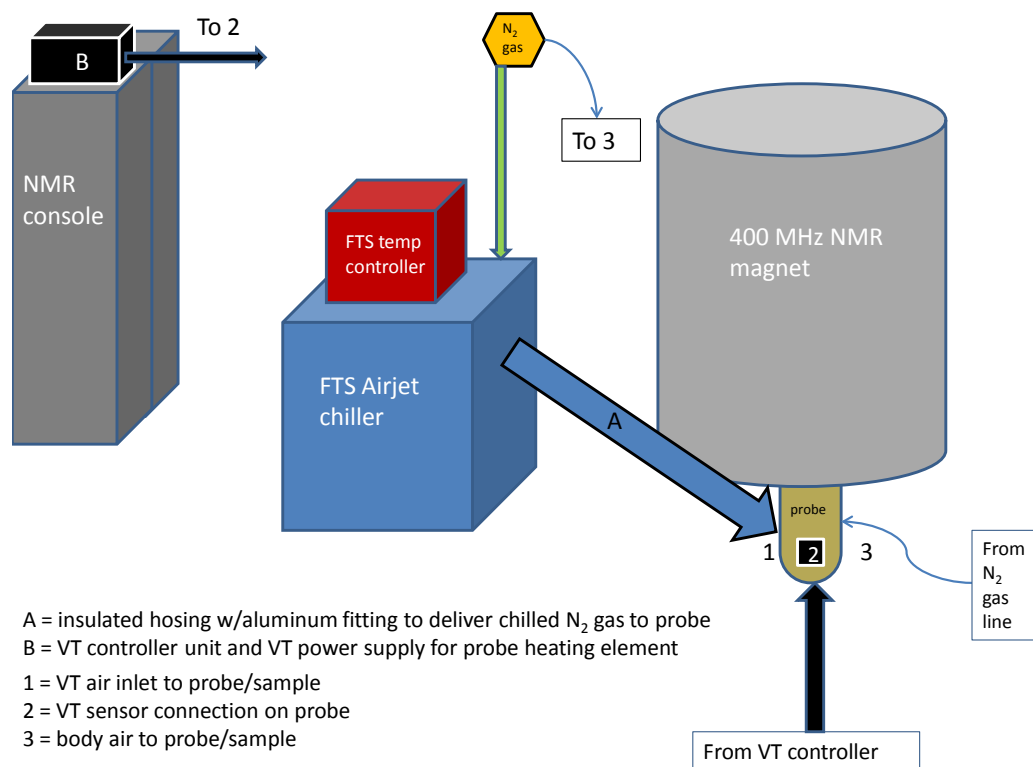


Figure 7.1. Schematic representation of VT NMR system for experiments.

Experimental Procedure

Preparation of sporulation medium

A medium, Chemically Defined Sporulation Medium (CDSM), was prepared using a derivative method from that of the original author⁵. In a large beaker, the following chemicals were added to a volume of distilled water (approximately 20 to 50 mL less than the desired volume): MOPS buffer, 8.3704 g/L; ammonium sulfate, 1.2458 g/L; potassium phosphate, monobasic, 0.5444 g/L; D-glucose, anhydrous, 3.6032 g/L; and L-glutamic acid, 1.4971 g/L; this was then mixed with a stir bar on a stirrer/hot plate until dissolved. L-lactic acid, 10 mL/L of a 0.5M solution (0.4504 g/L net final mass), and 20 mL/L of a premade metals solution (MT mix, 50x; 1L stock with final concentrations of:

MgCl₂, 0.2M; CaCl₂, 70mM; MnCl₂, 5mM; ZnCl₂, 0.1mM; FeCl₃, 0.5mM; thiamin HCl, 0.2mM; HCl, 2mM) were then added. The pH was adjusted to 7.00 by adding dropwise concentrated NaOH solution, then the volume was adjusted to the desired amount by addition of distilled water. This solution was then filtered through a sterile screw-top 0.2 µm pore-size SFCA (surfactant-free cellulose acetate) filter (Nalgene, Thermo Scientific, Waltham, MA) into a sterile screw-top bottle of the desired capacity and stored at RT until use.

In addition, two other solutions necessary for CDSM usage were made as needed. 100 mg of L-tryptophan and L-isoleucine were dissolved in 5.0 mL, respectively, of 0.2 M HCl and distilled water in 50 mL Falcon tubes, mixed with a vortex mixer until fully dissolved, then syringe-filtered using 0.2 µm sterile filters into sterile 15 mL Falcon tubes. These tubes were Parafilmed, with the L-tryptophan solution covered in aluminum foil to prevent light reacting with the tryptophan, and stored at RT until needed (final concentration 20 mg/mL). These solutions would be remade as needed as the tryptophan would eventually (over two to three weeks) break down as evidenced by a color change of the solution from clear to progressively darker shades of orange-red color.

Preparation of LB media

LB media was made via mixing, in the desired volume of distilled water, 10 g/L tryptone and 5 g/L each yeast extract and NaCl, and stirring until dissolved. The solution was transferred to a screw-top bottle, typically of about twice the volume as the volume of the solution, and autoclaved for sterility;

afterwards it was kept at RT until consumed or until visible contamination was apparent.

Preparation of media—deuterium-labeled media

To grow deuterium-labeled spores, deuterium-labeled media was prepared to either 25% or 40% D₂O concentration. The preparations described above were altered accordingly by replacing a given proportion of water in the LB and CDSM with the desired percentage of D₂O. Sterilization of deuterium-labeled media was universally performed via filtration through sterile screw-top filters in sterile bottles as opposed to autoclaving.

Sterility of media transfer

All transferring of media from stock bottles to experimental containers or glassware were done under sterile conditions via use of sterile glassware, flame-sterilization of the tops of the glassware and stock bottles, and (for volumes less than or equal to 25 mL) sterile transfer pipets.

Growth protocol – B.subtilis species

Initial overnight cultures of *B.subtilis* 1A578 and ATCC 6051 were made through incubating a small amount (~100 µL pipette tip-sized or smaller particles) of frozen stocks of these strains in a 125 mL Erlenmeyer flask containing 20 mL of LB media. These flasks were kept in incubator-shakers at 37°C overnight (16-18 hr) and 200 rpm shaking, and growth of the culture was verified in the morning via turbidity of the culture. For *B.subtilis* 1A578 only, the 20 mL of LB was supplemented by 20 µL of a 10 mg/mL solution of

chloramphenicol to ensure purity of the culture (given 1A578's chloramphenicol resistance locus).

This culture was then used to inoculate a larger-volume culture (typically 200 mL, though 100 mL volumes were also used on occasion) at 1% in LB media. This culture was allowed to grow in the same incubator (at 37°C/200 rpm) for one day. The culture was then centrifuged in a polypropylene 250mL centrifuge bottle for 20 minutes at 10,000xg (JA-14 rotor), the supernatant decanted, and the pellet resuspended in an equal volume of CDSM (as made above). The resuspended culture was supplemented with aliquots of the L-tryptophan and L-isoleucine solutions (250 µL/100 mL) before returning the flask to the incubator at 37°C/200 rpm. Cultures were then allowed to sporulate for between 3 to 7 days, with daily aliquots withdrawn for phase contrast analysis to observe relative proportion of cells that appear as phase-bright spores. Cultures were not purified unless they reached a minimum of 80% spores and appeared that no new spores were forming via phase-contrast images.

Growth protocol—B.pumilus SAFR-032

The growth protocol for *B.pumilus* SAFR-032 was functionally identical to the protocol for *B.subtilis* 1A578 and ATCC 6051 except that the media inoculated using the overnight culture was LB and not CDSM and no substitution/resuspension of media was performed; *B.pumilus* SAFR-032 was sporulated in LB media. This was done after initial testing using small volume cultures (50 mL) determined that the best number of spores seen via phase-

contrast occurred during growth in LB media and not in CDSM nor in another medium studied prior to these experiments, the modified Schaeffer medium (MSM)⁶.

Spore purification

The cultures containing sufficient spores to warrant continuing the protocol were centrifuged in 250 mL polypropylene centrifuge bottles at 4°C under the same conditions as listed above (10,000xg/20 minutes), with the supernatant decanted and the pellet 'washed' (resuspended in sterile distilled water of equivalent volume, followed by recentrifugation at 10,000xg/20 min). After decanting the wash supernatant, the pellet was resuspended in 20 mL of 50% EtOH:distilled water solution and transferred to a 30 mL polypropylene centrifuge tube; the sample was allowed to sit at 25°C for 2 hours without shaking. Following this the sample was centrifuged (JA-17 rotor) at 10,000xg for 20 minutes, decanted, and washed 3x with equal volume of sterile water, with centrifugation after each wash step including the last.

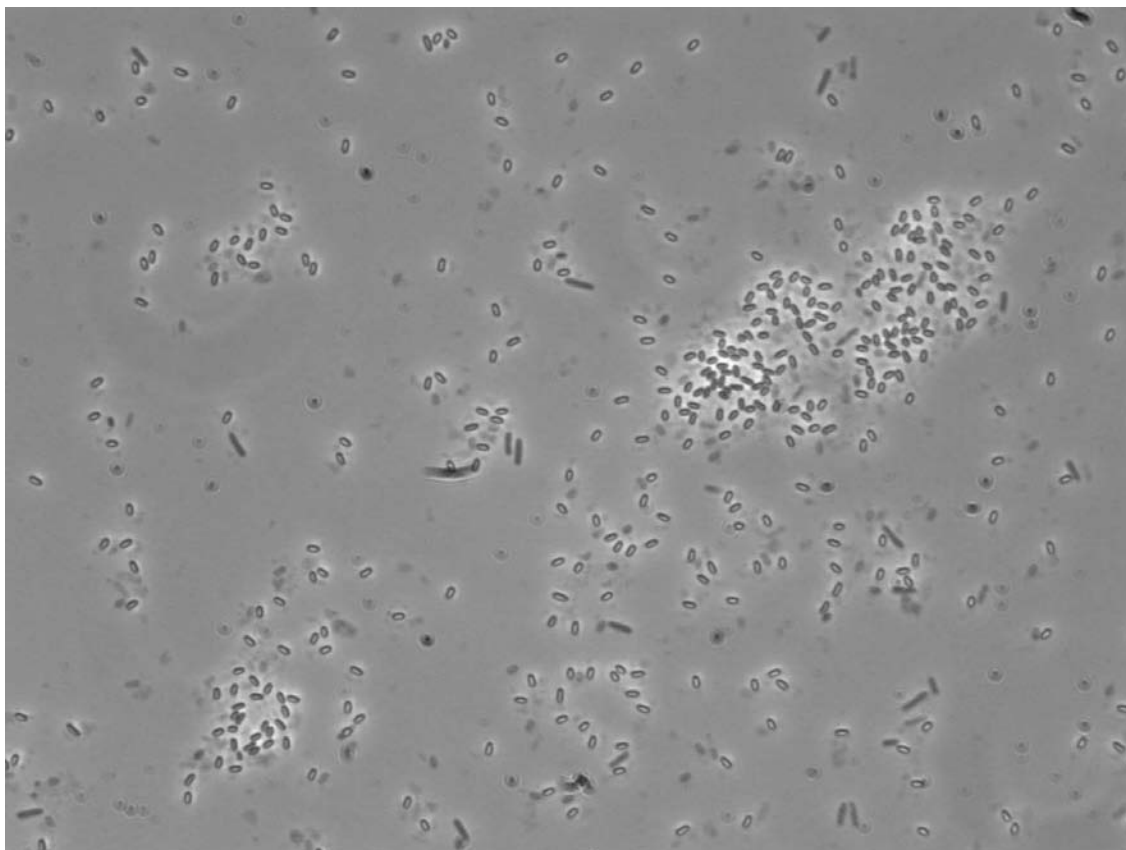


Figure 7.2. Phase contrast microscopy image of *B. pumilus* SAFR-032 spores grown in LB media and subsequently purified (1000x magnification). Spores exhibit a characteristic phase-bright center surrounded by phase-dark coat material.

Following the final wash step and decanting, the pellet was resuspended in 20 mL of water in the same centrifuge tube, parafilmmed, and stored at 4°C overnight. (The water used depended on whether the sample was grown in deuterated media, in which case D₂O was used, or not, in which case distilled water was used.) The following morning, the sample was vortex mixed to ensure the culture was resuspended and subsequently syringe-filtered into a clean sterile centrifuge tube by use of piggybacked syringe filters to catch debris in the media (3.1/1.2 µm). The filtered samples were then centrifuged immediately (10,000xg/20 min), decanted, and resuspended in ~8.0 mL of H₂O

or D₂O in a clean, tared glass vial. The vial was then placed in liquid nitrogen to flash-freeze the sample, followed by putting the vial in a glass container attached to the lyophilizer unit and lyophilizing the sample for a minimum of two days at ~-40°C chamber temperature and 0.05-0.2 mbar pressure. After lyophilization, the dried powder spore samples were weighed and stored at -20°C until used.

Additional samples

Bovine serum albumin (BSA, Sigma-Aldrich, St. Louis, MO) was suspended in D₂O (100 mg/8.0 mL), lyophilized, and used as a standard protein to compare deuterated protein NMR spectra to the spectra of the bulk spore sample.

Deuterated calcium dipicolinate crystals, prepared by other members of the lab according to the method described in Bailey *et al*⁷ and verified to be calcium dipicolinate via X-ray crystallography, were packed in an NMR rotor and similarly ran to observe its spectrum compared to the spore samples.

NMR experiments

Spores that were not grown in deuterated media were deuterated, when needed, by resuspension of already lyophilized spores which were purified and filtered with distilled water for a period of at least one week in D₂O ('D₂O soaking') followed by re-lyophilization. Alternatively, deuterated spores were soaked in distilled water to attempt to remove deuterium from the spores where water is accessible and exchangeable. This process is known as H-D exchange (and the incorporation of deuterium into the spores is D-H exchange).

All samples were lyophilized as powders prior to NMR experiments being conducted.

Powdered samples were packed into 5 mm NMR rotors (typical maximum spore mass that could be packed in those rotors was approximately 30 mg) and sealed using an o-ring cap. The packed rotors were placed horizontally into the static deuterium wideline probe, which was inserted into the magnetic field of the Oxford 400 MHz magnet. No sample spinning or temperature changes were done in these experiments. The RF pulses and data collection were performed by a Varian Unity*plus* NMR console controlled by the Varian VNMR 6.1C software.

Experiments used the solid-state echo (SSECHO) pulse sequence ($90_x-\tau_1-90_y-\tau_2$ -acquire)⁸, with a pulse width of 6 μ s for both 90° pulses, $\tau_1=60$ ms, $\tau_2=50$ ms, an acquisition time of 40 ms, and a recycle delay (*d1*) of 120s (based off of experimental determination that T_1 of deuterated spores was ~ 22 s and the rule of thumb that the recycle delay between pulses should be 5 times the T_1 time). Spectra were collected until either the spectrum appeared to be satisfactorily well-resolved or until the desired number of transients was collected (10,000). The FID was left-shifted so that the Fourier transformation was performed with the FID starting at the peak echo, with the resulting spectrum phased to provide maximum intensity of the central peak and equivalent peak heights for the deuterium Pake pattern horns.

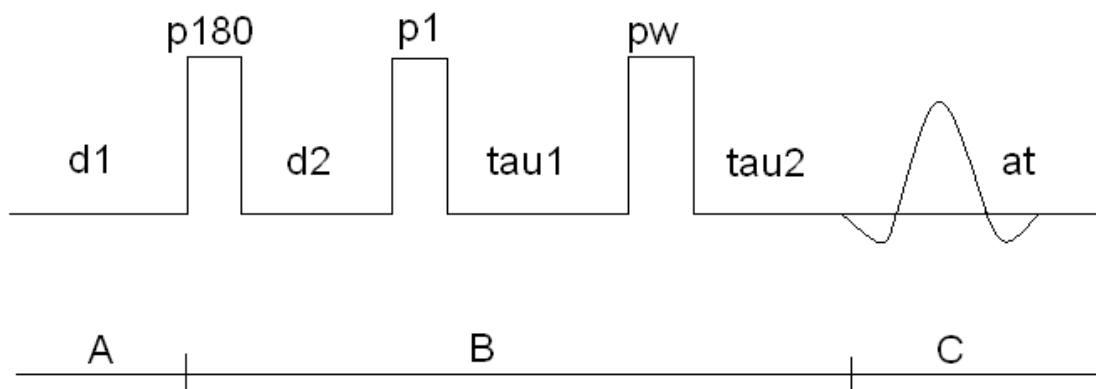


Figure 7.3. The schematic of the solid-state echo (SSECHO) pulse sequence, using parameters defined for Varian VNMR and VNMRJ software. The initial 90° pulse is $p1$, the second 90° pulse is pw . $p180$ and $d2$ are optional properties and were ignored ($p180$, $d2=0$).

The NMR experiments were divided into different sets depending on the sample:

- 1) Comparisons between different spore strains, to determine if there was any observable difference in their NMR spectra that might belie a physical or structural difference.
- 2) Comparisons between different states of the same spore species, i.e. attempting to determine the permeability and exchangeability of protons and deuterons by comparing a spore sample that is deuterated and then performing H-D exchange. This was also performed in the opposite manner, taking a non-deuterated spore species and deuterating them.
- 3) Attempts to identify features of the spore spectra through comparing their spectra to the spectra of deuterated BSA and calcium dipicolinate.

Results

Variable-temperature deuterium NMR of deuterium oxide

First, it is necessary to show what is considered to be ‘mobile’ and ‘immobile’ water in the context of deuterium solid-state NMR studies. As such, Figures 7.4 and 7.5 below are the spectra from a deuterium VT NMR experiment with pure deuterium oxide using the SSECHO pulse sequence. Figure 7.4 is the spectrum of D₂O with the SSECHO pulse sequence at -40°C; Figure 7.5 is the same sample and same pulse sequence at 0°C.

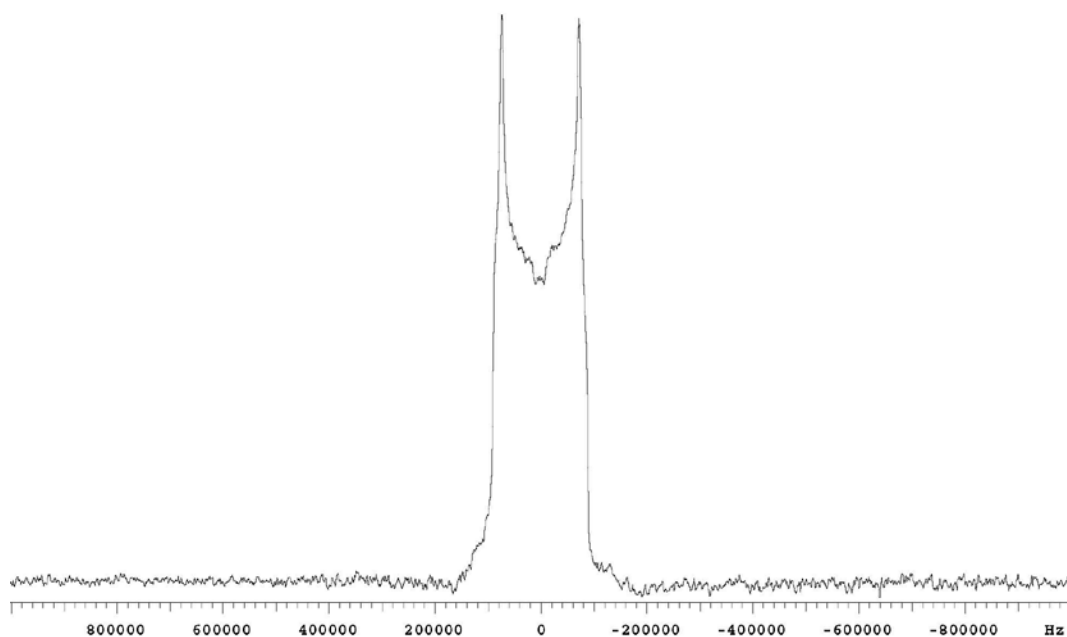


Figure 7.4. Solid-state VT ²H NMR spectrum of D₂O at -45°C.

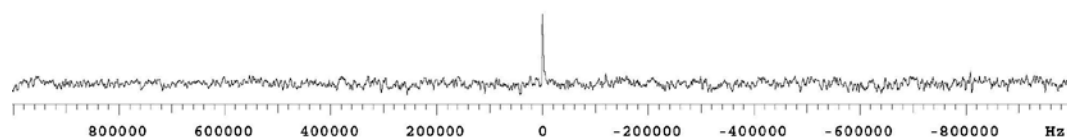


Figure 7.5. Same sample of D₂O using VT ssNMR, at 0°C.

As described in the background of the NMR theory, including deuterium NMR, the deuterium signal of immobile/solid molecules, in this case Figure 7.4 (being frozen D₂O), has a characteristic doublet peak similar to the Pake pattern but with a different range between the peaks (3/4ths of the quadrupolar coupling constant rather than being the dipolar coupling constant). As the sample was warmed from minus 45°C to 0°C, the Pake-pattern-like peaks quickly fade away, indicative that the sample warming has allowed for molecular motion to begin to occur, until at minus 5° and 0°C, a singlet signal which is associated with mobile (liquid) deuterium signals. Thus it appears that signals near to 0 Hz are most associated with mobile deuterium signals, while the Pake doublets are more associated with immobile deuterium.

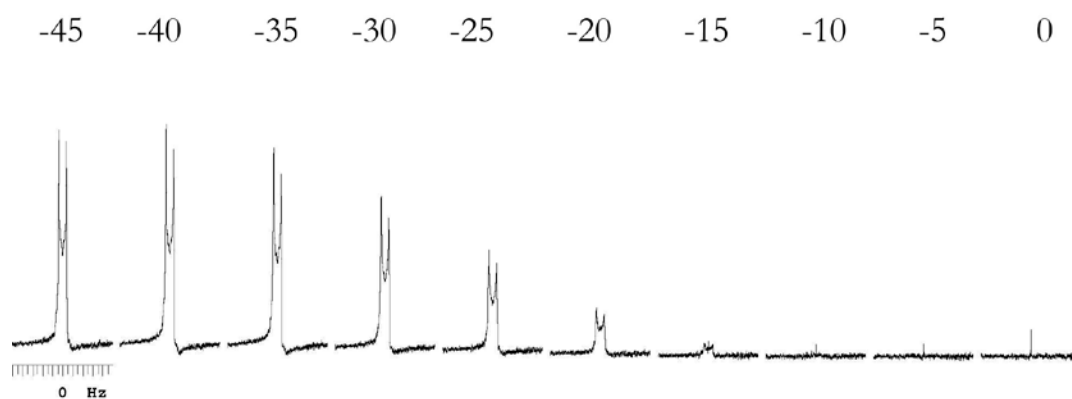


Figure 7.6. The temperature array (labeled with temperature, in °C) from which Figures 7.4 and 7.5 were taken; Figure 7.4 is at left (-45°C), Figure 7.5 at right (0°C).

We can reasonably assume that a sample which might have an array of different mobility states of deuterated molecules would have a variety of signals which would overlap, instead of the distinct signals that have been seen in Figure 7.4 and 7.5 above.

Solid-state deuterium NMR of bacterial spores

With this in mind, the spectra of the lyophilized powders of spores were interesting to look at when compared to the distinct features of D₂O. First, below, is the spectrum of *B.subtilis* ATCC 6051 spores grown in 25% D₂O LB and sporulated in 25% D₂O CDSM:

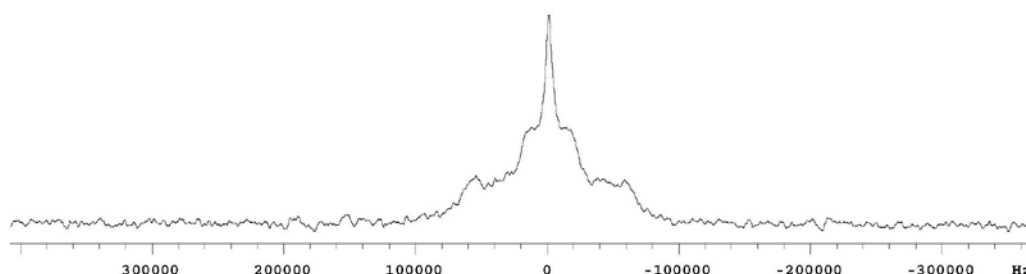


Figure 7.7. Deuterium solid-state NMR spectrum of 25% D₂O *B.subtilis* ATCC 6051 spores (17.0 mg). Note the change in the scale from figure 7.4 and 7.5.

The important feature to notice is that there is more than one deuterium environment present in the spore. There is a large central peak that is, as in Figure 7.5 above, associated with mobile deuterium present somewhere in the spore, but there are two distinct environments of immobile deuterium responsible for the two shoulders of the signal, the inner peaks separated by about 40 kHz, the outer by around 120 kHz. This is narrower than the separation of the Pake doublet for frozen D₂O from Figure 7.4 (~144 kHz). This indicates that some of the deuterium has become incorporated into immobile elements of the spore, perhaps in the cortex peptidoglycan or in the coat proteins, or in the core itself.

Similar lineshapes were observed for the *B.subtilis* 1A578 and *B.pumilus* SAFR-032 25% D₂O spectra, as shown below, though each have some slight differences:

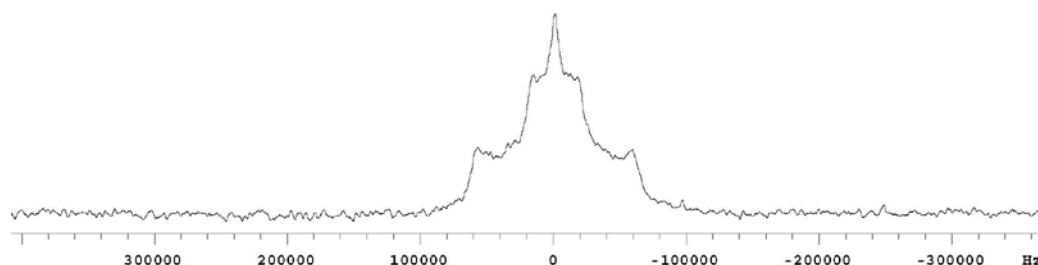


Figure 7.8. ²H NMR spectrum of 25% D₂O-labeled *B.subtilis* 1A578 spores, 19.7 mg, vs (vertical scale)=500k.

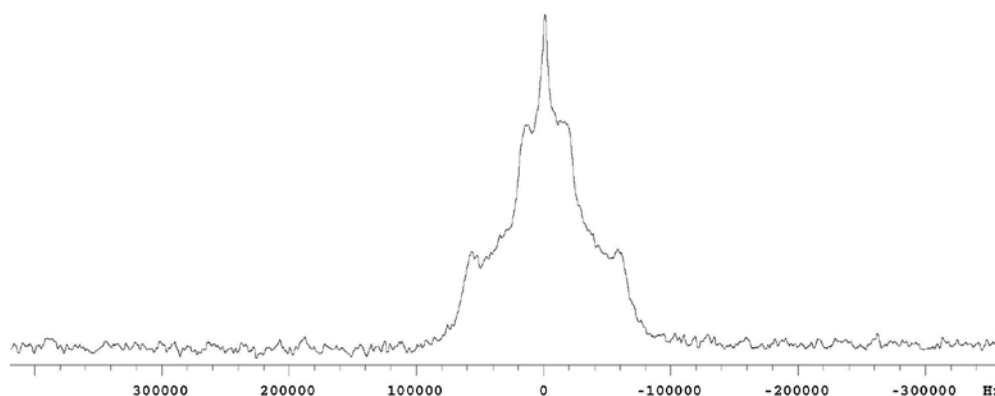


Figure 7.9. ²H NMR spectrum of 25% D₂O *B.pumilus* SAFR-032, 19.7 mg. vs=500k.

The *B.subtilis* 1A578 spores, when compared to the ATCC 6051 strain, appear to have a slightly shorter mobile peak than the ATCC 6051, possibly indicative of a lower water content. In contrast, the *B.pumilus* has a more intense signal based on the steeper transition from the outer immobile-associated Pake peaks to the inner pair to the mobile deuterium peak. This can

be seen more prominently if we overlay the three spectra overtop one another, as seen below in Figure 7.10.

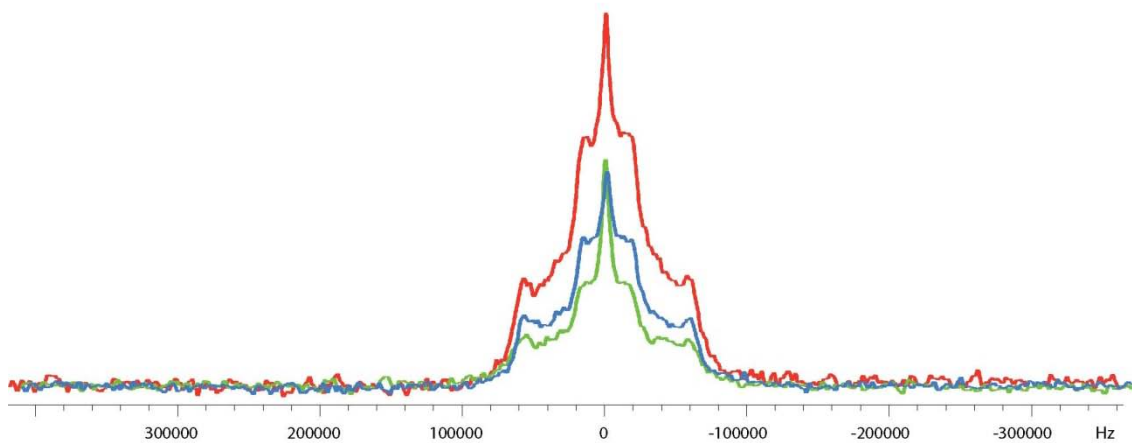


Figure 7.10. Overlays of Figures 7.7-7.9 on the same axis, all at $\nu_s=500\text{k}$. Red = Figure 7.9, the 25% D_2O -labeled *B.pumilus* SAFR-032; blue = 25% D_2O -labeled *B.subtilis* 1A578 (Figure 7.8); green = 25% D_2O -labeled *B.subtilis* ATCC 6051 (Figure 7.7).

Deuterium NMR of bacterial spores: exchange experiments

Subsequently, spores of these bacterial species were subjected to exchange experiments to determine the ability of external water to permeate and exchange with the water inside of the spore. These experiments took two forms. The first experiments took the deuterated spores from Figures 7.7-7.9 and to soak them in distilled water for one week, to attempt to remove deuterium from the spores where the external water could exchange with it. These spores were then rehydrated and re-run on deuterium solid-state NMR with the same parameters to obtain a post-exchange spectrum. This experiment is the H-D exchange experiment. The other experiment was to grow spores in non-deuterated media and soak them in D_2O to introduce deuterium into the spores, then collect a deuterium NMR spectrum to observe

where the exchanged deuterium ended up in the spore. This spectrum was compared with the spectra from spores grown in deuterated media (Figures 7.7-7.9) to observe any differences; this is the D-H exchange experiment. A schematic for these experiments is included below.

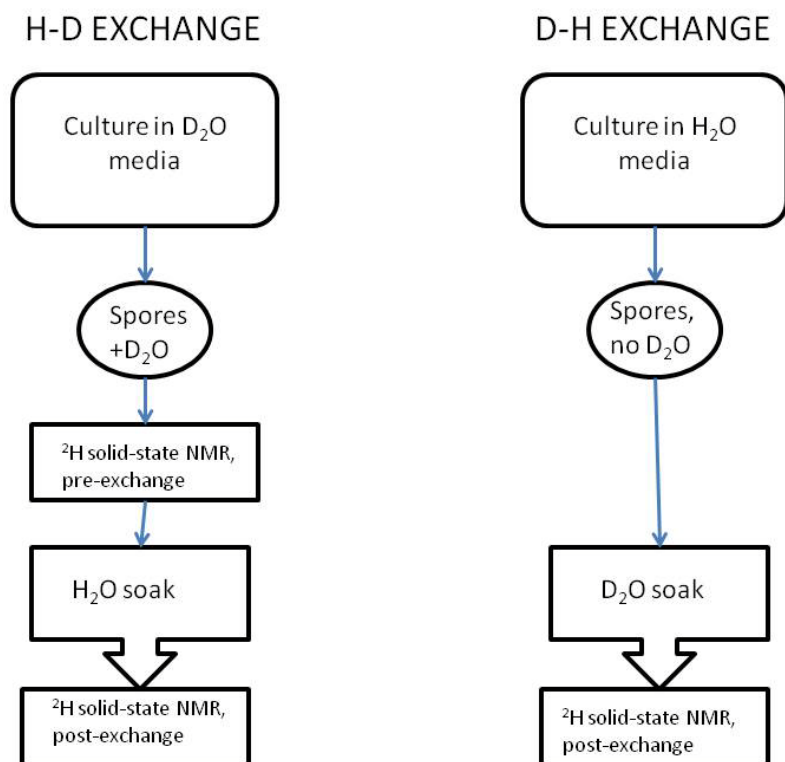


Figure 7.11. A flowchart comparison of the two exchange experiments, H-D and D-H exchange, respectively.

First, the deuterated spores from Figures 7.7-7.9 were recollected and soaked in distilled water for the H-D exchange experiments. These experiments, under the same parameters as their counterparts, are shown below as Figures 7.12-7.14.

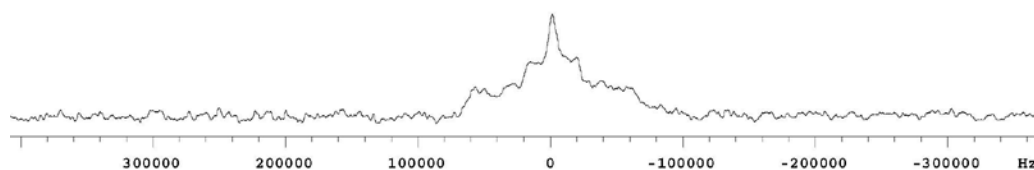


Figure 7.12. ^2H NMR spectrum of the H-D exchanged spore sample of *B.subtilis* ATCC 6051, 13.3 mg.

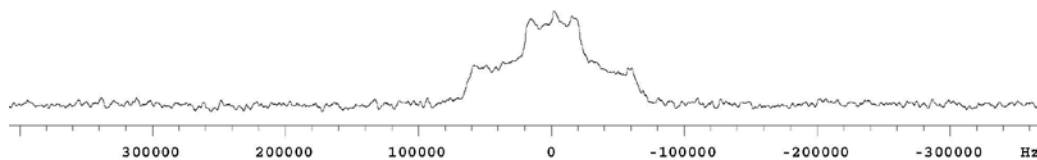


Figure 7.13. ^2H NMR spectrum of H-D exchanged *B.subtilis* 1A578 spores, 13.6 mg.

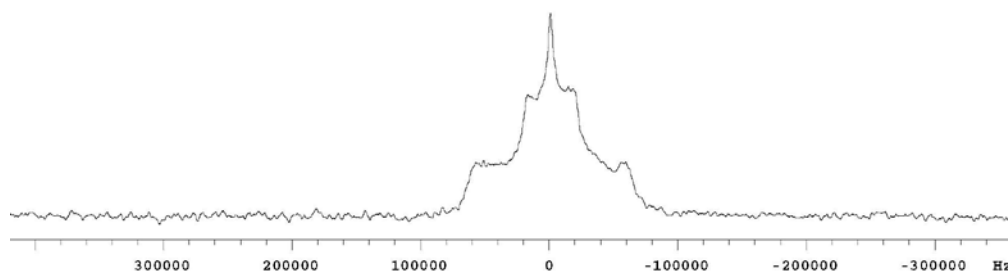


Figure 7.14. ^2H NMR spectrum of H-D exchanged *B.pumilus* SAFR-032 spores, 14.2 mg.

There are distinct differences in the *B.subtilis* H-D exchanged spores, when comparing the deuterated spores to the exchanged spores. In the *B.subtilis* ATCC 6051 spores, the main difference is the appearance that the mobile peak feature is smaller than it was in the deuterated spores; for

B.subtilis 1A578 this difference is much more pronounced, with the mobile deuterium peak hardly visible over the Pake pattern peaks. The difference is not obvious at first glance for the *B.pumilus* SAFR-032 spores, only manifested when the spectra are overlaid and scaled to account for the change in mass (the result of loss of sample in the resuspension, rehydrophilization, and repacking process); it is exhibited as a general loss of signal throughout which happens to be slightly larger for the central peak than the inner- and outer-immobile peaks.

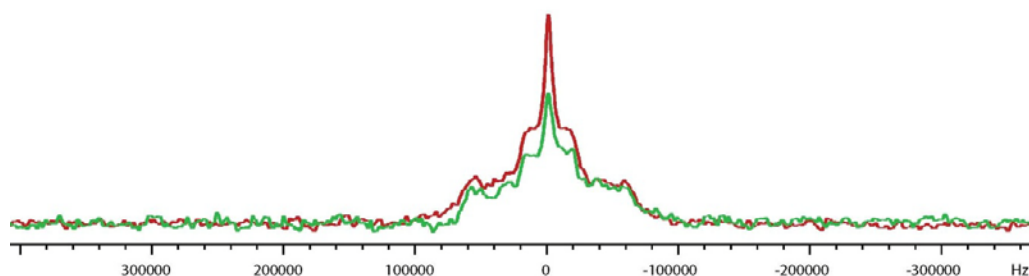


Figure 7.15. Overlaid spectra of Figures 7.7 and 7.12 (*B.subtilis* ATCC 6051 spores, 25% D₂O label (red) and post-H-D exchange (green), respectively) scaled to equal mass.

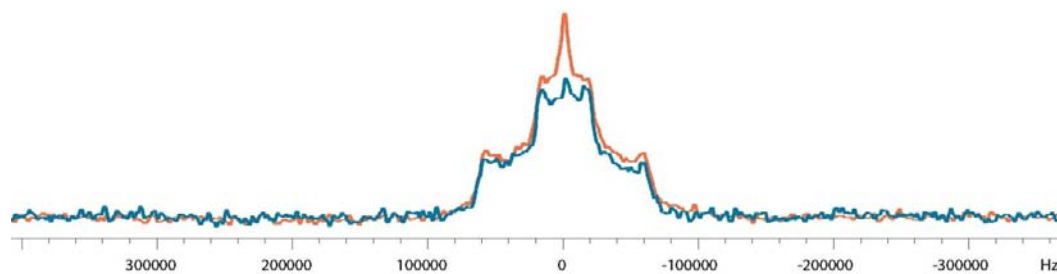


Figure 7.16. Comparison of *B.subtilis* 1A578 spores (25% D₂O labeled, orange; post-1-week H-D exchange, teal) via ²H NMR.

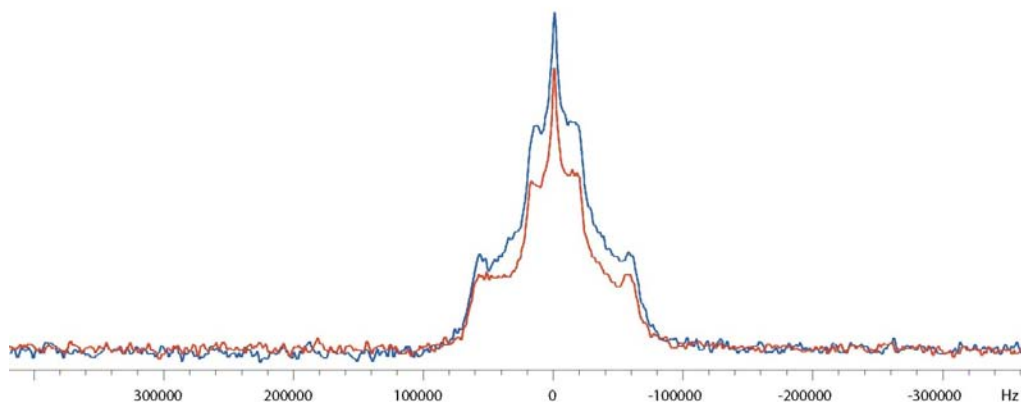


Figure 7.17. Comparison spectra of *B.pumilus* SAFR-032 (25% D₂O, blue; 1-week H-D exchange, red) spores via ²H NMR.

Interestingly, this exchange did not seem to be greatly affected by the duration of time the spores were allowed to soak. An experiment was performed using spores of *B.pumilus* SAFR-032 that were made in a 40% D₂O LB medium, where the spectrum was originally taken and the spores allowed to undergo H-D exchange for four weeks instead of the one week shown in Figures 7.15-7.17 above. The compared spectra are below as Figure 7.18. The decrease in the intensity of the peaks is not vastly different than those of the 25% D₂O comparison in Figure 7.17, indicating that the H-D exchange effects are not dependant on the initial level of spore deuteration, nor on duration of exchange.

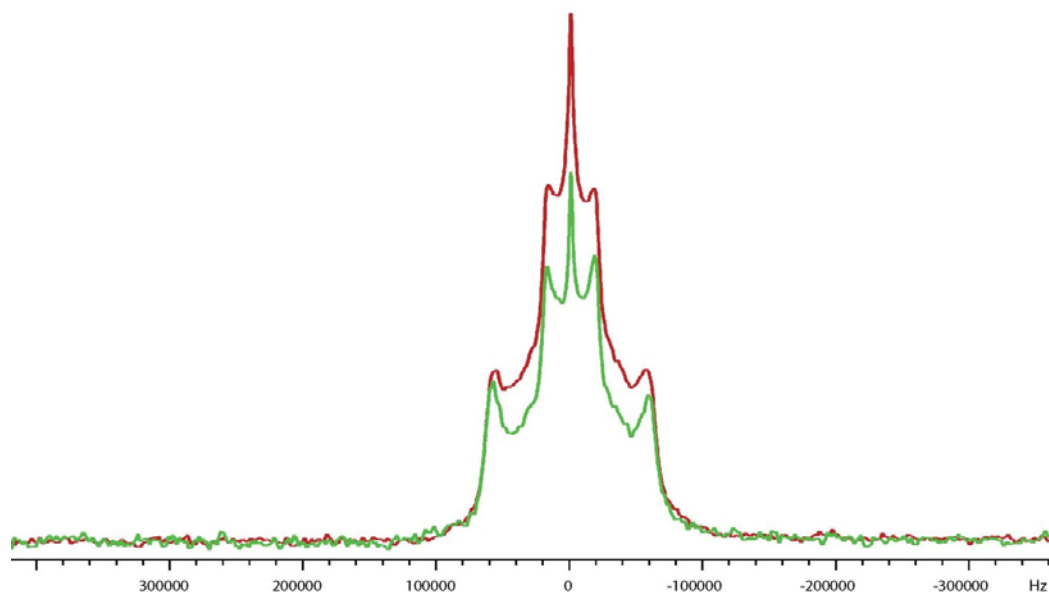


Figure 7.18. Compared spectra of 40% D₂O *B.pumilus* SAFR-032 spores (red) with spores soaked in water (H-D exchange) for four weeks (green).

In the D-H exchange experiments, spores were grown in normal media and only deuterated after sporulation was completed. ²H NMR spectra were obtained and compared to spectra of spores grown in deuterated media. This was done to see if the deuterium signal could be introduced through exchange into the spore after maturation through diffusion. The spectra (Figures 7.19-7.21, below) show that the *B.subtilis* ATCC 6051 does undergo deuterium exchange and incorporation when grown in normal media, but the *B.subtilis* 1A578 and *B.pumilus* SAFR-032 have no exchange in the immobile peak regions, solely in the mobile deuterium signal at ~0 Hz.

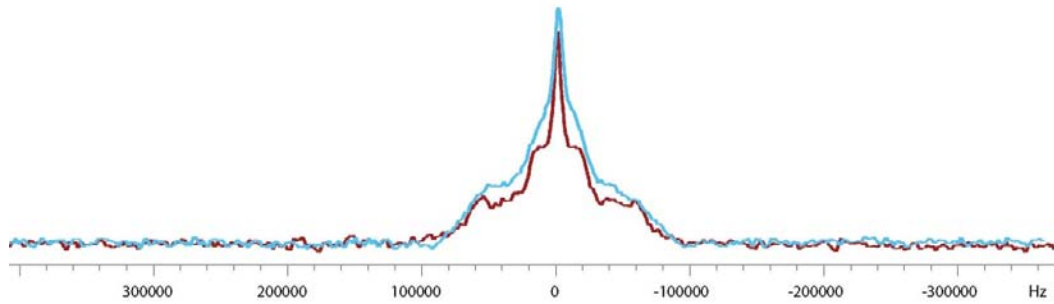


Figure 7.19. The overlaid spectra of *B. subtilis* ATCC 6051 spores by ^2H NMR; 25% D_2O spores (made in deuterated media), red; spores grown in media and deuterated post-sporulation (D-H exchange), light blue.

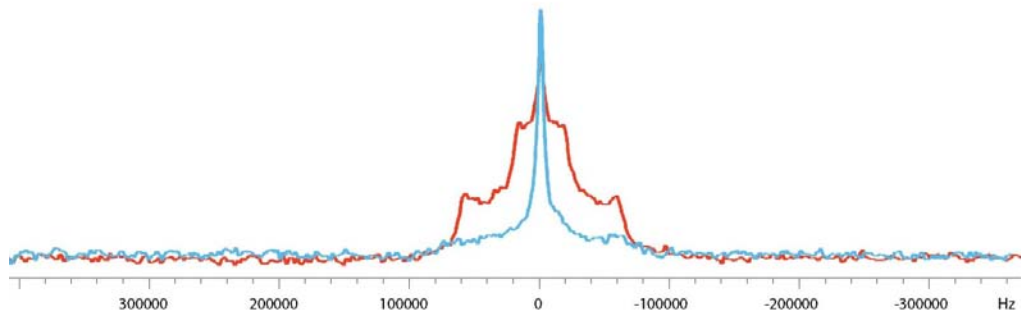


Figure 7.20. The comparison of 25% D_2O spores of *B. subtilis* 1A578 (red) and the post-sporulation deuterated spores of the same species (D-H exchange, light blue), similar to Figure 7.18.

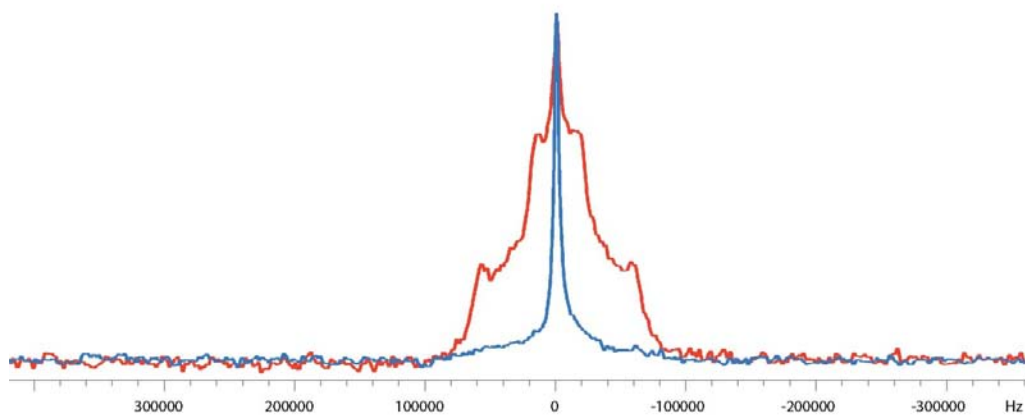


Figure 7.21. The comparison of 25% D_2O *B. pumilus* SAFR-032 spores, red, and D-H exchanged (post-sporulation) spores of SAFR-032, blue.

The difference between the before-and-after-exchange lineshapes is quite evident for the *B.subtilis* 1A578 and the *B.pumilus* SAFR-032, where both sets of immobile peaks do not appear when the spores were deuterated after sporulation. This seems to suggest that the immobile peaks are features of the spore that are inaccessible to external deuterated water within the spore. The ability of *B.subtilis* ATCC 6051 to undergo D-H exchange indicates physical differences in membrane permeability not apparent with the *B.subtilis* 1A578 and *B.pumilus* SAFR-032.

Deuterium NMR of deuterated bovine serum albumin and crystalline calcium dipicolinate trihydrate

Because there are multiple immobile deuterium regions in the spore spectra, it is important to try to assign those peak features to molecules or structures present in the spores. Spectra of deuterated chemicals of interest were taken to observe their lineshape in relation to those of the spores. Deuterated bovine serum albumin was used as an analog for potentially immobile proteins in the spore, while deuterated crystalline and amorphous calcium dipicolinate (made by other members of the group, as stated above) were used due to the high concentration of DPA in the spore core. The concept was to attempt to define the immobile deuterium signals as coming from known components of the spore, to understand where the immobile signals were occurring from, and why they would not be present in the D-H exchanged spore spectra above.

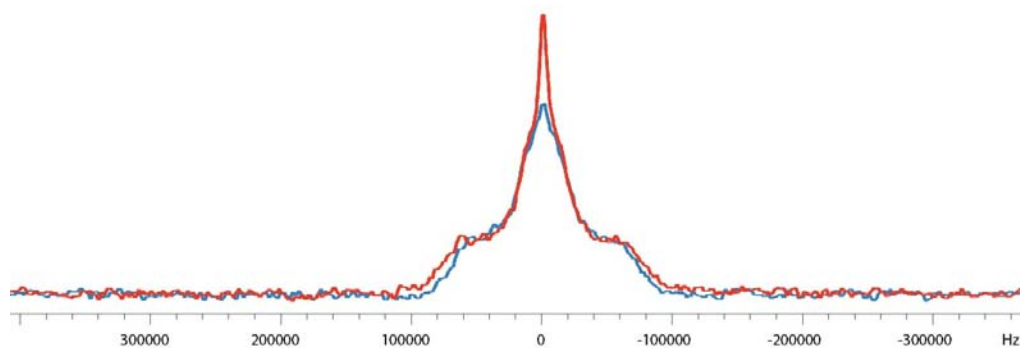


Figure 7.22. Two samples of deuterated bovine serum albumin studied via ^2H NMR: after 5 days' lyophilization, red (30.7 mg); after 19 days' lyophilization, blue (33.7 mg).

Apart from a slight decrease in the mobile peak, the two spectra appear identical; the decrease can be attributed to the additional time in the lyophilizer for the second sample. The width of the shoulder of the BSA peaks is similar to the difference between the outer immobile peaks in the spore spectra (~120 kHz).

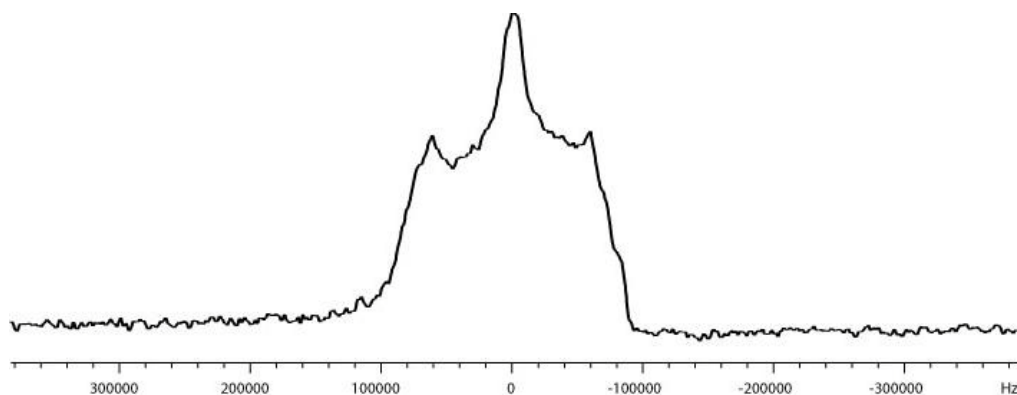


Figure 7.23. The solid-state deuterium NMR spectrum of amorphous (powder) calcium dipicolinate.

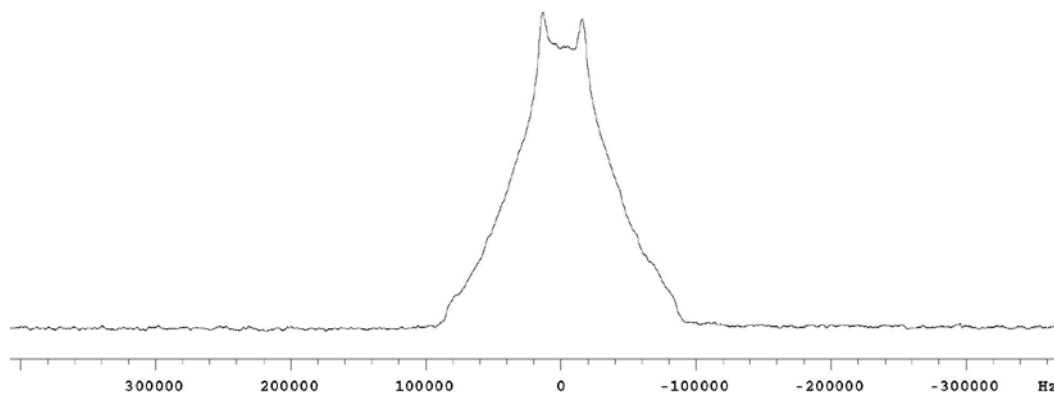


Figure 7.24. The solid-state ^2H NMR spectrum of crystallized deuterated calcium dipicolinate (70.0 mg).

The crystalline calcium dipicolinate spectrum is very broad, with no distinct mobile peak (which is explained by the sample being a crystal). The Pake peaks are separated by 30.8 kHz, similar to the inner immobile signals from the spore spectra but not the outer immobile signals as shown in Table 7.1. The crystal was confirmed by X-ray crystallography to be the trihydrate and not the sesquihydrate based on the crystal parameters and dimensions of the unit cell⁶. The amorphous calcium dipicolinate spectrum is also broad, with an approximately 116 kHz separation between its peaks, but differs in it having a mobile deuterium peak.

Peak dist. (kHz)	CaDP·3D ₂ O	BSA (5d lyo)	BSA (19d lyo)	D ₂ O, -45°C	25% BP SAFR	25% BS 6051	25% BS 578	40% BP SAFR
Inner	30.8	N/A	N/A	N/A	32.5	32.3	33.8	33.4
Outer	N/A	120.4	117.5	144.2	116.5	118.9	118.9	113.6

Table 7.1. List of distance (in kHz) between immobile Pake doublets for various ^2H NMR samples. N/A = not applicable (sample had only one identifiable doublet).

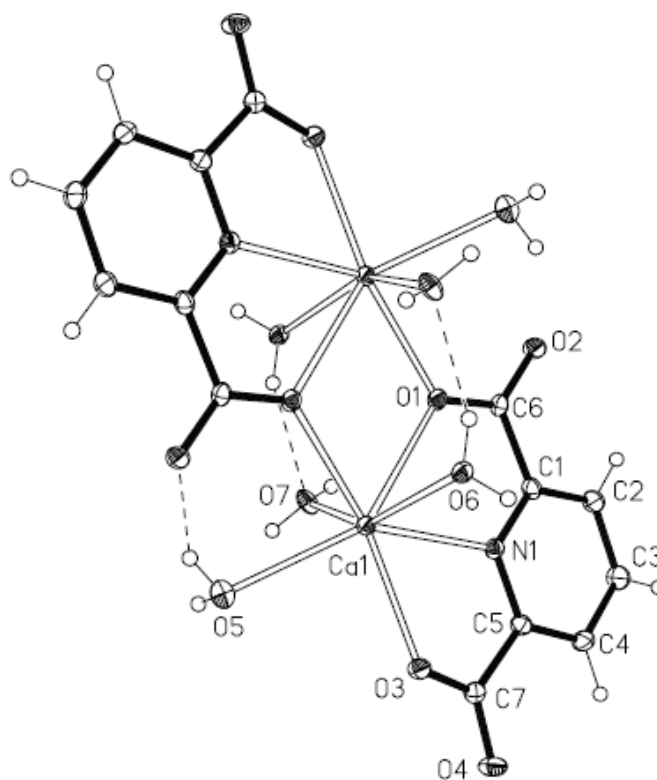


Figure 7.25. The crystal structure of calcium dipicolinate trihydrate, in this case a dimer, as determined by X-ray crystallography (courtesy Doug Powell).

Discussion

Deuterium NMR of spores: lineshape comparisons

Firstly, when the 25% deuterated-media-labeled spore spectra of *B.subtilis* ATCC 6051 and 1A578 and *B.pumilus* SAFR-032 are observed together, it does not appear as though there is anything particularly obvious in their spectra to indicate why SAFR-032 possesses the biological and spore resistance properties it does. Apart from a more intense signal, the overall lineshape of the three spectra are identical or near enough to it as to be identical to the naked eye. There are no defining alterations to this basic lineshape between strains or these two species to indicate a structural

difference between the SAFR-032 and the *B.subtilis* strains. This can be observed both in Figure 7.27 below as well as their data in Table 7.1. However, there must be some difference between these species given the different spectra shown in Figures 7.19-7.21 above when deuterated-media spores and spores deuterated post-sporulation are compared.

It seems obvious when looking at those figures that there are components of the spore that are deuterated when the spores form from bacteria grown in a partially-deuterated medium (and maintain deuteration under H-D exchange, as seen in Figures 7.15-7.17. These are spore components, not simply bulk D₂O that is immobile, as comparison of the bulk frozen D₂O spectrum with that of any of the spore species shows that the distance between the pure D₂O Pake doublet is wider than the entirety of the spore lineshape. The lack of exchange when the spores are deuterated during their dormancy indicates that those components are in a chemical environment which limits both their mobility and their accessibility to external substances; if this were not the case then we would expect that the spectra would appear more similar to the deuterated-media-grown spores.

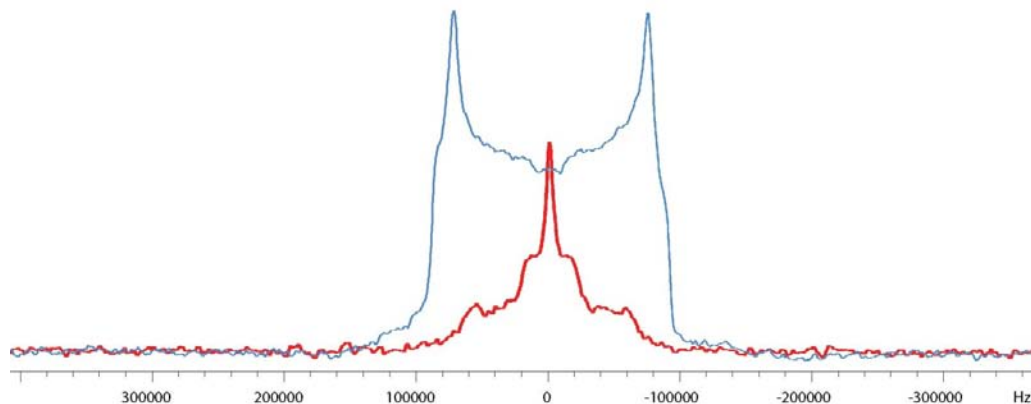


Figure 7.26. The peak features of *B.subtilis* ATCC 6051 spores (25% D₂O, red) are not attributable to the peak width of bulk frozen water (D₂O, blue).

In addition, there is the question of the overall lineshape of the spore samples as compared to other deuterated molecules. When one looks at the frozen D₂O in Figure 7.4, the two Pake peaks are (for solid-state NMR standards) well-defined and separated; there is good resolution of the two signals, save the overlap which is a necessary and expected feature of quadrupolar nuclei. This is interpreted as the D₂O being in a definitive frozen, immobile, crystalline structure. By contrast, the spectrum of deuterated bovine serum albumin does not appear as sharp and well-defined, with any immobile signal either seemingly buried by the mobile peak (which is wider than it is for most of the spore mobile signals) or present as a shoulder and not as a distinct peak feature. This lineshape is more suggestive of an amorphous protein solid more similar to a glassy substrate than a well-ordered crystalline structure, owing to the sample being a dissolved powder in D₂O prior to lyophilization.

Peak assignments of spore immobile deuterium signals

When we then look at the actual spore spectra, we see spectra that, for the most part, appear more like the BSA than the frozen D₂O (or the deuterated calcium dipicolinate trihydrate crystal, for that matter). The immobile signals are obvious and yet muddled, poorly resolved into very small peaks at best, shoulders and slight differences in lineshape at worst, with the exception of the 40% D₂O-containing LB-grown *B.pumilus* SAFR-032, and that can be explained by merely the increase in deuteration of the bacteria (and of the ensuing spore). By itself, this would not be definitive of anything. However, when coupled together with the knowledge that these immobile signals are not present when spores are deuterated after-the-fact strongly suggests that these signals are parts of the spore that are both immobile and inaccessible to external D₂O over the span of a week. This is reinforced by the opposite experiment, i.e. that the immobile signals remain when deuterated spores are soaked in distilled water to attempt to remove deuterons from the spore, also indicating a lack of exchangeability of external water with these immobile spore features. The conclusion is that these immobile signals due to non-crystalline immobile proteins and molecules present in the spore reside in regions that are inaccessible to water from outside the spore. This does not contradict, e.g., the knowledge that the initial steps to spore germination occur on the timescales of seconds to minutes^{9,10} because germination typically is dependent on reception of nutrients or other germinants by receptors, not on diffusion of chemicals through the entire spore.

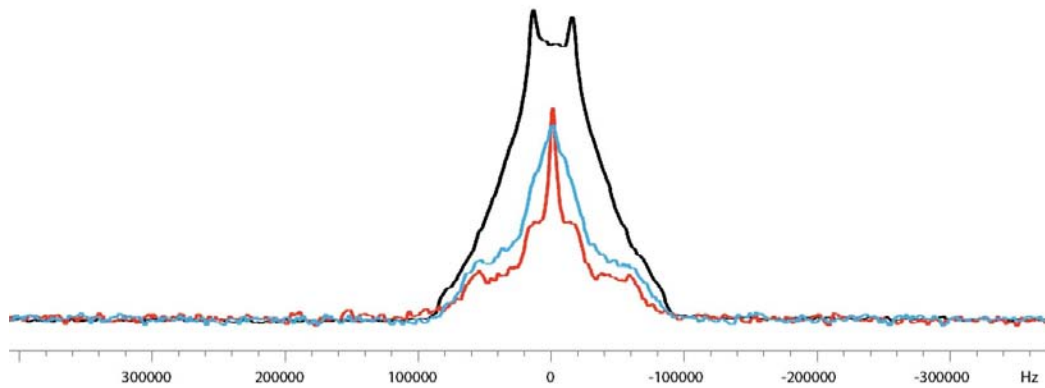


Figure 7.27. Overlaid spectra (not to scale) of: 25% D₂O *B. subtilis* ATCC 6051 spores, red; deuterated bovine serum albumin (19-day lyophilization), blue; deuterated calcium dipicolinate trihydrate crystal, black.

This is not to say that the calcium dipicolinate spectrum has no bearing on the spore spectra; the inner spore peaks are more similar to the CaDP peaks than those of the BSA. The inner peaks being distinctly separate from those of the outer immobile peaks, unlike the BSA, suggests that the two are in different environments, one most similar to the more crystalline environment of the calcium dipicolinate, the other most similar to amorphous glass-like proteins, which is analogous to the BSA spectrum. Since the calcium dipicolinate is associated only in the spore core, we assign the inner immobile signal as that being attributable to spore core contents including calcium dipicolinate, and the outer immobile signal as attributable to proteins outside of the core, including proteins in the spore coat and the peptidoglycan of the spore cortex.

Accessibility of spore core to external water

We can also glean information from the comparison of the spectra of the spores after the exchange experiments. The appearance in Figures 7.15-7.17

of the spectra of spores made in deuterated media and then soaked in distilled water indicates that the exchange of deuterium already incorporated into the spore is mostly confined to those mobile deuterons easily accessible to the external water, excluding the immobile deuterons in the spore core, as shown in Figure 7.28 below. Similarly, the spectra of spores soaked in D_2O after sporulation (Figures 7.19-7.21) suggests that, in general, the deuterium exchange only occurs for a small fraction (at most) of the immobile coat and core contents and is again confined to water that is unbound and easily accessible through diffusion, shown in Figure 7.29.

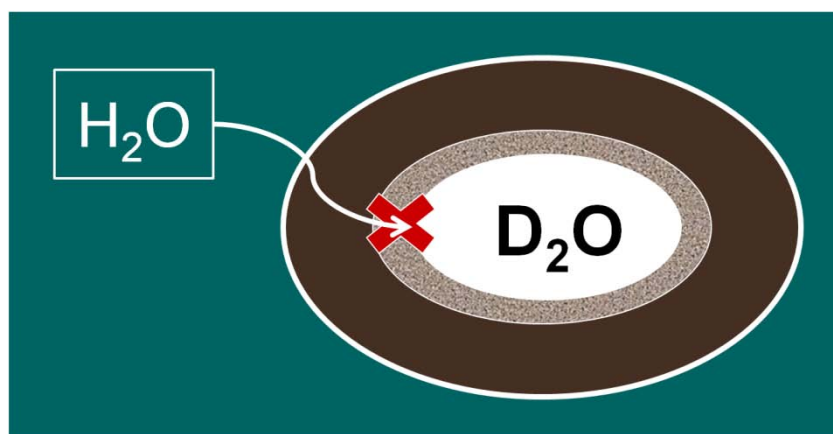


Figure 7.28. External water is not able to exchange with immobile deuterium bound in the spore core during H-D exchange experiments.

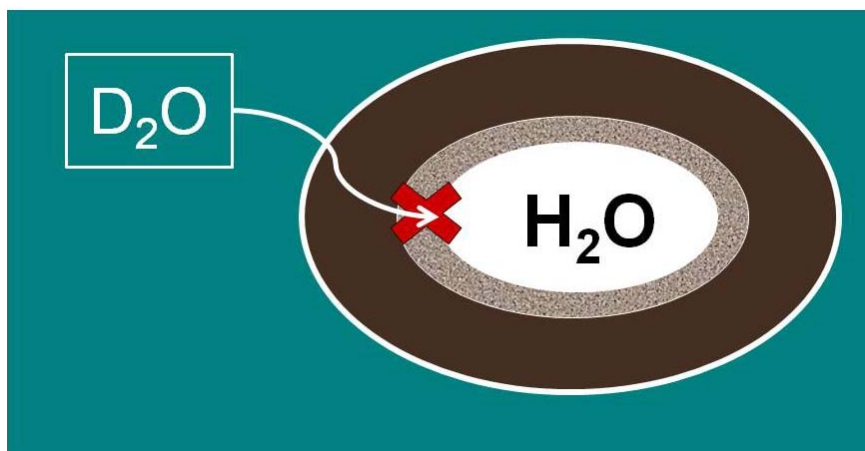


Figure 7.29. External deuterated water is unable to deuterate the spore core, as shown in D-H exchange experiments.

Figure 7.19 is odd in that it does not follow the similar trend set by the other two in that series—that *B.subtilis* ATCC 6051's D-H exchange spectra shows deuterium exchanging throughout the spore when the spore was grown in normal media, while this was not apparent in *B.subtilis* 1A578 or *B.pumilus* SAFR-032 spores under the same conditions. As mentioned in the results, the reasoning for this is unclear. One possibility is that there are differences in the physical structure or the membrane permeability of the *B.subtilis* 1A578 and *B.pumilus* SAFR-032 spores compared to the wild-type *B.subtilis*. The differences are more obvious with the *B.pumilus*, given its enhanced UV resistance and other factors; these changes to allow greater spore survival may have had physical effects on its structure that can be seen in these spectra. With the *B.subtilis* 1A578, it may be as simple a case as the addition of the chloramphenicol resistance may have had effects on its membrane permeability that would alter the way it is able to uptake deuterated water as a spore. This also raises a question with the wild-type *B.subtilis* that, if it was as permeable to

D₂O in the D-H exchange as Figure 7.19 suggests, why the deuterium signal in Figure 7.15 is not removed by H-D exchange? Again, this may result from a difference in permeability between the wild-type *B.subtilis* and the other two species.

Future research aims

Additional research is likely to be necessary to clear up that question, as well as to study other topics in this field. These research objectives would involve studying the deuterium NMR spectrum of deuterated spores both before and after exposure to conditions that could prove either lethal or which could induce either germination or damage to the spore but without being immediately lethal to the spore, such as dry and wet heating, UV exposure, heating or UV exposure under vacuum conditions, etc. The goal would be to observe if there is a change in the appearance of the lineshape (either a change or loss of the mobile/immobile peaks, or appearance of new signals) that could likewise be attributed to mobile water inside the spore or to spore components.

Another category of future research which could be performed is with mutant strains; for instance, using mutants that lack the ability to fully germinate (i.e. through failure to hydrolyze the cortex) but which do initiate the germination process and release the calcium dipicolinate and other ions and hydrate the core and observing the change in the lineshape (particularly if the inner immobile peaks disappear and the spectrum appears more similar to that of deuterated BSA).

Conclusions

Knowledge of the state of the water inside of bacterial spores would be useful to develop novel sporicidal methods, in particular when dealing with strains that are resistant to conventional means of sterilization. Deuterium solid-state NMR experiments can provide insight into this subject through qualitative analysis of the lineshapes of deuterated spores and their behavior when deuterium is removed or introduced through exchange experiments. In this work the nature of the water in the spore has been established as partly unbound, 'free' (mobile) water, and then as mainly amorphous glassy-state (immobile) water in two distinct environments associated with the coat and cortex proteins and with core molecules such as calcium dipicolinate. The immobile water is generally inaccessible to exchange with external water, unlike the mobile water signal; neither set of immobile signals is attributable to pure deuterium oxide indicating, if not binding, than at least close association with bound proteins occurs in the spore prior to dormancy.

In addition, the results given here seem to contradict the conclusions given (and mentioned earlier in this work) by Sunde *et al*¹¹ in their rejection of the spore core being in a glassy state. Their conclusion was that, based on measurement of deuterium NMR relaxation times, "...the core is not in a glassy state...Core water is both bound and mobile, and there is no contradiction in this"¹¹ (Sunde *et al* 2009, 19338). Our data suggest the opposite: the core water is indeed in a glassy state based on the spectra of deuterated spores. The distinct chemical environment assigned to a biomolecule known to be present in the spore core indicates the core environment is different than that of

the rest of the spore; this environment appearing as a Pake doublet indicates it is not based on mobile deuterium; and the peaks being not well resolved indicates it is not a crystalline solid. Therefore we can only conclude that the water inside of the spore core is in an amorphous, glassy solid state. What mobile water we see in the spectra is not core-associated, based on the deuterium exchange experiments; more likely it is associated with the more permeable and exchangeable outer layers of the spore.

CHAPTER 8: TREATMENT OF BACTERIAL SPORES WITH OXINE®, A PROPRIETARY CHLORINE DIOXIDE-BASED BIOCIDAL AGENT

Introduction

In the previous chapter of this dissertation, bacterial spores were studied using deuterium solid-state NMR spectroscopy to determine the nature of the water inside of the dormant spore core. In the chapter prior to that, it was discussed and mentioned that bacterial spores were able to survive extreme conditions compared to vegetative cells of the same species, and that some species, notably the *B.pumilus* SAFR-032, were much more resistant to UV radiation and peroxide treatment than spores of other species, such as *B.subtilis* spp. The natural question that results such as those poses is what can be done to sterilize surfaces exposed to spores such as those, if they are resistant to common biocidal methods such as UV exposure and peroxide treatment. To that end, this chapter describes a collaboration between the Rice Group and a manufacturer of biocidal agents to test bacterial spores against a chlorine dioxide-based agent.

Structure, mechanism of biocidal action, and uses of chlorine dioxide

Chlorine dioxide, ClO₂, is a chemical that has become widely used in several fields due to its antimicrobial properties¹⁻⁴ and its use in bleaching of wood pulp⁵. It is a yellow-greenish gas at room temperature, with a formula weight of 67.46 g/mol; it is soluble in water up to 20 g/L^{2,6,7}. It has a boiling point of 11°C and a melting point of -59°C; OSHA states that the gaseous form could also be yellow-red in color, with liquid ClO₂ being reddish-brown and solid

ClO₂ being a yellowish-red crystal⁶. Chlorine dioxide has an odor similar to chlorine⁷. In solution, chlorine dioxide concentration can be determined through colorimetric methods, with ClO₂ concentrations determined at 360 nm^{28,29} and/or 445 nm (unpublished work).

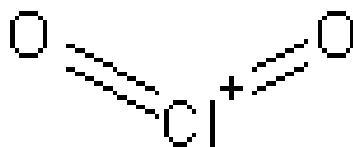
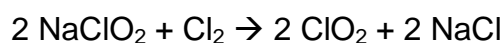


Figure 8.1. Structure of chlorine dioxide.

Chlorine dioxide gas is unstable², and OSHA gives several risks including being an explosion hazard when heated or in air at >10% concentration⁶. Thus, for most non-industrial uses, ClO₂ gas is generated on-site for use⁸. Chlorine dioxide can be formed in a variety of manners; two common ones are as products of the reaction of sodium chlorite (NaClO₂) with other compounds, as shown below⁷:



Or



Chlorine dioxide can also be formed from an electrochemical reaction⁸ or from passing chlorine gas over solid sodium chlorite; for large-scale production (e.g. for bleaching of wood pulp) sodium chlorate is reacted with peroxide and sulfuric acid².

Chlorine dioxide has demonstrated effectiveness in a wide range of antimicrobial or sterilization situations. In the aftermath of the 2001 anthrax incidents, gas-phase chlorine dioxide was used to decontaminate affected

structures^{9,11}. One paper indicated that liquid ClO₂ exposure to *B.anthraxis* spores caused inactivation of the spores (~7-log reduction) within 5 minutes of exposure⁸. This is tempered by an article suggesting that there are differences in the exposure of gaseous ClO₂ required for spore inactivation when tested against common office building structural materials, such as drywall, cinder block, and pine wood, and that the exposure required was in excess of what was needed to kill spores on common biological indicators⁴. ClO₂ also has demonstrated sporicidal ability against other species; a paper from 1986 reported efficacy of ClO₂ in killing spores of *B.cereus* and *C.perfringens*, with the sporicidal properties of ClO₂ against *B.cereus* not dependent on the conditions used (20-80 ppm, 4.5-8.5 pH, or *B.cereus* grown and sporulated in two different media)¹⁰.

Chlorine dioxide has been used against other bacteria and spores. Chlorine dioxide has been indicated to disinfect hot-water circulation systems that may be susceptible to *Legionella* colonization¹². A polymer-encapsulated stabilized ClO₂ solution demonstrated >99% kill against *P.aeruginosa*, *E.coli*, and vegetative *B.subtilis* on contact for 60 minutes, and 90% kill against *S.aureus*; while the initial kill against *B.subtilis* spores is low, the continuous contact and release of ClO₂ leads to a 75% inactivation of the spores after 72 hours¹³. Chlorine dioxide has been used to prevent or reduce soft rot in tomatoes (by *Erwinia carotovora* subsp. *carotovora*)¹⁴; it has also been used in food processing to decontaminate produce, either in static batches or as a continuous tunnel-exposure treatment³. ClO₂ was shown to have comparable

or better sporicidal properties compared to chlorine against *B.cereus* spores in water, regardless of whether the chlorine dioxide was alkaline or acidified, though it was shown that spore-killing ability rapidly diminished after 10s when trying to kill *B.cereus* and *B.thuringiensis* spores in MGM media unless at high concentrations (due to the concentrations of organic and inorganic compounds in the media)¹.

Chlorine dioxide's mechanism of action is mainly the result of it being a powerful oxidant. Its half reaction is given as⁷:



It oxidizes selectively, preferring "...one-electron transfer mechanisms, wherein it attacks electron-rich centers in organic molecules and, in the process, is reduced to chlorite ion"². The oxidation leads to cell damage; the EPA states that "chlorine dioxide kills microorganisms by disrupting transport of nutrients across the cell wall"⁹. A 1967 paper on the mechanism of the disinfectant action of chlorine dioxide stated that the rapid rate of disinfection and chlorine dioxide's oxidative power "...suggested that chemical disruption of the bacterial cell wall was the likely mechanism"¹⁵; it also suggested that the main effect was inhibition of protein synthesis. This was also seen in a more recent paper that found denaturation of bovine serum albumin and *S.cerevisiae* glucose-6-phosphate dehydrogenase occurred after exposure to ClO_2 ⁷. That same paper pointed out that ClO_2 is reactive to varying degrees with amino acids, with the most-reactive being sulfur or aromatic species, such as Cys, Trp, and Tyr⁷.

Effects on the cell wall by chlorine dioxide were also suggested to have been responsible for some non-lethal expressive behavior by cells. In one paper in the *Journal of Bacteriology* it was demonstrated that sub-lethal doses of chlorine dioxide against *B.subtilis* induced formation of biofilms¹⁶. The main described mechanism for this was activation of the KinC protein via induced changes in the membrane potential, thus triggering a biofilm-inducing pathway in a similar method as surfactin.

Chlorine dioxide's disinfectant properties, as well as reduced levels of chlorinated byproducts such as trihalomethanes when compared to chlorine^{2,5,7,17}, have seen it used in bleaching of wood pulp for paper production⁵, and in water treatment plants^{17,2}.

Recently, chlorine dioxide has entered the conversation as to how best to sterilize spacecraft. The typical protocol is the use of dry heat sterilization, which dates to the Viking missions to Mars¹⁸; however, increasing usage of thermolabile or other heat-sensitive components, such as in the ESA's Beagle 2 mission, pose a challenge to the use of dry heat sterilization methods¹⁹. A recent paper compared two methods of potential low-temperature sterilization, using vaporous hydrogen peroxide and gaseous chlorine dioxide; both methods were equally effective at 5-log or greater reduction in viability of the various *Bacillus* spore species tested, although this occurred within 20 minutes for the peroxide versus 60 minutes for ClO₂²⁰.

As has been mentioned previously in this work, the presence of hyper-resistant bacterial species, including spore-forming bacteria, has been observed

even within nominally clean-room areas such as the Spacecraft Assembly Facility at the Jet Propulsion Laboratory^{21,22}. One such strain, *B.pumilus* SAFR-032, has been repeatedly isolated^{22,23} and has demonstrated resistance to temperatures and UV conditions lethal to other strains of *B.pumilus* and other *Bacillus* species²³. *B.pumilus* SAFR-032 has also been reported to be resistant to peroxide treatment through novel genes in its sequence²⁴ and through additional peroxide catalases in its spore coat²⁵. While some progress has been made in sterilization of surfaces contaminated by *B.pumilus* SAFR-032 through supercritical-fluid carbon dioxide (SF-CO₂)²⁶ or SF-CO₂ with added hydrogen peroxide²⁷, more alternatives in sterilization of *B.pumilus* SAFR-032 may be necessary or beneficial.

A stabilized chlorine dioxide solution, prepared by activation with citric acid (Oxine® , Bio-Cide International, Inc., Norman, OK, USA) had previously been tested against spores of *B.subtilis*, along with hypochlorite solution, for efficacy and mechanism of attack²⁸. The authors reported no difference in the percentage of killed spores between exposure with hypochlorite and ClO₂, and no difference in mutagenesis by the two compounds. However, chlorine dioxide treatment did not bleach the spores in appearance when pelleted compared to hypochlorite (vs. a control), and spores treated with ClO₂ proceeded further in germinating before being shown as non-viable compared to hypochlorite. These results were the same whether the authors tested a wild-type strain (PS533) or a strain deficient in the α/β small acid-soluble proteins (SASPs) (PS578).

Based off of these results, it seemed necessary to test the *B.pumilus* SAFR-032 against a known control (*B.subtilis* ATCC 6051) to determine whether there is any greater or lesser efficacy of the Oxine®/chlorine dioxide on the *B.pumilus*, and if any additional information on the mechanism of action of Oxine® could be determined via scanning-electron microscopy (SEM).

Experimental Protocol

Spore preparation

The spore preparation method for Oxine exposure is substantively similar to the previously mentioned protocol for spore preparation for deuterium NMR, with a few modifications. In short, cultures of either *B.pumilus* SAFR-032 or *B.subtilis* ATCC 6051 (the wild-type strain) were grown in media until the cultures exhibited sufficient sporulation. The *B.pumilus* SAFR-032 was grown in LB media until sporulation occurred due to nutrient exhaustion, which typically occurred after three days. *B.subtilis* ATCC 6051 was initially grown in LB media for one day, then centrifuged (10,000xg, 20 min., 4°C), the LB supernatant decanted, and the pellet resuspended in an equal volume of chemically-defined sporulation medium (CDSM)³⁰. The choice of media was based on prior experiments which determined that sporulation was most complete in CDSM for *B.subtilis* but best in LB for *B.pumilus*. *B.pumilus* was grown at 32°C, with the *B.subtilis* grown at 37°C, both in incubator-shakers at 200 rpm. The amount of sporulation was determined through the use of phase-contrast microscopy (Olympus BX-50) at 1000x magnification using wet-mounted 5-10µL aliquots of culture.

Cultures reaching a desired percentage of spores as observed by phase contrast microscopy were then purified using an adapted protocol of Zhao *et al*^{β1}. Cultures were centrifuged (10,000xg, 20 min, 4°C), decanted, and resuspended in Milli-Q deionized water; this suspension was then centrifuged once again (a 'water wash' step), decanted, and then resuspended in 20 mL of sterile 50% EtOH:distilled water in a centrifuge tube. This was shaken at room temperature at 200 rpm for 4h, and then centrifuged under the same parameters as above, with three water-wash steps using sterile distilled water. The resulting final pellet was resuspended in sterile distilled water and an aliquot taken for phase contrast microscopy to ensure purity of the spore sample and sufficient number of spores (at least 95%). Subsequently the spores were diluted with distilled water until their absorbance at 600 nm (the optical density, OD₆₀₀) was 1.0 using a Beckman-Coulter DU-640 UV-vis spectrophotometer.

Preparation of chlorine dioxide

An aqueous solution of 2% stabilized chlorine dioxide (Oxine[®]; Bio-Cide International, Inc., Norman, OK, USA) was used in all exposure experiments. The product was activated by citric acid addition in a ratio of 0.2 g per mL of Oxine[®] solution without stirring (30 min, room temperature), causing the formation of chlorine dioxide. Each experiment used a freshly activated Oxine[®] solution. The total concentration of activated Oxine (after dilution) was measured using a proprietary iodometric titration method (Bio-Cide International). The concentration of free chlorine dioxide gas, which is a

fraction of the total Oxine® concentration, was determined using a Hach Colorimeter with $\lambda = 445$ nm. The activated Oxine® was then diluted in water to a total concentration of 500 ppm, followed by subsequent dilutions to approximately total concentrations 200 ppm, 100 ppm, and 50 ppm for selected experiments. For liquid experiments (performed but not reported in this work), reported concentrations include dilution of the Oxine® with the spore suspension medium. Experiments relying on a spray application of Oxine® utilized 1 L of chosen dilutions in a hand-held pump-up sprayer (RL Flo-Master model 1401, Root-Lowell Manufacturing Co., Lowell, MI), which had been pressurized and flushed with at least 100 mL of the solution prior to use.

Exposure of dried spores to chlorine dioxide

Spores in liquid suspensions do not represent the low moisture environment of a clean room or spacecraft assembly facility, so dried spore experiments were performed to evaluate differences in survival. 100 μ L of a liquid spore suspension was deposited onto three sterile microscope slide coverslips. These spores were then left to dry at room temperature for 24 h under sterile conditions. Following the drying, the spores were sprayed for less than one second with a fine mist of Oxine® that lightly covered the microscope coverslip. Reaction with Oxine® was allowed to proceed at room temperature under sterile conditions, and once the desired exposure time (10 min, 60 min, or 24h) was reached, the coverslip was transferred to a 50 mL conical centrifuge tube and submerged with 10 mL 0.1 N sodium thiosulfate for neutralization. Next, the submerged spores were placed in a ultrasonic water bath to dislodge

the spores (Ultrasonic Cleaner B-220, Branson Cleaning Equipment, Shelton, CT) for 2 min followed by vigorous vortex mixing for 10 s, a procedure previously used to remove *B. cereus* spores from metal coupons.³¹ Spore suspensions were serially diluted with PBS, streaked onto TSA plates, incubated at 37°C, and colonies were counted after 24 h, again confirming no growth after 48 h.

Additional experiments were later performed using the same protocol as listed above with the *B.pumilus* SAFR-032 spores; however, the spores would be deposited onto spacecraft-grade aluminum coupons provided to the Rice Group (Dr. Parag Vaishampayan, JPL). The aluminum coupons were autoclaved for sterility prior to spore deposition. In addition to exposure to a solution of activated Oxine®, additional coupons were exposed to a solution of inactivated Oxine® solution to which no citric acid had been added, to test whether the solution would diffuse into the spore and be activated by the spore core environment, as well as exposure to a 3.5% w/v solution of hydrogen peroxide. As per the previous paragraph, coupons were neutralized after the exposure time was reached with sodium thiosulfate, sonicated to dislodge spores from the coupons, serially diluted with PBS, plated on TSA, incubated at 37°C, and the resulting colonies counted at 24 h.

Evaluation of spore damage with electron microscopy

Samples of dried spores on microscope coverslips were prepared using the procedure described above. However, the spores were not exposed to sodium thiosulfate and thus the Oxine® was not deliberately neutralized. For analysis with scanning electron microscopy, a small amount of silver oxide

adhesive was used to secure the glass coverslip onto an aluminum support.

The samples were sputter coated with a thin layer (~ 2 nm) of iridium metal prior to viewing them with a Zeiss Neon 40 EsB SEM. Unneutralized aluminum coupons in the later experiment were likewise observed through SEM.

Results

Spore preparations

After purification, the *B. pumilus* SAFR-032 spores exhibited high hydrophobicity, often sticking to plastics (polypropylene and polyethylene tubes and micropipette tips) and glass (test tubes and serological pipets). This was also visible during phase contrast microscopy, where regions of the applied spore suspension that dried showed high numbers of spores. However, sonication was able to dislodge spores from the glass or plastic surface. In contrast, *B. subtilis* ATCC 6051 spores stayed in suspension with limited attachment to plastic or glass. In addition, *B. subtilis* ATCC 6051 spores showed viable counts similar to what was expected based on OD₆₀₀ values (e.g., 10⁶ CFU/mL for an OD₆₀₀ of 0.01), whereas, in the absence of sonication, the *B. pumilus* SAFR-032 suspensions showed inconsistent viable counts relative to the OD₆₀₀ (data not shown).

Preparation of chlorine dioxide

In general, the activated Oxine® solutions after dilution showed a total “Oxine® concentration” of approximately 500 ppm, a free chlorine dioxide (dissolved gas) concentration of 200 ppm, and a pH of 2.7 to 3. So, the majority of the Oxine® was not completely converted. Free ClO₂ gas levels of 80-90

ppm were measured for 200 ppm total Oxine® concentration, while a 50 ppm total Oxine® concentration lead to 18 ppm free ClO₂. Similarly, in the later experiments using the aluminum coupons, the activated Oxine® solution had a concentration of 70.4 ppm, but a free ClO₂ concentration of 39 ppm. The chlorine dioxide gas has some potential to dissipate from the liquid over time, especially from agitation caused by dilution or stirring. All solutions were made fresh prior to use and all subsequent dilution labels refer to the total Oxine® concentration.

Dried spores' exposure to chlorine dioxide

An initial experiment with 50 ppm Oxine® sprayed onto dried microscope coverslips coated with *B. subtilis* ATCC 6051 and *B. pumilus* SAFR-032 spores showed a slight decrease in viable counts after 5 minutes of exposure. The decrease was within one standard deviation of the unexposed controls (data not shown). As shown in Table 8.1, dried spores were rendered nonviable after being sprayed with 47 and 187 ppm Oxine® solutions. As expected, higher Oxine® concentration required lesser time to inactive the spores. As a control, an additional set of dried spores were kept in a sterile room temperature environment for 8 days with minimal loss in activity, with the viable count decreasing less than 10⁻¹ CFU. Prior to exposure, the numbers of spores on the coverslip is much lower than in the solution phase experiments, and thus a spore concentration lower than 10² CFU could not be reliably detected when taking into account the submersion in 10 mL 0.1 N sodium thiosulfate and followed by using 100 µL of that 10 mL suspension for streaking on agar plates.

Oxine® concentration (ppm)	Exposure time	Colony Forming Units	
		<i>B. subtilis</i> ATCC 6051	<i>B. pumilus</i> SAFR-032
0	-	$4.59 \pm 1.71 \times 10^4$	$1.30 \pm 0.32 \times 10^5$
47	10 min	$3.50 \pm 2.12 \times 10^2$	$2.40 \pm 0.10 \times 10^4$
47	60 min	$4.70 \pm 3.11 \times 10^3$	$1.10 \pm 0.14 \times 10^3$
47	24 h	n.d.	n.d.
187	10 min	n.d.	n.d.
187	60 min	n.d.	n.d.
187	24 h	n.d.	n.d.

Table 8.1. Viable results after spraying Oxine® onto dry microscope cover slips coated with *B.subtilis* ATCC 6051 and *B.pumilus* SAFR-032 spores.

In the later experiment with the aluminum coupons, the exposure time was set at 1 and 24 hours, and spores were plated onto duplicate sets of plates. The plates were checked after 24 hours of incubation for signs of growth, and the number of observed colonies is reported below as Tables 8.2 (for the 1-hour exposure time) and 8.3 (for the 24-hour exposure time). The results appear to indicate near total spore kill at 24 hours' incubation time with the activated Oxine®, with hydrogen peroxide only approaching total kill for the longer exposure time. Exposure to inactive Oxine® appears not to be hazardous to the spores, having similar viability as the unexposed control coupons. An experiment was performed with *B.subtilis* ATCC 6051 previous to this, but owing to contamination of the plates with fungus and a lack of replicate platings, that data is not included here.

		10 ⁻¹	10 ⁻²	10 ⁻³	10 ⁻⁴	10 ⁻⁵	10 ⁻⁶
CONTROL	A	TNTC	TNTC	TNTC	TNTC	79	8
	B	TNTC	TNTC	TNTC	TNTC	109*	5
Peroxide, 3.5%	A	TNTC	TNTC	TNTC	181	6	2
	B	TNTC	TNTC	TNTC	113	5	2
Inactive Oxine	A	TNTC	TNTC	TNTC	298	27	7
	B	TNTC	TNTC	TNTC	260	16	0
Active Oxine	A	201	14	0	0	1	0
	B	TNTC	18	1	1	0	0*

Table 8.2. Plate countings of post-exposure *B.pumilus* SAFR-032 spores exposed on aluminum coupons, 1 hour exposure time, 24 hour incubation time. Inactivated Oxine® concentration = 108.5 ppm ClO₂; activated Oxine® concentration = 70.4 ppm, 39 ppm free. Numbers are colonies counted on TSA plates for the given serial dilution. TNTC = too numerous to count (>300 colonies, or >100 colonies in one quarter of the plate). * = agar plate appeared damaged or potentially contaminated. A and B are duplicate platings.

		10 ⁻¹	10 ⁻²	10 ⁻³	10 ⁻⁴	10 ⁻⁵	10 ⁻⁶
Control	A	TNTC	TNTC	TNTC	TNTC	31	2*
	B	TNTC	TNTC	TNTC	TNTC	20	2
Peroxide, 3.5%	A	0	0	0	0	0	0
	B	1	0	0	0	0	0
Inactive Oxine	A	TNTC	TNTC	TNTC	TNTC	48*	8
	B	TNTC	TNTC	TNTC	TNTC	78	3
Active Oxine	A	3	0	0	0	0	0
	B	3	0	0	0	0	0

Table 8.3. Plate countings for post-exposure spores of *B. pumilus* SAFR-032 spores on Al coupons, 24 hour exposure time, 24 hour incubation time. Concentrations are identical to Table 8.2. * = potential contamination or plate damage.

Discussion

The present work described here extends on the work previously performed by Young and Setlow²⁸ by conducting tests of Oxine® effect on dried spores. These dried spores showed greater survival at equivalent concentration and exposure time than liquid spore suspensions exposed to Oxine® (data not shown), though as seen above in Table 8.1, the viability of the

dried spores decreases over longer exposure times and with higher concentrations. Interestingly, there does not appear to be a large difference in the viability results between dried *B.pumilus* and *B.subtilis* spores.

In the data for *B.pumilus* SAFR-032 on aluminum coupons, seen in Tables 8.2 and 8.3 above, the activated Oxine® has a much more prominent effect than the results on the glass cover slips. The activated Oxine® had about a 3-log decrease in viable colony counts on TSA plates after one hour of exposure and showed nearly total killing effect after 24 hours of exposure. This does correspond to the same enhanced killing over time seen with the glass cover slip test. It was more effective at shorter times, however, than exposure to peroxide; this might be the result of the enhanced peroxidase activity known to be present in SAFR-032 delaying any immediate loss of viability. The Oxine® must clearly be activated, however; either inactive Oxine® cannot diffuse through the outer spore layers to affect the spore, or it cannot be activated by the environment in the interior of the spore core.



Figure 8.2. SEM image of pre-treatment dried *B.subtilis* ATCC 6051 spores on glass cover slips, magnification 10,000x. The spores appear oval in shape, in line with the expected size and shape of bacterial spores.

The SEM results appear to show a potential mechanism of action of the Oxine® on the spores of both species. For the *B.subtilis* ATCC 6051 spores, as can be seen in Figures 8.2 through 8.4, the effect of the Oxine® appears to be a chemical degradation of the spore; many of the spores appear collapsed, indicating possible dissolution of the core and subsequent cortex collapse. Spores that appear intact are smaller in size than collapsed spores and have visible rings of material surrounding them, indicating additional oxidation by the activated chlorine dioxide; these effects are most prominent at the interface of the spore and the glass surface of the cover slip. Similar effects are apparent in

SEM images of treated *B.pumilus* SAFR-032 spores, as seen in Figures 8.5 and 8.6 below; spores appear smaller and some are collapsed, though there are fewer of both. The reduced size could be attributable to chemical dissolution of exosporium, which may also be responsible for the absence of unknown connecting material between spores seen in Figure 8.5. This material may be responsible for some of the enhanced peroxide resistance in *B.pumilus* SAFR-032 as previously reported^{24,25}.

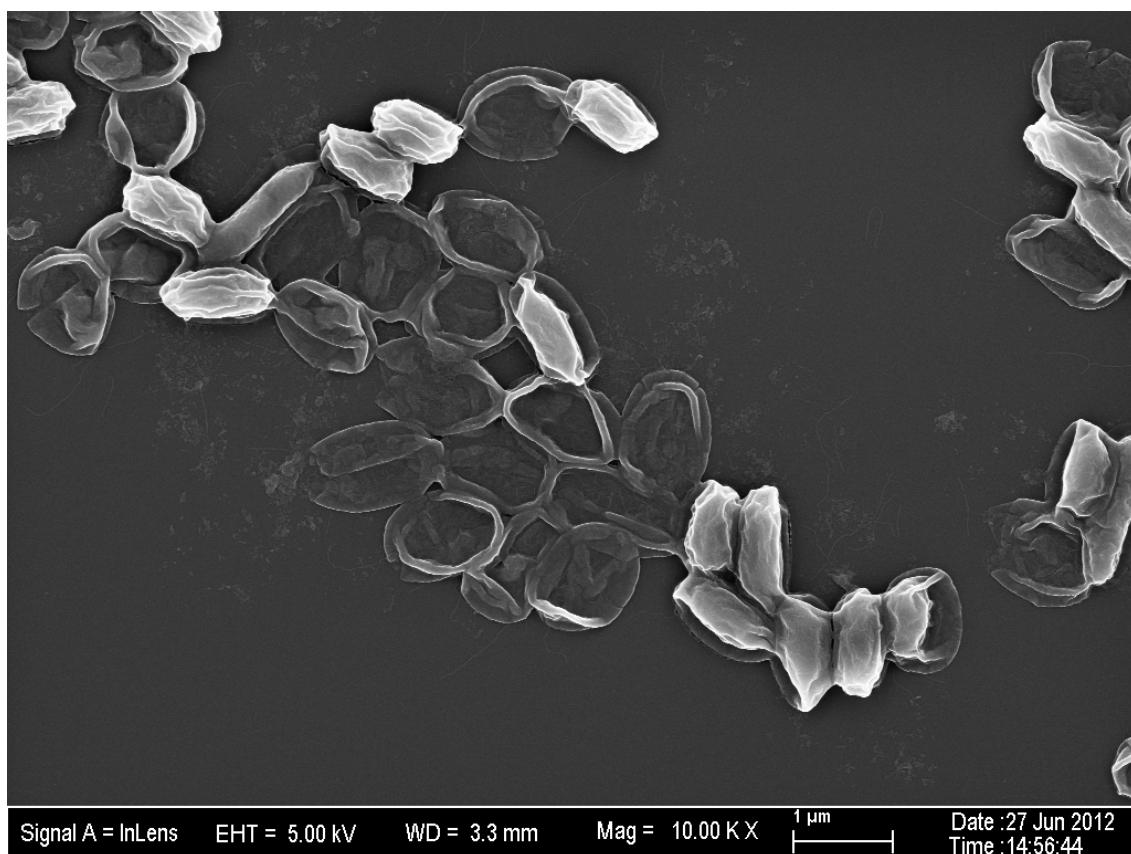


Figure 8.3. Post-Oxine®-treatment *B.subtilis* ATCC 6051 spores as seen via SEM, 10,000x magnification. A number of spores appear to have collapsed, a ring of outer material surrounding a nearly-hollow center; other spores are more intact but smaller and with a halo of material affected by the chemical treatment occurring at the interface between the spores and the glass cover slip.

When observing the aluminum spacecraft-grade coupons with spores using SEM, the appearance of the images in all examples shows numerous pits, cavities, and other surface deformities on the coupon. It is surmised that these surfaces may be the result of autoclaving the aluminum coupons, as one recent paper used an alternative sterilization method due to oxidation damage to the coupon during autoclaving³². Curiously, for the peroxide sample, there is no evidence of intact spores, or spore bodies at all; there is the possibility that owing to the lack of inactivation and the time delay between exposure and SEM imaging (approximately 1 week), the spores may have dissolved entirely on that particular coupon. Inactivated Oxine® and the control coupons both have similar appearances further contributing to the lack of biocidal activity by inactive Oxine®.

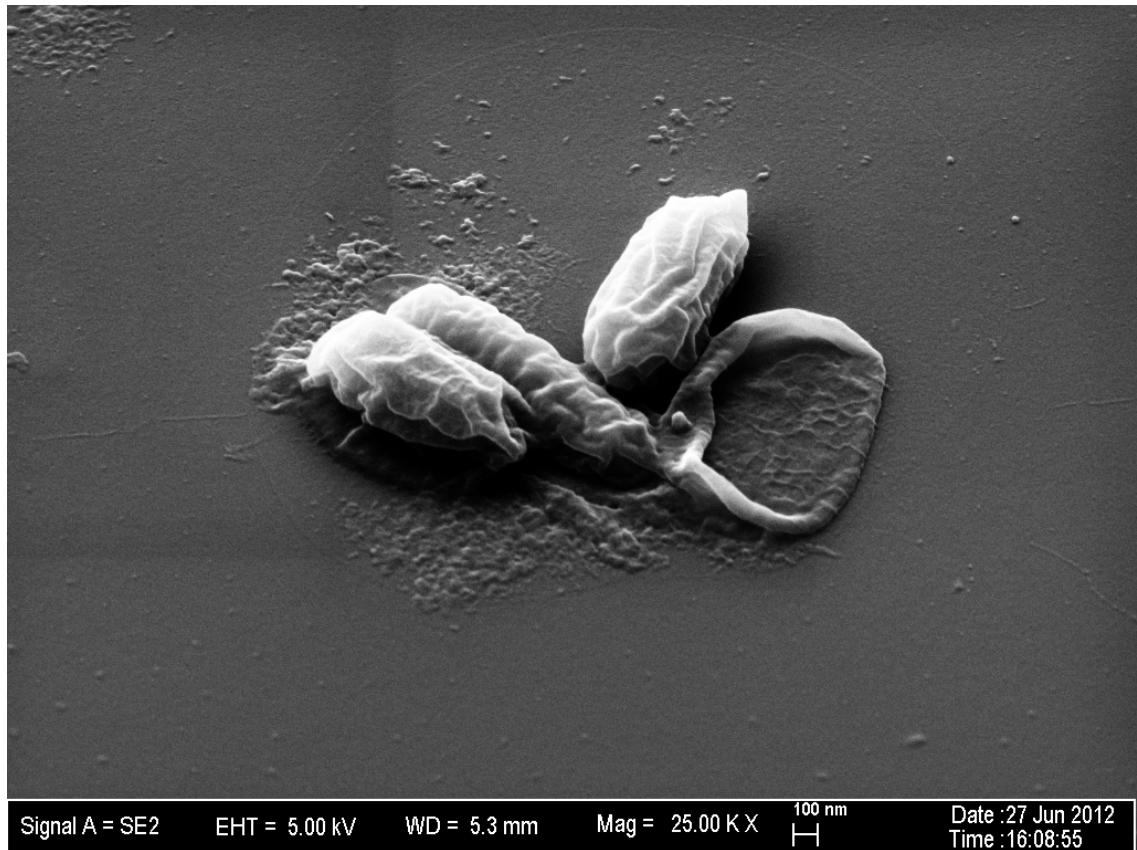


Figure 8.4. Enhanced-magnification (25,000x) and tilted (45°) SEM image of post-Oxine®-treated *B. subtilis* ATCC 6051 spores. From this image it appears that the Oxine® has degraded the spore core material, causing the cortex to collapse; the cortex and coat appear mostly intact.

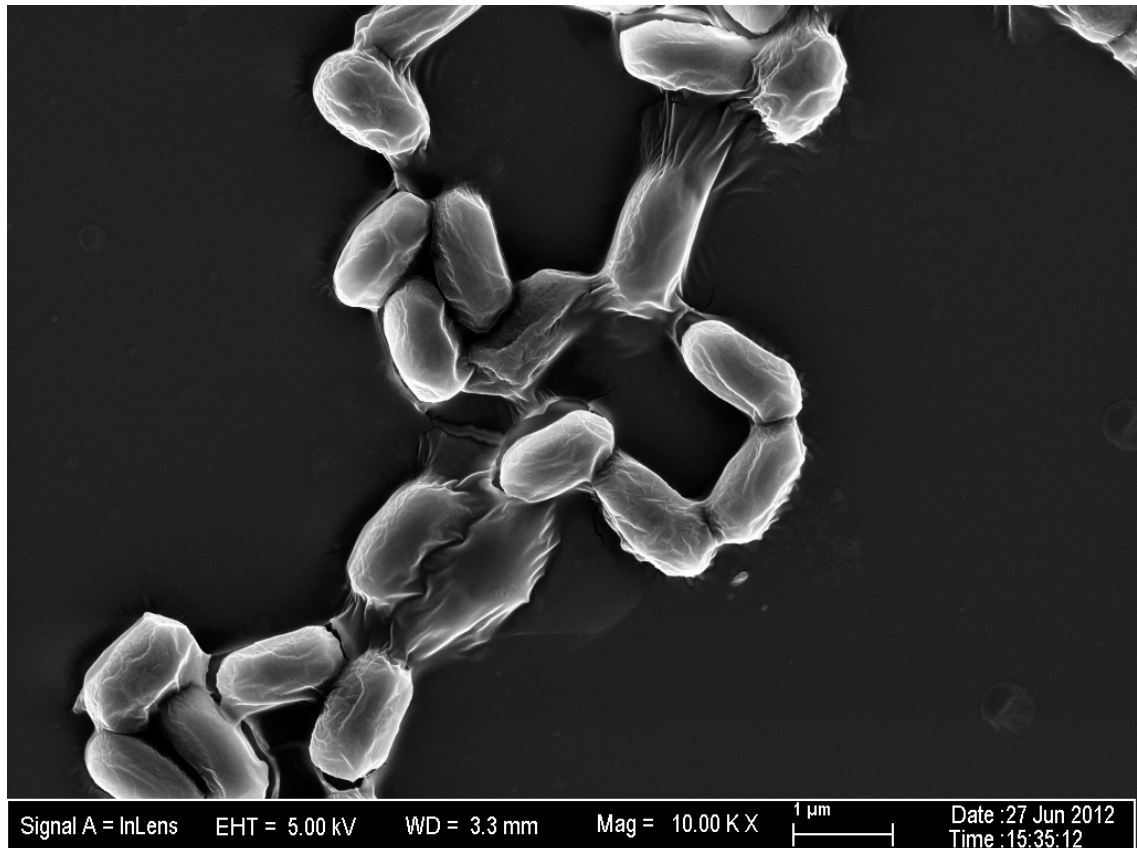


Figure 8.5. Pre-treatment *B.pumilus* SAFR-032 spores as seen on glass cover slips via SEM (10,000x magnification). There appears to be an unknown material, possibly exosporium, connecting some of the spores together. The overall shape of the spores is still oval, though slightly smaller in size versus the *B.subtilis* ATCC 6051.

The lack of spores on the peroxide coupon is equaled only by the lack of spores on the SEM image of the activated Oxine®-treated spores. However, occasional collapsed spores are visible on that coupon, whereas no spores are evident on the peroxide-treated coupon; it appears that the spore visible in Figure 8.10 has suffered the same damage and loss of structure as those seen in both *B.subtilis* ATCC 6051 and *B.pumilus* SAFR-032 spores treated by Oxine® on glass cover slips. Spores found on the inactive Oxine® exposure coupons and the controls appear normal, though it is harder to distinguish due

to there being multiple layers of spores and apparent crevasses and other defects in the aluminum coupon surface. In several SEM images there are unknown crystal-like structures which are not spores and have not been identified; it is unclear whether they are the result of oxidative damage to the coupon from autoclaving or some sort of dried precipitate from the spore deposition. For the images associated with the peroxide and Oxine®, it is further unclear whether the damage to the coupon is entirely a result of the autoclave oxidation or chemical damage from the peroxide or Oxine®; further testing will have to be performed to clarify the results found here.

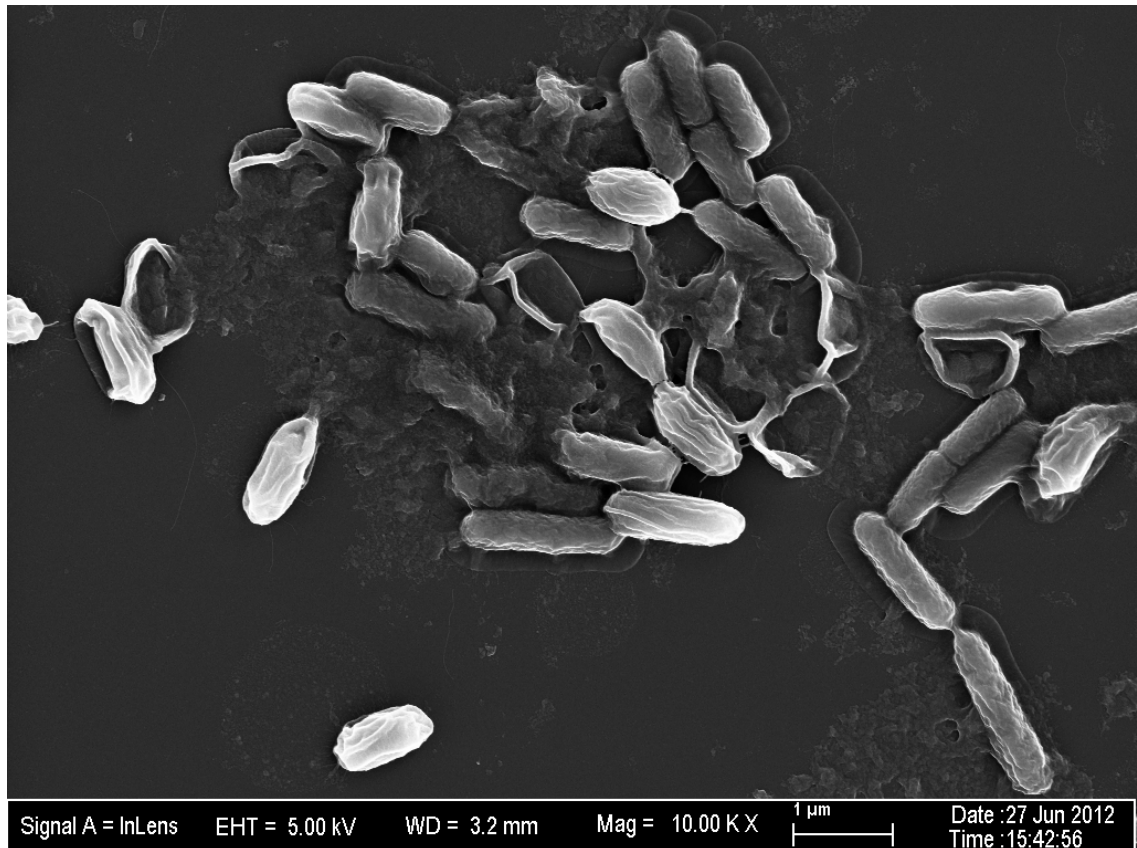


Figure 8.6. Post-Oxine®-treated *B.pumilus* SAFR-032 spores as seen via SEM at 10,000x magnification. Several spores appear similarly affected to those of *B.subtilis* with a ring of material surrounding a dissolved/collapsed center; some of that material has leaked from the spores onto the surface of the glass cover slip. Some rod-like bodies are present, which were not present in the pre-treatment or control images, or images at lower magnification elsewhere on the cover slip; their identities are unknown.

Conclusions

Some spore species, such as *B.pumilus* SAFR-032, are highly resistant to conventional methods of treatment, such as UV radiation exposure and peroxide treatment. In order to find methods of sterilization that will be effective, new biocidal agents are required. Bio-Cide International's Oxine® was tested against *B.subtilis* ATCC 6051 and *B.pumilus* SAFR-032; it demonstrates sporicidal effects against both, though more thorough testing will

be necessary to better clarify concentrations and exposure times required for sporicidal effects to occur. The apparent mechanism of action is a chemical degradation of the spore core causing the spore core contents to leak from the spore and the spore coat and cortex to collapse. Oxine® demonstrates effects on dried spores on glass cover slips and on aluminum coupons, though the presence of unknown structures on the aluminum coupons may be the result of oxidative damage to the aluminum as a result of the autoclaving sterilization method. These results, however, show promise for the use of Oxine® as a sporicidal agent.

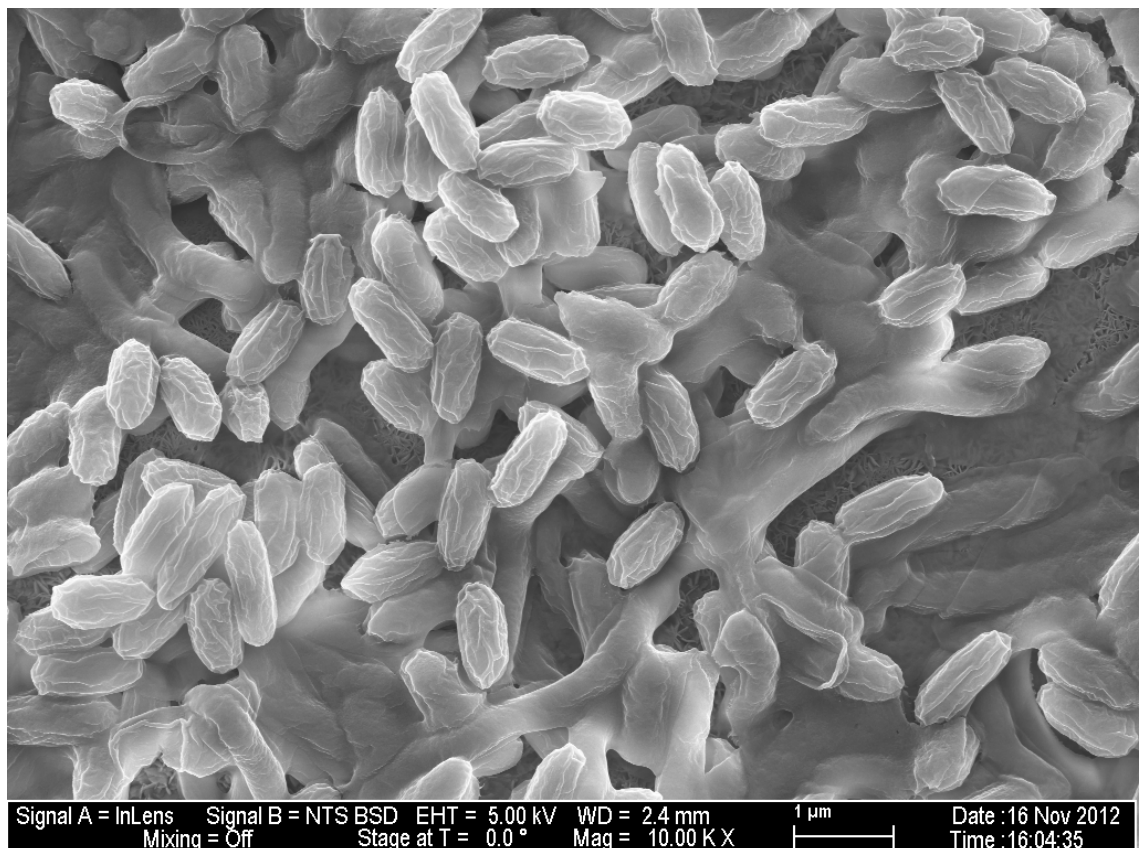


Figure 8.7. SEM image of *B. pumilus* SAFR-032 spores on an aluminum coupon, 10,000x magnification. The spores are normally-shaped, though there are unusual structures underneath the topmost layer of spores, which may be overhangs and crevasses in the surface of the metal coupon.

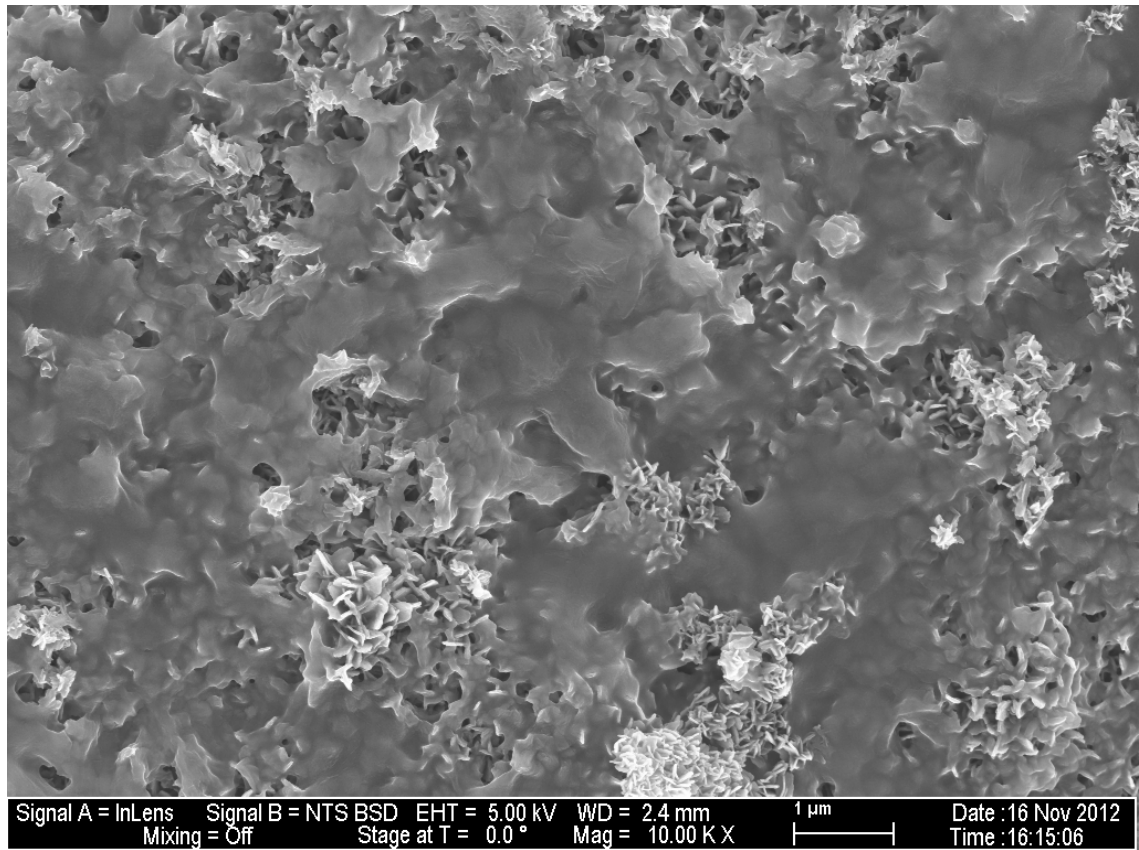


Figure 8.8. SEM image of aluminum coupon, initially covered in *B.pumilus* SAFR-032 spores, after treatment with 3.5% w/v hydrogen peroxide (magnification 10,000x). No spores are apparent in this image, and there are unusual crystal-shaped structure visible on the lower surface of the coupon; what these shapes are is unknown. The lack of spores is possibly the result of the peroxide entirely dissolving the spores.

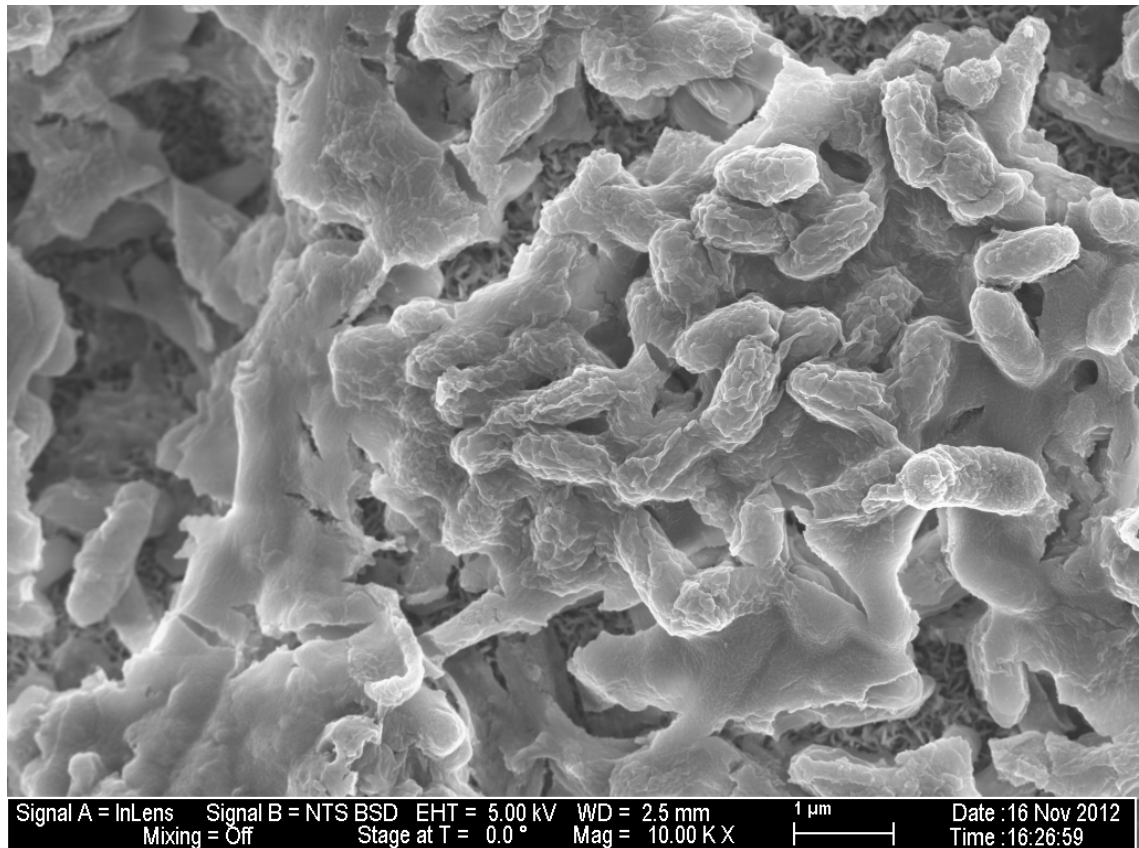


Figure 8.9. SEM image of *B. pumilus* SAFR-032 spores on an aluminum coupon, after treatment with inactive Oxine®, magnification 10,000x. Spores are present throughout the image, though it is obvious there are large pits and other structures, from the left side of the image. The spore bodies appear intact and oval in shape. The unknown crystal structures are visible underneath the top-most layer.

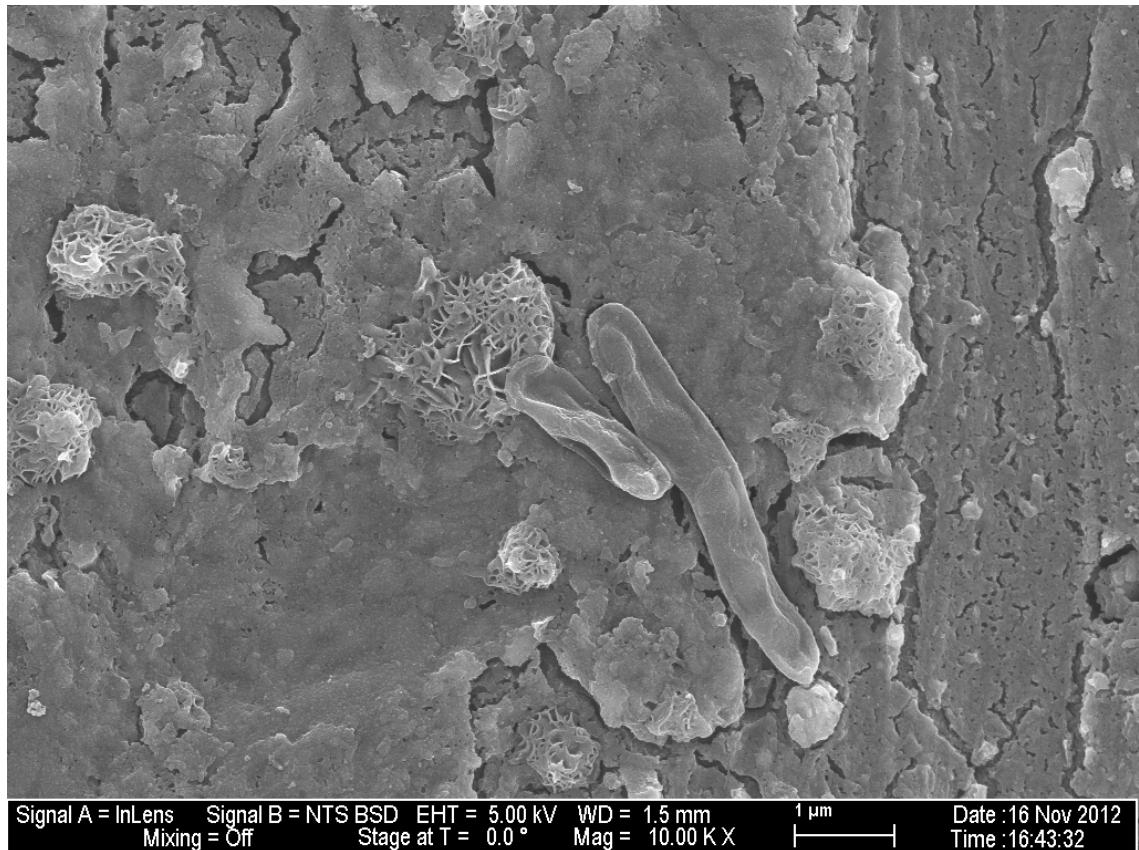


Figure 8.10. SEM image of an aluminum coupon coated in *B.pumilus* SAFR-032 spores treated with activated Oxine®, magnification 10,000x. Few spores were present in the observations of this coupon, though the collapsed spore body at center of this figure is one of them. The spore appears to be collapsed similarly to those in Figures 8-3 and 8-6. There does not appear to be as much layering as in previous figures, though the crystal-shaped bodies are more obvious even on the surface layer.

REFERENCES

CHAPTER 1: THE RNA WORLD HYPOTHESIS AND THE COLD ORIGIN OF LIFE

1. Voet, Donald, and Judith G. Voet. *Biochemistry*. 3rd ed. New York: John Wiley & Sons, Inc., 2004.
2. Gilbert, Walter. "The RNA world." *Nature* **319** (1986) 618.
3. Westheimer, F.H. "Polyribonucleic acids as enzymes." *Nature* **319** (1986) 534-6.
4. Orgel, L.E. "Evolution of the Genetic Apparatus." *J Mol Biol* **38** (1968) 381-93.
5. Crick, F.H.C. "The Origin of the Genetic Code." *J Mol Biol* **38** (1968) 367-79.
6. Orgel, Leslie E. "Prebiotic Chemistry and the Origin of the RNA World." *Crit Rev Biochem Mol Biol* **39** (2004) 99-123.
7. Wächtershäuser, Günter. "Before Enzymes and Templates: Theory of Surface Metabolism." *Microbiol Rev* **52** (1988) 452-484.
8. Miller, Stanley L., and Harold C. Urey. "Organic Compound Synthesis on the Primitive Earth." *Science* **130** (1959) 245-51.
9. Chyba, Christopher, and Carl Sagan. "Endogenous production, exogenous delivery and impact-shock synthesis of organic molecules: an inventory for the origins of life." *Nature* **355** (1992) 125-32.
10. Barks, Hannah L., Ragan Buckley, Gregory A. Grieves, Ernesto Di Mauro, Nicholas V. Hud, and Thomas M. Orlando. "Guanine, Adenine, and Hypoxanthine Production in UV-Irradiated Formamide Solutions: Relaxation of the Requirements for Prebiotic Purine Nucleobase Formation." *ChemBioChem* **11** (2010) 1240-3.
11. Powner, Matthew W., Béatrice Gerland, and John D. Sutherland. "Synthesis of activated pyrimidine ribonucleotides in prebiotically plausible conditions." *Nature* **459** (2009) 239-42.
12. Larralde, Rosa, Michael P. Robertson, and Stanley L. Miller. "Rates of decomposition of ribose and other sugars: Implications for chemical evolution." *PNAS* **92** (1995) 8158-60.

13. Levy, Matthew, and Stanley L. Miller. "The stability of the RNA bases: Implications for the origin of life." *PNAS* **95** (1998) 7933-8.
14. Bada, J.L., C. Bigham, and S. L. Miller. "Impact melting of frozen oceans on the early Earth: Implications for the origin of life." *PNAS* **91** (1994) 1248-50.
15. Oró, J. "Mechanism of Synthesis of Adenine from Hydrogen Cyanide under Possible Primitive Earth Conditions." *Nature* **191** (1961) 1193-4.
16. Miyakawa, Shin, H. James Cleaves, and Stanley L. Miller. "The Cold Origin of Life: A. Implications Based on the Hydrolytic Stabilities of Hydrogen Cyanide and Formamide." *Orig Life Evol Biosph* **32** (2002) 195-208.
17. Miyakawa, Shin, H. James Cleaves, and Stanley L. Miller. "The Cold Origin of Life: B. Implications Based on Pyrimidines and Purines Produced from Frozen Ammonium Cyanide Solutions." *Orig Life Evol Biosph* **32** (2002) 209-218.
18. Monnard, Pierre-Alain, Anastassia Kanavarioti, and David W. Deamer. "Eutectic Phase Polymerization of Activated Ribonucleotide Mixtures Yields Quasi-Equimolar Incorporation of Purine and Pyrimidine Nucleobases." *J Am Chem Soc* **125** (2003) 13734-40.
19. Vlassov, A.V., B.H. Johnston, L.F. Landweber, and S.A. Kazakov. "RNA Catalysis in Frozen Solutions." *Dokl Biochem Biophys* **402** (2005) 207-9.
20. Vlassov, Alexander V., Sergei A. Kazakov, Brian H. Johnston, and Laura F. Landweber. "The RNA World on Ice: A New Scenario for the Emergence of RNA Information." *J Mol Evol* **61** (2005) 264-73.
21. Szostak, Jack W., David P. Bartel, and P. Luigi Luisi. "Synthesizing life." *Nature* **409** (2001) 387-90.
22. Müller, U.F. "Re-creating an RNA world." *Cell Mol Life Sci* **63** (2006) 1278-93.
23. Joyce, Gerald F. "The antiquity of RNA-based evolution." *Nature* **418** (2002) 214-21.
24. Spirin, A.S. "The RNA World and Its Evolution." *Molecular Biology* **39** (2005) 466-472.
25. Monnard, Pierre-Alain, and David W. Deamer. "Membrane Self-Assembly Processes: Steps Toward the First Cellular Life." *The Anatomical Record* **268** (2002) 196-207.
26. Orgel, Leslie E. "The origin of life – a review of facts and speculations." *Trends Biochem Sci* **23** (1998) 491-5.

27. Lazcano, Anthony, and Stanley L. Miller. "The Origin and Early Evolution of Life: Prebiotic Chemistry, the Pre-RNA World, and Time." *Cell* **85** (1996) 793-8.
28. Valley, John W., William H. Peck, Elizabeth M. King, and Simon A. Wilde. "A cool early Earth." *Geology* **30** (2002) 351-4.
29. Attwater, James, Aniela Wochner, Vitor B. Pinheiro, Alan Coulson, and Philipp Holliger. "Ice as a protocellular medium for RNA replication." *Nat Commun* **1**:76 (2010) 9p. DOI: 10.1038/ncomms1076.

CHAPTER 2: EXTREMOPHILIC ORGANISMS

1. Lowe, Susan E., Mahendra K. Jain, and J. Gregory Zeikus. "Biology, Ecology, and Biotechnological Applications of Anaerobic Bacteria Adapted to Environmental Stresses in Temperature, pH, Salinity, or Substrates." *Microbiol Rev* **57** (1993) 451-509.
2. Canganella, Francesco, and Juergen Wiegel. "Extremophiles: from abyssal to terrestrial ecosystems and possibly beyond." *Naturwissenschaften* **98** (2011) 253-79.
3. Chyba, Christopher F., and Cynthia B. Phillips. "Possible ecosystems and the search for life on Europa." *PNAS* **98** (2001) 801-4.
4. Hansen, Candice J., L. Esposito, A.I.F. Stewart, J. Colwell, A. Hendrix, W. Pryor, D. Shemansky, and R. West. "Enceladus' Water Vapor Plume." *Science* **311** (2006) 1422-5.
5. Teolis, B.D., M.E. Perry, B.A. Magee, J. Westlake, and J.H. Waite. "Detection and measurement of ice grains and gas distribution in the Enceladus plume by Cassini's Ion Neutral Mass Spectrometer." *J Geophys Res* **115** (2010) A09222 (12p.)
6. Smith, P.H., L.K. Tamppari, R.E. Arvidson, D. Bass, D. Blaney, W.V. Boynton, A. Carswell, D.C. Catling, B.C. Clark, T. Duck, E. DeJong, D. Fisher, W. Goetz, H.P. Gunnlaugsson, M.H. Hecht, V. Hipkin, J. Hoffman, S.F. Hviid, H.U. Keller, S.P. Kounaves, C.F. Lange, M.T. Lemmon, M.B. Madsen, W.J. Markiewicz, J. Marshall, C.P. McKay, M.T. Mellon, D.W. Ming, R.V. Morris, W.T. Pike, N. Renno, U. Staufer, C. Stoker, P. Taylor, J.A. Whiteway, and A.P. Zent. "H₂O at the Phoenix Landing Site." *Science* **325** (2009) 58-61.
7. Kostama, V.-P., M.A. Ivanov, J. Raitala, T. Törmänen, J. Korteniemi, and G. Neukum. "Evidence for multiple ice deposits on the northeastern rim of Hellas basin, Mars." *Earth Plan Sci Lett* **294** (2010) 321-31.

8. Pikuta, Elena V., Richard B. Hoover, and Jane Tang. "Microbial Extremophiles at the Limits of Life." *Crit Rev Microbiol* **33** (2007) 183-209.
9. Morita, Richard Y. "Psychrophilic Bacteria." *Bacteriol Rev* **39** (1975) 144-167.
10. Georlette, D., V. Blaise, T. Collins, S. D'Amico, E. Gratia, A. Hoyoux, J.-C. Marx, G. Sonan, G. Feller, and C. Gerday. "Some like it cold: biocatalysis at low temperatures." *FEMS Microbiol Rev* **28** (2004) 25-42.
11. D'Amico, Salvino, Tony Collins, Jean-Claude Marx, Georges Feller, and Charles Gerday. "Psychrophilic microorganisms: challenges for life." *EMBO Reports* **7** (2006) 385-89.
12. Deming, Jody W. "Psychrophiles and polar regions." *Curr Opin Microbiol* **5** (2002) 301-9.
13. Hoover, Richard B., and Elena V. Pikuta. "Psychrophilic and Psychrotolerant Microbial Extremophiles in Polar Environments." In *Polar Microbiology: The Ecology, Biodiversity, and Bioremediation Potential of Microorganisms in Extremely Cold Environments*; Bej, Asim K., et al., eds. Boca Raton: CRC Press, 2010: 115-156.
14. Junge, Karen, Hajo Eicken, and Jody W. Deming. "Bacterial Activity at -2 to -20°C in Arctic Wintertime Sea Ice." *Appl Env Microbiol* **70** (2004) 550-7.
15. Junge, Karen, Hajo Eicken, Brian D. Swanson, and Jody W. Deming. "Bacterial incorporation of leucine into protein down to -20°C with evidence for potential activity in sub-eutectic saline ice formations." *Cryobiology* **52** (2006) 417-29.
16. Price, P. Buford. "A habitat for psychrophiles in deep Antarctic ice." *PNAS* **97** (2000) 1247-51.
17. D'Elia, Tom, Ram Verrapaneni, and Scott O. Rogers. "Isolation of Microbes from Lake Vostok Accretion Ice." *Appl Env Microbiol* **74** (2008) 4962-5.
18. Lanoil, Brian, Mark Skidmore, John C. Priscu, Sukkyun Han, Wilson Foo, Stefan W. Vogel, Slawek Tulaczyk, and Hermann Engelhardt. "Bacteria beneath the West Antarctic Ice Sheet." *Env Microbiol* **11** (2009) 609-15.
19. Panikov, N.S., P.W. Flanagan, W.C. Oechel, M.A. Mastepanov, and T.R. Christensen. "Microbial activity in soils frozen to below -39°C." *Soil Biol Biochem* **38** (2006) 785-94.
20. Stetter, Karl O. "Hyperthermophilic procaryotes [sic]." *FEMS Microbiol Rev* **18** (1996) 149-58.

21. Rastogi, Gurdeep, Geetha L. Muppidi, Raghu N. Gurram, Akash Adhikari, Kenneth M. Bischoff, Stephen R. Hughes, William A. Apel, Sookie S. Bang, David J. Dixon, and Rajesh K. Sani. "Isolation and characterization of cellulose-degrading bacteria from the deep subsurface of the Homestake gold mine, Lead, South Dakota, USA." *J Ind Microbiol Biotechnol* **36** (2009) 585-98.
22. Rothschild, Lynn J., and Rocco L. Mancinelli. "Life in extreme environments." *Nature* **409** (2001) 1092-1101.
23. Cava, Felipe, Aurelio Hidalgo, and José Berenguer. "*Thermus thermophilus* as biological model." *Extremophiles* **13** (2009) 213-31.
24. Averhoff, Beater, and Volker Müller. "Exploring research frontiers in microbiology: recent advances in halophilic and thermophilic extremophiles." *Res Microbiol* **161** (2010) 506-514.
25. Gibbs, Richard A. "DNA Amplification by the Polymerase Chain Reaction." *Anal Chem* **62** (1990) 1206-1214.
26. Burgess, Sara A., Denise Lindsay, and Steve H. Flint. "Thermophilic bacilli and their importance in dairy processing." *Int J Food Microbiol* **144** (2010) 215-25.
27. Ventosa, A., and J.J. Nieto. "Biotechnological applications and potentialities of halophilic microorganisms." *World J Microbiol Biotechnol* **11** (1995) 85-94.
28. Siglioccolo, Alessandro, Alessandro Paiardini, Maria Piscitelli, and Stefano Pascarella. "Structural adaption of extreme halophilic proteins through decrease of conserved hydrophobic contact surface." *BMC Struct Biol* **11**:50 (2011) (12p.).
29. Oren, Aharon. "Industrial and environmental applications of halophilic microorganisms." *Env Technol* **31** (2010) 825-34.
30. Daly, Michael J. "A new perspective on radiation resistance based on *Deinococcus radiodurans*." *Nat Rev Microbiol* **7** (2009) 237-45.
31. Cox, Michael M., James L. Keck, and John R. Battista. "Rising from the Ashes: DNA Repair in *Deinococcus radiodurans*." *PLoS Genetics* **6** (2010) e1000815 (3p.)
32. Cox, Michael M., and John R Battista. "*Deinococcus radiodurans*—the consummate survivor." *Nat Rev Microbiol* **3** (2005) 882-92.
33. Bartlett, D.H. "Pressure effects on *in vivo* microbial processes." *Biochim Biophys Acta* **1595** (2002) 367-381.

34. Fang, Jiansong, and Chiaki Kato. "Deep-Sea Piezophilic Bacteria: Geomicrobiology and Biotechnology." In *Geomicrobiology*, Sudhir K. Jain, Abdul Arif Khan, and Mahendra Rai, eds. Enfield; Science Publishers Ltd., 2010; 47-77.
35. Horikoshi, Koki. "Barophiles: deep-sea microorganisms adapted to an extreme environment." *Curr Opin Microbiol* **1** (1998) 291-5.
36. Oger, Phillipe M., and Mohamed Jebbar. "The many ways of coping with pressure." *Res Microbiol* **161** (2010) 799-809.
37. Simonato, Francesca, Stefano Campanaro, Federico M. Lauro, Alessandro Vezzi, Michela D'Angelo, Nicola Vitulo, Giorgio Valle, and Douglas H. Bartlett. "Piezophilic adaptation: a genomic point of view." *J Biotechnol* **126** (2006) 11-25.
38. Abe, Fumiyoshi, and Koki Horikoshi. "The biotechnological potential of piezophiles." *Trends Biotechnol* **19** (2001) 102-8.
39. Amils, Ricardo, Elena González-Toril, David Fernández-Remolar, Felipe Gómez, Ángeles Aguilera, Nuria Rodríguez, Mustafá Malki, Antonio García-Moyano, Alberto G. Fairén, Vicenta de la Fuente, and José Luis Sanz. "Extreme environments as Mars terrestrial analogs: The Rio Tinto case." *Plan Space Sci* **55** (2007) 370-81.
40. Horikoshi, Koki. "Alkaliphiles: Some Applications of Their Products for Biotechnology." *Microbiol Mol Biol Rev* **63** (1999) 735-50.
41. Sarethy, Indira P., Yashi Saxena, Aditi Kapoor, Manisha Sharma, Sanjeev K. Sharma, Vandana Gupta, and Sanjay Gupta. "Alkaliphilic bacteria: applications in industrial biotechnology." *J Ind Microbiol Biotechnol* **38** (2011) 769-90.
42. Campos, Victor L., Cristian Valenzuela, Pablo Yarza, Peter Kämpfer, Roberto Vidal, C. Zaror, Maria-Angelica Mondaca, Arantxa Lopez-Lopez, and Ramon Rosselló-Móra. "*Pseudomonas arsenicoxydans* sp nov., an arsenite-oxidizing strain isolated from the Atacama desert." *Syst Appl Microbiol* **33** (2010) 193-7.

CHAPTER 3: RHODAMINE-B FLUORESCENCE STUDIES OF

POLY(ADENYLIC) ACID, A POTENTIAL CRYOPROTECTANT, IN RELATION TO LIPOTEICHOIC ACID

1. Rothschild, Lynn J., and Rocco L. Mancinelli. "Life in extreme environments." *Nature* **409** (2001) 1092-1101.

2. D'Amico, Salvino, Tony Collins, Jean-Claude Marx, Georges Feller, and Charles Gerday. "Psychrophilic microorganisms: challenges for life." *EMBO Reports* **7** (2006) 385-9.
3. Kohshima, Shiro. "A novel cold-tolerant insect found in a Himalayan glacier." *Nature* **310** (1984) 225-7.
4. Junge, Karen, Hajo Eicken, Brian D. Swanson, and Jody W. Deming. "Bacterial incorporation of leucine into protein down to -20°C with evidence for potential activity in sub-eutectic saline ice formations." *Cryobiology* **52** (2006) 417-29.
5. Junge, Karen, Hajo Eicken, and Jody W. Deming. "Bacterial Activity at -2 to -20°C in Arctic Wintertime Sea Ice." *Appl Env Microbiol* **70** (2004) 550-7.
6. Price, P. Buford. "Microbial life in glacial ice and implications for a cold origin of life." *FEMS Microbiol Ecol* **59** (2007) 217-31.
7. Treberg, Jason R., Connie E. Wilson, Robert C. Richards, K. Vanya Ewart, and William R. Driedzic. "The freeze-avoidance response of smelt *Osmerus mordax*: initiation and subsequent suppression of glycerol, trimethylamine oxide and urea accumulation." *J Exp Biol* **205** (2002) 1419-27.
8. Lillford, Peter J., and Chris B. Holt. "In vitro uses of biological cryoprotectants." *Phil Trans R Soc Lond B* **357** (2002) 945-51.
9. Venketesh, S., and C. Dayananda. "Properties, Potentials, and Prospects of Antifreeze Proteins." *Crit Rev Biotechnol* **82** (2008) 57-82.
10. Neuhaus, Francis C., and James Baddiley. "A Continuum of Anionic Charge: Structures and Functions of D-Alanyl-Teichoic Acids in Gram-Positive Bacteria." *Microbiol Mol Biol Rev* **67** (2003) 686-723.
11. Schirner, Kathrin, Jon Marles-Wright, Richard J. Lewis, and Jeff Errington. "Distinct and essential morphogenic functions for wall- and lipo-teichoic acids in *Bacillus subtilis*." *EMBO J* **28** (2009) 830-42.
12. Armstrong, J.J., J. Baddiley, J.G. Buchanan, B. Carss, and G.R. Greenberg. "Isolation and Structure of Ribitol Phosphate Derivatives (Teichoic Acids) from Bacterial Cell Walls." *J Chem Soc* (1958) 4344-54.
13. Baddiley, James. "Bacterial Cell Walls and Membranes. Discovery of the Teichoic Acids." *BioEssays* **10** (1989) 207-10.
14. Schmidt, Richard R., Christian M. Pedersen, Yan Qiao, and Ulrich Zähringer. "Chemical synthesis of bacterial lipoteichoic acids: An insight on its biological significance." *Org Biomol Chem* **9** (2011) 2040-52.

15. Morath, Siegfried, Andreas Stadelmaier, Armin Geyer, Richard R. Schmidt, and Thomas Hartung. "Synthetic Lipoteichoic Acid from *Staphylococcus aureus* Is a Potent Stimulus of Cytokine Release." *J Exp Med* **195** (2002) 1635-40.
16. Morath, Siegfried, Sonja von Aulock, and Thomas Hartung. "Structure/function relationships of lipoteichoic acids." *J Endotoxin Res* **11** (2005) 348-56.
17. Schröder, Nicholas W.J., Siegfried Morath, Christian Alexander, Lutz Hamann, Thomas Hartung, Ulrich Zähringer, Ulf B. Göbel, Joerg R. Weber, and Ralf R. Schumann. "Lipoteichoic Acid (LTA) of *Streptococcus pneumoniae* and *Staphylococcus aureus* Activates Immune Cells via Toll-like Receptor (TLR)-2, Lipopolysaccharide-binding Protein (LBP), and CD14, whereas TLR-4 and MD-2 Are Not Involved." *J Biol Chem* **278** (2003) 15587-94.
18. Weber, Joerg R., Philippe Moreillon, and Elaine I. Tuomanen. "Innate sensors for Gram-positive bacteria." *Curr Opin Immunol* **15** (2003) 408-15.
19. Draing, Christian, Stefanie Sigel, Susanne Deininger, Stephanie Traub, Rebekka Munke, Christoph Mayer, Lars Hareng, Thomas Hartung, Sonja von Aulock, and Corinna Hermann. "Cytokine induction by Gram-positive bacteria." *Immunobiology* **213** (2008) 285-296.
20. Wickham, Jason R., Jeffrey L. Halye, Stepan Kastanov, Jana Khandogin, and Charles V. Rice. "Revisiting Magnesium Chelation by Teichoic Acid with Phosphorus Solid-State NMR and Theoretical Calculations." *J Phys Chem B* **113** (2009) 2177-83.
21. Garimella, Ravindranath, Jeffrey L. Halye, William Harrison, Phillip E. Klebba, and Charles V. Rice. "Conformation of the Phosphate D-Alanine Zwitterion in Bacterial Teichoic Acid from Nuclear Magnetic Resonance Spectroscopy." *Biochemistry* **48** (2009) 9242-9.
22. McBride, Shonna M., and Abraham L. Sonenshein. "The *dlt* operon confers resistance to cationic antimicrobial peptides in *Clostridium difficile*." *Microbiology* **157** (2011) 1457-65.
23. Ginsburg, Isaac. "Role of lipoteichoic acid in infection and inflammation." *Lancet Infect Dis* **2** (2002) 171-9.
24. Fabretti, Francesca, Christian Theliacker, Lucilla Baldassarri, Zbigniew Kaczynski, Andrea Kropec, Otto Holst, and Johannes Huebner. "Alanine Esters of Enterococcal Lipoteichoic Acid Play a Role in Biofilm Formation and Resistance to Antimicrobial Peptides." *Infect Immun* **74** (2006) 4164-71.

25. Wickham, Jason R., and Charles V. Rice. "Solid-state NMR studies of bacterial lipoteichoic acid adsorption on different surfaces." *Solid State Nuc Mag Res* **34** (2008) 154-61.
26. Rice, Charles V., Jason R. Wickham, Margaret A. Eastman, William Harrison, Mark P. Pereira, and Eric D. Brown. "Magnetic resonance tells microbiology where to go: bacterial teichoic acid protects liquid water at sub-zero temperatures." *Proc SPIE* **7097** (2008) 70970O (10p.)
27. McGown, Linda B., and Kasem Nithipatikom. "Molecular Fluorescence and Phosphorescence." *Appl Spectros Rev* **35** (2000) 353-93.
28. Ingle, James D., Jr., and Stanley R. Crouch. *Spectrochemical Analysis*. Prentice-Hall, Inc.; New York, 1988.
29. Valeur, Bernard, and Mário N. Berberan-Santos. "A Brief History of Fluorescence and Phosphorescence before the Emergence of Quantum Theory." *J Chem Ed* **88** (2011) 731-8.
30. Beija, Mariana, Carlos A.M. Alfonso, and José M.G. Martinho. "Synthesis and applications of Rhodamine derivatives as fluorescent probes." *Chem Soc Rev* **38** (2009) 2410-33.
31. Arbeloa, F. López, T. López Arbeloa, M.J. Tapia Estévez, and I. López Arbeloa. "Photophysics of Rhodamines. Molecular Structure and Solvent Effects." *J Phys Chem* **95** (1991) 2203-8.
32. Snare, M.J., F.E. Treloar, K.P. Chigginio, and P.J. Thistlewaite. "The photophysics of Rhodamine B." *J Photochem* **18** (1982) 335-46.
33. Montenay-Garestier, Thérèse, Claude Hélène, and A.M. Michelson. "Étude par luminescence des interactions dans les acides oligo et polyadényliques." *Biochim Biophys Acta* **182** (1969) 342-54.
34. Terstereci, H. Nur, Ali Usanmaz, & Ahmet M. Önal. "Viscosity Molecular Weight Determination of Polyadenylic Acid." *J Macromol Sci A* **32** (1995) 553-562.
35. D'Elia, Michael A., Kathryn E. Millar, Terry J. Beveridge, and Eric D. Brown. "Wall Teichoic Acid Polymers Are Dispensable for Cell Viability in *Bacillus subtilis*." *J Bacteriol* **188** (2006) 8313-6.
36. Karstens, T., and K. Kobs. "Rhodamine B and Rhodamine 101 as Reference Substances for Fluorescence Quantum Yield Measurements." *J Phys Chem* **84** (1980) 1871-2.

CHAPTER 4: GENERAL PRINCIPLES OF DEUTERIUM NUCLEAR

MAGNETIC RESONANCE SPECTROSCOPY

1. Rabenstein, Dallas L. "NMR Spectroscopy: Past and Present." *Anal Chem* **73** (2001) 215A-223A.
2. Emsley, J.W., and J. Feeney. "Milestones in the first fifty years of NMR." *Prog Nuc Mag Spec* **28** (1995) 1-9.
3. Andrew, E.R., and E. Szczesniak. "A historical account of NMR in the solid state." *Prog Nuc Mag Spec* **28** (1995) 11-36.
4. Duer, Melinda J. *Introduction to Solid-State NMR Spectroscopy*. Blackwell Publishing; Walden, MA, 2004.
5. Basler, Wolf D. "Introduction to Nuclear Magnetic Resonance." *Adv Colloid Interface Sci* **23** (1985) 3-20.
6. Darbeau, Ron W. "Nuclear Magnetic Resonance (NMR) Spectroscopy: A Review and a Look at Its Use as a Probative Tool in Deamination Chemistry." *Appl Spec Rev* **41** (2006) 401-25.
7. Veeman, W.S. "Nuclear magnetic resonance, a simple introduction to the principles and applications." *Geoderma* **80** (1997) 225-42.
8. House, Waylon V. "Introduction to the principles of NMR." *IEEE Trans Nuc Sci* **NS-27** (1980) 1220-6.
9. Gladden, L.F. "Nuclear magnetic resonance in chemical engineering: principles and applications." *Chem Eng Sci* **49** (1994) 3339-408.
10. Freeman, Ray. "Pioneers of High-Resolution NMR." *Concepts Mag Res* **11** (1999) 61-70.
11. King, Glenn F., and Philip W. Kuchel. "Theoretical and Practical Aspects of NMR Studies of Cells." *Immunomethods* **4** (1994) 85-97.
12. Lesot, Philippe, and Jacques Courtieu. "Natural abundance deuterium NMR spectroscopy: Developments and analytical applications in liquids, liquid crystals and solid phases." *Prog Nuc Mag Res Spec* **55** (2009) 128-59.
13. Fyfe, Colin A., Stephanie A. Isbell and Nicolas E. Burlinson. "Nuclear Magnetic Resonance Imaging as a Probe of the Freezing-Thawing Phenomena of Liquids in Heterogeneous Systems." *Mag Res Chem* **32** (1994) 276-83.
14. Siminovitch, David J. "Solid-state NMR studies of proteins: the view from static ^2H NMR experiments." *Biochem Cell Biol* **76** (1998) 411-22.

15. Mantsch, Henry H., Hazime Saito, and Ian C.P. Smith. "Deuterium magnetic resonance, applications in chemistry, physics and biology." *Prog NMR Spec* **11** (1977) 211-71.
16. Xiong, Jincheng, and Gary E. Maciel. "Deuterium NMR Studies of Local Motions of Benzene Adsorbed on Ca-Montmorillonite." *J Phys Chem B* **103** (1999) 5543-9.
17. Lee, David K., Tomonori Saito, Alan J. Benesi, Michael A. Hickner, and Harry R. Allcock. "Characterization of Water in Proton-Conducting Membranes by Deuterium NMR T₁ Relaxation." *J Phys Chem B* **115** (2011) 776-83.
18. Garnier-Lhomme, Marie, Axelle Grélard, Richard D. Byrne, Cécile Loudet, Erick J. Dufourc, and Banafshé Larijani. "Probing the dynamics of intact cells and nuclear envelope precursor membrane vesicles by deuterium solid state NMR spectroscopy." *Biochim Biophys Acta* **1768** (2007) 2516-27.
19. Davis, James H. "The description of membrane lipid conformation, order and dynamics by ²H-NMR." *Biochim Biophys Acta* **737** (1983) 117-71.

CHAPTER 5: VARIABLE-TEMPERATURE DEUTERIUM NMR OF

POLY(ADENYLIC) ACID AND OTHER POTENTIAL CRYOPROTECTANTS

1. Fischer, Werner. "Physiology of Lipoteichoic Acids in Bacteria." *Adv Microbial Physiol* **29** (1988) 233-302.
2. Reichmann, Nathalie T., and Angelika Gründling. "Location, synthesis and function of glycolipids and polyglycerolphosphate lipoteichoic acid in Gram-positive bacteria of the phylum *Firmicutes*." *FEMS Microbiol Lett* **319** (2011) 97-105.
3. Schmidt, Richard R., Christian M. Pedersen, Yan Qiao, and Ulrich Zähringer. "Chemical synthesis of bacterial lipoteichoic acids: An insight on its biological significance." *Org Biomol Chem* **9** (2011) 2040-2052.
4. Neuhaus, Francis C., and James Baddiley. "A Continuum of Anionic Charge: Structures and Functions of D-Alanyl-Teichoic Acids in Gram-Positive Bacteria." *Microbiol Mol Biol Rev* **67** (2003) 686-723.
5. Sutcliffe, Iain C. "The Lipoteichoic Acids and Lipoglycans of Gram-positive Bacteria: A Chemotaxonomic Perspective." *Sys Appl Microbiol* **17** (1994) 467-480.
6. Morath, Siegfried, Sonja von Aulock, and Thomas Hartung. "Structure/function relationships of lipoteichoic acids." *J Endotoxin Res* **11** (2005) 348-356.

7. Schirner, Kathrin, Jon Marles-Wright, Richard J. Lewis, and Jeff Errington. "Distinct and essential morphogenic functions for wall- and lipo-teichoic acids in *Bacillus subtilis*." *EMBO J* **28** (2009) 830-842.
8. Beveridge, T.J., and R.G.E. Murray. "Sites of Metal Deposition in the Cell Wall of *Bacillus subtilis*." *J Bacteriol* **141** (1980) 876-887.
9. Baddiley, James. "Structure, Biosynthesis, and Function of Teichoic Acids." *Acc Chem Res* **3** (1970) 98-105.
10. Morath, Siegfried, Armin Geyer, and Thomas Hartung. "Structure-Function Relationship of Cytokine Induction by Lipoteichoic Acid from *Staphylococcus aureus*." *J Exp Med* **193** (2001) 393-397.
11. Morath, Siegfried, Andreas Stadelmaier, Armin Geyer, Richard R. Schmidt, and Thomas Hartung. "Synthetic Lipoteichoic Acid from *Staphylococcus aureus* Is a Potent Stimulus of Cytokine Release." *J Exp Med* **193** (2002) 1635-1640.
12. Draing, Christian, Stefanie Sigel, Susanne Deininger, Stephanie Traub, Rebekka Munke, Christoph Mayer, Lars Hareng, Thomas Hartung, Sonja von Aulock, and Corinna Hermann. "Cytokine induction by Gram-positive bacteria." *Immunobiology* **213** (2008) 285-296.
13. Wickham, Jason R., Jeffrey L. Halye, Stepan Kastanov, Jana Khandogin, and Charles V. Rice. "Revisiting Magnesium Chelation by Teichoic Acid with Phosphorus Solid-State NMR Theoretical Calculations." *J Phys Chem B* **113** (2009) 2177-2183.
14. Halye, Jeffrey L., and Charles V. Rice. "Cadmium Chelation by Bacterial Teichoic Acid from Solid-State Nuclear Magnetic Resonance Spectroscopy." *Biomacromolecules* **11** (2010) 333-340.
15. Rice, Charles V., William Harrison, Karl Kirkpatrick, and Eric D. Brown. "Cryoprotection from Bacterial Teichoic Acid." *Proc. SPIE* **7441** (2009) 74410M (7p.)
16. Rice, Charles V., Jason R. Wickham, Margaret A. Eastman, William Harrison, Mark P. Pereira, and Eric D. Brown. "Magnetic resonance tells microbiology where to go: bacterial teichoic acid protects liquid water at sub-zero temperatures." *Proc. SPIE* **7097** (2008) 70970O (10p.)
17. Haines, R.B. "The Effect of Freezing on Bacteria." *Proc R Soc Lond B* **124** (1938) 451-463.
18. Rice, Charles V. "RNA World Meets Snowball Earth." *Proc. SPIE* **7819** (2010) 781912 (8p.)

19. Anderson, James T. "RNA Turnover: Unexpected Consequences of Being Tailed." *Curr Biol* **15** (2005) R635-R638.
20. Kuntz, I.D., Jr., T.S. Brassfield, G.D. Law, and G.V. Purcell. "Hydration of Macromolecules." *Science* **163** (1969) 1329-1331.

CHAPTER 6: OVERVIEW OF SPORE-FORMING BACTERIA AND

SPORULATION

1. Bartlett, D.H. "Pressure effects on *in vivo* microbial processes." *Biochim Biophys Acta* **1595** (2002) 367-81.
2. Rothschild, Lynn J., and Rocco L. Mancinelli. "Life in extreme environments." *Nature* **409** (2001) 1092-1101.
3. Price, Buford P. "A habitat for psychrophiles in deep Antarctic ice." *PNAS* **97** (2000) 1247-51.
4. Collins, R. Eric, Gabriele Rocap, and Jody W. Deming. "Persistence of bacterial and archaeal communities in sea ice through an Arctic winter." *Env Microbiol* **12** (2010) 1828-41.
5. Azua-Bustos, Armando, Catalina Urrejola, and Rafael Vicuña. "Life at the dry edge: Microorganisms of the Atacama Desert." *FEBS Letters* **586** (2012) 2939-45.
6. Wierzchos, J., B. Cámara, A. De Los Ríos, A.F. Davila, I.M. Sánchez Almazo, O. Artieda, K. Wierzchos, B. Gómez-Silva, C. McKay, and C. Ascaso. "Microbial colonization of Ca-sulfate crusts in the hyperarid core of the Atacama Desert: implications for the search for life on Mars." *Geobiology* **9** (2011) 44-60.
7. McKay, Christopher P., E. Imre Friedmann, Benito Gómez-Silva, Luis Cáceres-Villanueva, Dale T. Andersen, and Ragnhild Landheim. "Temperature and Moisture Conditions for Life in the Extreme Arid Region of the Atacama Desert: Four Years of Observations Including the El Niño of 1997-1998." *Astrobiology* **3** (2003) 393-406.
8. Campos, Victor L., Cristian Valenzuela, Pablo Yarza, Peter Kämpfer, Roberto Vidal, C. Zaror, Maria-Angelica Mondaca, Arantxa Lopez-Lopez, and Ramon Rosselló-Móra. "*Pseudomonas arsenicoxydans* sp nov., an arsenite-oxidizing strain isolated from the Atacama desert." *Syst Appl Microbiol* **33** (2010) 193-7.

9. Drees, Kevin P., Julia W. Neilson, Julio L. Betancourt, Jay Quade, David A. Henderson, Barry M. Pryor, and Raina M. Maier. "Bacterial Community Structure in the Hyperarid Core of the Atacama Desert, Chile." *Appl Env Microbiol* **72** (2006) 7902-8.
10. Moreno, M.L., F. Piubeli, M.R.L. Bonfá, M.T. Garcia, L.R. Durrant, and E. Mellado. "Analysis and characterization of cultivable extremophilic hydrolytic bacterial community in heavy-metal-contaminated soils from the Atacama Desert and their biotechnological potentials." *J Appl Microbiol* **113** (2012) 550-9.
11. Errington, Jeffery. "*Bacillus subtilis* Sporulation: Regulation of Gene Expression and Control of Morphogenesis." *Microbiol Rev* **57** (1993) 1-33.
12. Higgins, Douglas, and Jonathan Dworkin. "Recent progress in *Bacillus subtilis* sporulation." *FEMS Microbiol Rev* **36** (2012) 131-48.
13. Holt, S.C., and E.R. Leadbetter. "Comparative Ultrastructure of Selected Aerobic Spore-forming Bacteria: a Freeze-Etching Study." *Bacteriol Rev* **33** (1969) 346-78.
14. Cano, Raúl J., and Monica K. Borucki. "Revival and Identification of Bacterial Spores in 25- to 40-Million-Year-Old Dominican Amber." *Science* **268** (1995) 1060-4.
15. Setlow, P. "Spores of *Bacillus subtilis*: their resistance to and killing by radiation, heat and chemicals." *J Appl Microbiol* **101** (2006) 514-25.
16. Warth, A.D. "Molecular Structure of the Bacterial Spore." In *Advances in Microbial Physiology*, 17th edition. Eds. A.H. Rose and J. Gareth Morris. Academic Press, Ltd.; New York, 1978: 1-45.
17. Carrera, M., R.O. Zandomeni, J. Fitzgibbon, and J.-L. Sagripanti. "Difference between the spore sizes of *Bacillus anthracis* and other *Bacillus* species." *J Appl Microbiol* **102** (2007) 303-12.
18. Carrera, M., R.O. Zandomeni, and J.-L. Sagripanti. "Wet and dry density of *Bacillus anthracis* and other *Bacillus* species." *J Appl Microbiol* **105** (2008) 68-77.
19. Driks, Adam. "*Bacillus subtilis* Spore Coat." *Microbiol Mol Biol Rev* **63** (1999) 1-20.

20. Popham, David L., Jari Helin, Catherine E. Costello, and Peter Setlow. "Analysis of the Peptidoglycan Structure of *Bacillus subtilis* Endospores." *J Bacteriol* **178** (1996) 6451-8.
21. Warth, A.D., and J.L. Strominger. "Structure of the Peptidoglycan from Spores of *Bacillus subtilis*." *Biochemistry* **11** (1972) 1389-96.
22. Warth A.D., and J.L. Strominger. "Structure of the Peptidoglycan from Vegetative Cell Walls of *Bacillus subtilis*." *Biochemistry* **10** (1971) 4349-58.
23. Moeller, Ralf, Peter Setlow, Günther Reitz, and Wayne L. Nicholson. "Roles of Small, Acid-Soluble Spores Proteins and Core Water Content in Survival of *Bacillus subtilis* Spores Exposed to Environmental Solar UV Radiation." *Appl Env Microbiol* **75** (2009) 5202-8.
24. Setlow, Barbara, Swaroopa Atluri, Ryan Kitchel, Kasia Koziol-Dube, and Peter Setlow. "Role of Dipicolinic Acid in Resistance and Stability of Spores of *Bacillus subtilis* with or without DNA-Protective α/β -Type Small Acid-Soluble Proteins." *J Bacteriol* **188** (2006) 3740-7.
25. Nicholson, Wayne L., Nobuo Munakata, Gerda Horneck, Henry J. Melosh, and Peter Setlow. "Resistance of *Bacillus* Endospores to Extreme Terrestrial and Extraterrestrial Environments." *Microbiol Mol Biol Rev* **64** (2000) 548-72.
26. Piggot, Patrick J., and David W. Hilbert. "Sporulation of *Bacillus subtilis*." *Curr Opin Microbiol* **7** (2004) 579-86.
27. Setlow, Peter. "Spore germination." *Curr Opin Microbiol* **6** (2003) 550-6.
28. Paredes-Sabja, Daniel, Peter Setlow, and Mahfuzur R. Sarker. "Germination of spores of *Bacillales* and *Clostridiales* species: mechanisms and proteins involved." *Trends Micro* **19** (2011) 85-94.
29. Paidhungat, Madan, Katerina Ragkousi, and Peter Setlow. "Genetic Requirements for Induction of Germination of Spores of *Bacillus subtilis* by Ca^{2+} -Dipicolinate." *J Bacteriol* **183** (2001) 4886-93.
30. Leuschner, Renata G.K., Dudley P. Ferdinando, and Peter J. Lillford. "Structural analysis of spores of *Bacillus subtilis* during germination and outgrowth." *Colloids and Surfaces B* **19** (2000) 31-41.
31. Driks, Adam. "The *Bacillus* Spore Coat." *Phytopathology* **94** (2004) 1249-51.

32. Driks, Adam. "Maximum shields: the assembly and function of the bacterial spore coat." *Trends Micro* **10** (2002) 251-4.
33. Takamatsu, H., and K. Watabe. "Assembly and genetics of spore protective structures." *Cell Mol Life Sci* **59** (2002) 434-44.
34. Riesenman, Paul J., and Wayne L. Nicholson. "Role of the Spore Coat Layers in *Bacillus subtilis* Spore Resistance to Hydrogen Peroxide, Artificial UV-C, UV-B, and Solar UV Radiation." *Appl Env Microbiol* **66** (2000) 620-6.
35. Moeller, Ralf, Andrew C. Schuerger, Günther Reitz, and Wayne L. Nicholson. "Protective Role of Spores Structural Components in Determining *Bacillus subtilis* Spore Resistance to Simulated Mars Surface Conditions." *Appl Env Microbiol* **78** (2012) 8849-53.
36. Atrih, Abdelmadjid, and Simon J. Foster. "The role of peptidoglycan structure and structural dynamics during endospore dormancy and germination." *Antonie van Leeuwenhoek* **75** (1999) 299-307.
37. Mallidis, C.G., and J. Scholfield. "Relation of the heat resistance of bacterial spores to chemical composition and structure II. Relation to cortex and structure." *J Appl Bacteriol* **63** (1987) 207-15.
38. Atrih, Abdelmadjid, Peter Zöllner, Günter Allmaier, and Simon J. Foster. "Structural Analysis of *Bacillus subtilis* 168 Endospore Peptidoglycan and Its Role during Differentiation." *J Bacteriol* **178** (1996) 6173-83.
39. Ebmeier, Sarah E., Irene S. Tan, Katie Rose Clapham, and Kumaran S. Ramamurthi. "Small proteins link coat and cortex assembly during sporulation in *Bacillus subtilis*." *Mol Microbiol* **84** (2012) 682-96.
40. Magge, Anil, Amanda C. Granger, Paul G. Wahome, Barbara Setlow, Venkata R. Vepachedu, Charles A. Loshon, Lixin Peng, De Chen, Yong-qing Li, and Peter Setlow. "Role of Dipicolinic Acid in the Germination, Stability, and Viability of Spores of *Bacillus subtilis*." *J Bacteriol* **190** (2008) 4798-807.
41. Li, Yunfeng, Andrew Davis, George Korza, Pengfei Zhang, Yong-qing Li, Barbara Setlow, Peter Setlow, and Bing Hao. "Role of a SpoVA Protein in Dipicolinic Acid Uptake into Developing Spores of *Bacillus subtilis*." *J Bacteriol* **194** (2012) 1875-84.

42. Kong, Lingbo, Peter Setlow, and Yong-Qing Li. "Analysis of the Raman spectra of Ca²⁺-dipicolinic acid alone and in the bacterial spore core in both aqueous and dehydrated environments." *Analyst* **137** (2012) 3683-9.
43. Ghiamati, E., R. Manoharan, W.H. Nelson, and J.F. Sperry. "UV Resonance Raman Spectra of Bacillus Spores." *Appl Spec* **46** (1992) 357-64.
44. Setlow, Peter. "Small, Acid-Soluble Spore Proteins of *Bacillus* Species: Structure, Synthesis, Genetics, Function, and Degradation." *Annu Rev Microbiol* **42** (1988) 319-38.
45. Setlow, Peter. "Mechanisms for the Prevention of Damage to DNA in Spores of *Bacillus* Species." *Annu Rev Microbiol* **49** (1995) 29-54.
46. Moeller, Ralf, Peter Setlow, Günther Reitz, and Wayne L. Nicholson. "Roles of Small, Acid-Soluble Spore Proteins and Core Water Content in Survival of *Bacillus subtilis* Spores Exposed to Environmental Solar UV Radiation." *Appl Env Microbiol* **75** (2009) 5202-8.
47. Setlow, Barbara, and Peter Setlow. "Small, Acid-Soluble Proteins Bound to DNA Protect *Bacillus subtilis* Spores from Killing by Dry Heat." *Appl Env Microbiol* **61** (1995) 2787-90.
48. Setlow, Barbara, and Peter Setlow. "Dipicolinic Acid Greatly Enhances Production of Spore Photoproduct in Bacterial Spores upon UV Irradiation." *Appl Env Microbiol* **59** (1993) 640-3.
49. Nicholson, W.L. "Roles of *Bacillus* endospores in the environment." *Cell Mol Life Sci* **59** (2002) 410-6.
50. Vreeland, Russell H., William D. Rosenzweig, and Dennis W. Powers. "Isolation of a 250 million-year-old halotolerant bacterium from a primary salt crystal." *Nature* **407** (2000) 897-900.
51. Deakin, Laura J., Simon Clare, Robert P. Fagan, Lisa F. Dawson, Derek J. Pickard, Michael R. West, Brendan W. Wren, Neil F. Fairweather, Gordon Dougan, and Trevor D. Lawley. "The *Clostridium difficile* *spo0A* Gene Is a Persistence and Transmission Factor." *Infect Immun* **80** (2012) 2704-11.
52. Best, Emma L., Warren N. Fawley, Peter Parnell, and Mark H. Wilcox. "The Potential for Airborne Dispersal of *Clostridium difficile* from Symptomatic Patients." *Clin Infect Dis* **50** (2010) 1450-7.
53. Chaudhry, Rama. "Botulism: A diagnostic challenge." *Ind J Med Res* **134** (2011) 10-12.

54. Schmid, G., and A. Kaufmann. "Anthrax in Europe: its epidemiology, clinical characteristics, and role in bioterrorism." *Clin Microbiol Infect* **8** (2002) 479-88.
55. Spotts Whitney, Ellen A., Mark E. Beatty, Thomas H. Taylor, Jr., Robbin Weyant, Jeremy SObel, Matthew J. Arduino, and David A. Ashford. "Inactivation of *Bacillus anthracis* Spores." *Emerg Infect Dis* **9** (2003) 623-7.
56. Venkateswaran, Kasthuri, Masataka Satomi, Shirley Chung, Roger Kern, Robert Koukol, Cecilia Basic, and David White. "Molecular Microbial Diversity of a Spacecraft Assembly Facility." *Sys Appl Microbiol* **24** (2001) 311-20.
57. Rummel, J.D., and L. Billings. "Issues in planetary protection: policy, protocol and implementation." *Space Policy* **20** (2004) 49-54.
58. Kerney, Krystal R., and Andrew C. Schuerger. "Survival of *Bacillus subtilis* Endospores on Ultraviolet-Irradiated Rover Wheels and Mars Regolith under Simulated Martian Conditions." *Astrobiology* **11** (2011) 477-85.
59. Schuerger, Andrew C., Rocco L. Mancinelli, Roger G. Kern, Lynn J. Rothschild, and Christopher P. McKay. "Survival of endospores of *Bacillus subtilis* on spacecraft surfaces under simulated martian environments: implications for the forward contamination of Mars." *Icarus* **165** (2003) 253-76.
60. Nicholson, Wayne L., Lashelle E. McCoy, Krystal R. Kerney, Douglas W. Ming, D.C. Golden, and Andrew C. Schuerger. "Aqueous extracts of a Mars analogue regolith that mimics the Phoenix landing site do not inhibit spore germination or growth of model spacecraft contaminants *Bacillus subtilis* 168 and *Bacillus pumilus* SAFR-032." *Icarus* **220** (2012) 904-10.
61. Probst, Alexander, Rainer Facius, Reinhard Wirth, Marco Wolf, and Christine Moissl-Eichinger. "Recovery of *Bacillus* Spore Contaminants from Rough Surfaces: a Challenge to Space Mission Cleanliness Control." *Appl Env Microbiol* **77** (2011) 1628-37.
62. Sapru, V. and T.P. Labuza. "Glassy State in Bacterial Spores Predicted by Polymer Glass-Transition Theory." *J Food Sci* **58** (1993) 445-8.
63. Ablett, Steve, Arthur H. Darke, Peter J. Lillford, and David R. Martin. "Glass formation and dormancy in bacterial spores." *Int J Food Sci Tech* **34** (1999) 59-69.

64. Sunde, Erik P., Peter Setlow, Lars Hederstedt, and Bertil Halle. "The physical state of water in bacterial spores." *PNAS* **106** (2009) 19334-9.
65. National Center for Biotechnology Information. "Bacillus pumilus SAFR-032 16S ribosomal RNA gene, partial sequence – Nucleotide – NCBI." <http://www.ncbi.nlm.nih.gov/nucore/AY167879> . Accessed January 14, 2013.
66. Link, L., J. Sawyer, K. Venkateswaran, and W. Nicholson. "Extreme Spore UV Resistance of *Bacillus pumilus* Isolates Obtained from an Ultraclean Spacecraft Assembly Facility." *Microbial Ecology* **47** (2004) 159-63.
67. Newcombe, David A., Andrew C. Schuerger, James N. Benardini, Danielle Dickinson, Roger Tanner, and Kasthuri Venkateswaran. "Survival of Spacecraft-Associated Microorganisms under Simulated Martian UV Irradiation." *Appl Env Microbiol* **71** (2005) 8147-56.
68. Giola, Jason, Shailaja Yerrapragada, Xiang Qin, Huaiyang Jiang, Okezie C. Igboeli, Donna Muzny, Shannon Dugan-Rocha, Yan Ding, Alicia Hawes, Wen Liu, Lesette Perez, Christie Kovar, Huyen Dinh, Sandra Lee, Lynne Nazareth, Peter Blyth, Michael Holder, Christian Buhay, Madhan R. Tirumalai, Yamei Liu, Indrani Dasgupta, Lina Bokhetache, Masaya Fujita, Fathi Karouia, Prahathees Eswara Moorthy, Johnathan Siefert, Akif Uzman, Prince Buzumbo, Avana Verma, Hiba Zwiya, Brain D. McWilliams, Adeola Olowu, Kenneth D. Clinkenbeard, David Newcombe, Lis Golebiewski, Joseph F. Petrosino, Wayne L. Nicholson, George E. Fox, Kasthuri Venkateswaran, Sarah K. Highlander, and George M. Weinstock. "Paradoxical DNA Repair and Peroxide Resistance Gene Conservation in *Bacillus pumilus* SAFR-032." *PLoS ONE* **2** (2007) e928 (10p). DOI:10.1371/journal.pone.0000928
69. Checinska, Aleksandra, Malcolm Burbank, and Andrzej J. Paszczynski. "Protection of *Bacillus pumilus* Spores by Catalases." *Appl Env Microbiol* **78** (2012) 6413-22.
70. Vaishampayan, Parag A., Elke Rabbow, Gerda Horneck, and Kasthuri J. Venkateswaran. "Survival of *Bacillus pumilus* Spores for a Prolonged Period of Time in Real Space Conditions." *Astrobiology* **12** (2012) 487-97.
71. Nicholson, Wayne L., Andrew C. Schuerger, and Peter Setlow. "The solar UV environment and bacterial spore UV resistance: considerations for Earth-to-Mars transport by biological processes and human spaceflight." *Mutation Research* **571** (2005) 249-64.

72. Mileikowsky, Curt, Francis A. Cucinotta, John W. Wilson, Brett Gladman, Gerda Horneck, Lennart Lindegren, Jay Melosh, Hans Rickman, Mauri Valtonen, and J.Q. Zheng. "Natural Transfer of Viable Microbes in Space. 1. From Mars to Earth and Earth to Mars." *Icarus* **145** (2000) 391-427.
73. Nicholson, Wayne L. "Ancient micronauts: interplanetary transport of microbes by cosmic impacts." *Trends Micro* **17** (2009) 243-50.

CHAPTER 7: DEUTERIUM SOLID-STATE NMR EXPERIMENTS ON BACTERIAL SPORES—INSIGHTS INTO THE NATURE OF WATER INSIDE THE SPORE CORE

1. Conn, H.J. "The Identity of *Bacillus subtilis*." *J Infect Dis* **46** (1930) 341-50.
2. Anderson, Linda M., Tina M. Henkin, Glenn H. Chambliss, and Kenneth F. Bott. "New Chloramphenicol Resistance Locus in *Bacillus subtilis*." *J Bacteriol* **158** (1984) 386-8.
3. Burkholder, Paul R., and Norman H. Giles, Jr. "Induced Biochemical Mutations in *Bacillus subtilis*." *Amer J Bot* **34** (1947) 345-8.
4. Zeigler, Daniel R., Zoltán Prágai, Sabrina Rodriguez, Bastien Chevreux, Andrea Muffler, Thomas Albert, Renyuan Bai, Markus Wyss, and John B. Perkins. "The Origins of 168, W23, and Other *Bacillus subtilis* Legacy Strains." *J Bacteriol* **190** (2008) 6983-95.
5. Hageman, James H., Gary W. Shankweiler, Pamela R. Wall, Karen Franich, Gloria W. McCowan, Suan M. Cauble, Jesus Grajeda, and Casilda Quinones. "Single, Chemically Defined Sporulation Medium for *Bacillus subtilis*: Growth, Sporulation, and Extracellular Protease Production." *J Bacteriol* **160** (1984) 438-41.
6. Schaeffer, Pierre, Jacqueline Millet, and Jean-Paul Aubert. "Catabolic Repression of Bacterial Sporulation." *PNAS* **54** (1965) 704-11.
7. Bailey, Glen F., Saima Karp, and L.E. Sacks. "Ultraviolet-Absorption Spectra of Dry Bacterial Spores." *J Bacteriol* **89** (1965) 984-7.
8. *User Guide: Solid-State NMR: Varian NMR Spectrometer Systems with VNMR 6.1C Software*. Varian, Inc.; Palo Alto, 2002.
9. Hashimoto, Tadayo, W.R. Frieben, and S.F. Conti. "Germination of Single Bacterial Spores." *J Microbiol* **98** (1969) 1011-20.

10. Leuschner, Renata G.K., Dudley P. Ferdinando, and Peter J. Lillford. "Structural analysis of spores of *Bacillus subtilis* during germination and outgrowth." *Colloids and Surfaces B* **19** (2000) 31-41.
11. Sunde, Erik P., Peter Setlow, Lars Hederstedt, and Bertil Halle. "The physical state of water in bacterial spores." *PNAS* **106** (2009) 19334-9.

CHAPTER 8: TREATMENT OF BACTERIAL SPORES WITH OXINE®, A PROPRIETARY CHLORINE DIOXIDE-BASED BIOCIDAL AGENT

1. Beuchat, Larry R., Charles A. Pettigrew, Mario E. Tremblay, Brian J. Roselle, and Alan J. Scouten. "Lethality of chlorine, chlorine dioxide, and a commercial fruit and vegetable sanitizer to vegetative cells and spores of *Bacillus cereus* and spores of *Bacillus thuringiensis*." *J Ind Microbiol Biotechnol* **32** (2005) 301-8.
2. Gordon, Gilbert, and Aaron A. Rosenblatt. "Chlorine Dioxide: The Current State of the Art." *Oxine: Science and Engineering* **27** (2005) 203-7.
3. Novak, J, A. Dermici, and Y. Han. "Novel Chemical Processes: Ozone, Supercritical CO₂, Electrolyzed Oxidizing Water, and Chlorine Dioxide Gas." *Food Sci Tech Int* **14** (2008) 437-41.
4. Rastogi, Vipin K., Shawn P. Ryan, Lalena Wallace, Lisa S. Smith, Saumil Sh. Shah, and G. Blair Martin. "Systematic Evaluation of the Efficacy of Chlorine Dioxide in Decontamination of Building Interior Surfaces Contaminated with Anthrax Spores." *Appl Env Microbiol* **76** (2010) 3343-51.
5. Solomon, Keith R. "Chlorine in the bleaching of pulp and paper." *Pure & Appl Chem* **68** (1996) 1721-30.
6. Occupational Safety and Health Administration. "Occupational Safety and Health Guidelines for Chlorine Dioxide."
<http://www.osha.gov/SLTC/healthguidelines/chlorinedioxide/recognition.html>
(accessed November 27, 2012).
7. Sharma, Virender K., and Mary Sohn. "Reactivity of chlorine dioxide with amino acids, peptides, and proteins." *Environ Chem Lett* **10** (2012) 255-64.
8. Buhr, T.L., A.A. Young, Z.A. Minter, C.M. Wells, and D.A. Shegogue. "Decontamination of a hard surface contaminated with *Bacillus anthracis* ΔSterne and *B.anthraxis* Ames spores using electrochemically generated liquid-phase chlorine dioxide (eClO₂)." *J Appl Microbiol* **111** (2011) 1057-64.
9. Environmental Protection Agency. "Anthrax Spore Decontamination using Chlorine Dioxide."
<http://www.epa.gov/pesticides/factsheets/chemicals/chlorinedioxidefactsheet.htm>
(updated November 1, 2012) (accessed November 27, 2012).

10. Foegeding, P.M., V. Hemstapat, and F.G. Giesbrecht. "Chlorine Dioxide Inactivation of *Bacillus* and *Clostridium* Spores." *J Food Sci* **51** (1986) 197-201.
11. Spotts Whitney, Ellen A., et al. "Inactivation of *Bacillus anthracis* Spores." *Emerg Infect Dis* **9** (2003) 623-7.
12. Kim, B.R., et al. "Literature review—efficacy of various disinfectants against *Legionella* in water systems." *Water Res* **36** (2002) 4433-44.
13. Leung, W.K., A.P.S. Lau, and K.L. Leung. "Bactericidal and sporicidal performance of a polymer-encapsulated chlorine dioxide-coated surface." *J Appl Microbiol* **106** (2009) 1463-72.
14. Mahovic, Michael J., Joel D. Tenney, and Jerry A. Bartz. "Applications of Chlorine Dioxide Gas for Control of Bacterial Soft Rot in Tomatoes." *Plant Dis* **91** (2007) 1316-20.
15. Benarde, Melvin A., W. Brewster Snow, Vincent P. Olivieri, and Burton Davidson. "Kinetics and Mechanism of Bacterial Disinfection by Chlorine Dioxide." *Appl Microbiol* **15** (1967) 257-65.
16. Shemesh, Moshe, Roberto Kolter, and Richard Losick. "The Biocide Chlorine Dioxide Stimulates Biofilm Formation in *Bacillus subtilis* by Activation of the Histidine Kinase KinC." *J Bacteriol* **192** (2010) 6352-6.
17. Smith, Roger P., and Calvin C. Willhite. "Chlorine Dioxide and Hemodialysis." *Reg Toxicol Pharmacol* **11** (1990) 42-62.
18. Rummel, J.D., and L. Billings. "Issues in Planetary protection: policy, protocol and implementation." *Space Policy* **20** (2004) 49-54.
19. Pillinger, Judith M., C.T. Pillinger, S. Sancisi-Frey, and J.A. Spry. "The microbiology of spacecraft hardware: Lessons learned from the planetary protection activities on the Beagle 2 spacecraft." *Res Microbiol* **157** (2006) 19-24.
20. Pottage, T., S. Macken, K. Giri, J.T. Walker, and A.M. Bennett. "Low-Temperature Decontamination with Hydrogen Peroxide or Chlorine Dioxide for Space Applications." *Appl Env Microbiol* **78** (2012) 4169-74.
21. Venkateswaran, Kasthuri, Masataka Satomi, Shirley Chung, Roger Kern, Robert Koukol, Cecilia Basic, and David White. "Molecular Microbial Diversity of a Spacecraft Assembly Facility." *System Appl Microbiol* **24** (2001) 311-20.
22. Ghosh, Sudeshna, Shariff Osman, Parag Vaishampayan, and Kasthuri Venkateswaran. "Recurrent Isolation of Extremotolerant Bacteria from the Clean Room Where Phoenix Spacecraft Components Were Assembled." *Astrobiology* **10** (2010) 325-35.

23. Link, L., J. Sawyer, K. Venkateswaran, and W. Nicholson. "Extreme Spore UV Resistance of *Bacillus pumilus* Isolates Obtained from an Ultraclean Spacecraft Assembly Facility." *Microbial Ecology* **47** (2004) 159-63.
24. Giola, Jason, Shailaja Yerrapragada, Xiang Qin, Huaiyang Jiang, Okezie C. Igboeli, Donna Muzny, Shannon Dugan-Rocha, Yan Ding, Alicia Hawes, Wen Liu, Lesette Perez, Christie Kovar, Huyen Dinh, Sandra Lee, Lynne Nazareth, Peter Blyth, Michael Holder, Christian Buhay, Madhan R. Tirumalai, Yamei Liu, Indrani Dasgupta, Lina Bokhetache, Masaya Fujita, Fathi Karouia, Prahathees Eswara Moorthy, Johnathan Siefert, Akif Uzman, Prince Buzumbo, Avanai Verma, Hiba Zwiya, Brain D. McWilliams, Adeola Olowu, Kenneth D. Clinkenbeard, David Newcombe, Lis Golebiewski, Joseph F. Petrosino, Wayne L. Nicholson, George E. Fox, Kasthuri Venkateswaran, Sarah K. Highlander, and George M. Weinstock. "Paradoxical DNA Repair and Peroxide Resistance Gene Conservation in *Bacillus pumilus* SAFR-032." *PLoS ONE* **2** (2007) e928 (10p.) DOI:10.1371/journal.pone.0000928
25. Checinska, Aleksandra, Malcolm Burbank, and Andrzej J. Paszczynski. "Protection of *Bacillus pumilus* Spores by Catalases." *Appl Env Microbiol* **78** (2012) 6413-22.
26. Shieh, Edison, Andrzej Paszczynski, Chien M. Wai, Qingyong Lang, and Ronald L. Crawford. "Sterilization of *Bacillus pumilus* spores using supercritical fluid carbon dioxide containing various modifier solutions." *J Microbiol Meth* **76** (2009) 247-52.
27. Checinska, Aleksandra, Ingrid A. Fruth, Tonia L. Green, Ronald L. Crawford, and Andrzej J. Paszczynski. "Sterilization of biological pathogens using supercritical fluid carbon dioxide containing water and hydrogen peroxide." *J Microbiol Meth* **87** (2011) 70-75.
28. Young, S.B., and P. Setlow. "Mechanisms of killing of *Bacillus subtilis* spores by hypochlorite and chlorine dioxide." *J Appl Microbiol* **95** (2003) 54-67.
29. Masschelein, W.J. *Chlorine Dioxide: Chemistry and Environmental Impact of Oxychlorine Compounds*. Ann Arbor Science Publishers, Inc.; Ann Arbor, 1979.
30. Hageman, James H., Gary W. Shankweiler, Pamela R. Wall, Karen Franich, Gloria W. McCowan, Suan M. Cauble, Jesus Grajeda, and Casilda Quinones. "Single, Chemically Defined Sporulation Medium for *Bacillus subtilis*: Growth, Sporulation, and Extracellular Protease Production." *J Bacteriol* **160** (1984) 438-441.
31. Tauveron, Grégoire, Christian Slomianny, Céline Henry, and Christine Faille. "Variability among *Bacillus cereus* strains in spore surface properties and

influence on their ability to contaminate food service equipment.” *Int J Food Microbiol* **110** (2006) 254-62.

32. Vaishampayan, Parag, Elke Rabbow, Gerda Horneck, and Kasthuri J. Venkateswaran. “Survival of *Bacillus pumilus* Spores for a Prolonged Period of Time in Real Space Conditions.” *Astrobiology* **12** (2012) 487-97.